

# ARTS User Guide

edited by

**Patrick Eriksson and Stefan Buehler**

February 25, 2020  
ARTS Version 2.2.66

**The content and usage of ARTS are not only described by this document. An overview of ARTS documentation and help features are given in Section 1.2. For continuous reports on changes of the source code and this user guide, subscribe to the ARTS developers mailing list at <http://www.radiativetransfer.org/contact/>.**

**We welcome gladly comments and reports on errors in the software or the document. Send then an e-mail to: `patrick.eriksson(at)chalmers.se` or `sbuehler(at)ltu.se`.**

**If you use data generated by ARTS in a scientific publication, then please mention this and cite the most appropriate of the ARTS publications. The relevant publications are summarised at <http://www.radiativetransfer.org/docs/>.**

Copyright (C) 2000-2012

Stefan Buehler <sbuehler (at) ltu.se>

Patrick Eriksson <patrick.eriksson (at) chalmers.se>

The ARTS program is free software; you can redistribute it and/or modify it under the terms of the GNU General Public License as published by the Free Software Foundation; either version 2, or (at your option) any later version.

This program is distributed in the hope that it will be useful, but WITHOUT ANY WARRANTY; without even the implied warranty of MERCHANTABILITY or FITNESS FOR A PARTICULAR PURPOSE. See the GNU General Public License for more details.

You should have received a copy of the GNU General Public License along with the program; if not, write to the Free Software Foundation, Inc., 59 Temple Place - Suite 330, Boston, MA 02111-1307, USA.

## Contributing authors

Author/email	Main contribution(s)
Stefan Buehler <sup>a</sup> sbuehler (at) ltu.se	Editor, Sections 1, 6 and 17.
Claudia Emde <sup>c</sup> claudia.emde (at) dlr.de	Sections 8 and 18.
Patrick Eriksson <sup>b</sup> patrick.eriksson (at) chalmers.se	Editor, Sections 3, 4, 5, 7, 9, 10, 11, 12, 16, 13, 14, 15, and 19.
Oliver Lemke <sup>a</sup> olemke (at) core-dump.info	Latex fixes.

The present address is given for active contributors, while for others the address to the institute where the work was performed is given:

- <sup>a</sup> Department of Computer Science, Electrical and Space Engineering, Division of Space Technology, Luleå University of Technology, Box 812, SE-98128 Kiruna, Sweden.
- <sup>b</sup> Department of Earth and Space Sciences, Chalmers University of Technology, SE-41296 Gothenburg, Sweden.
- <sup>c</sup> Institute of Environmental Physics, University of Bremen, P.O. Box 33044, D-28334 Bremen, Germany.



# Contents

<b>I</b>	<b>Overview</b>	<b>1</b>
<b>1</b>	<b>Introduction</b>	<b>3</b>
1.1	What is ARTS?	3
1.2	Documentation	4
1.2.1	Guide documents	4
1.2.2	Articles	4
1.2.3	Built-in documentation	5
1.2.4	Test and include controlfiles	5
1.2.5	Source code documentation	5
1.2.6	Build instructions	5
1.2.7	Command line parameters	6
1.3	ARTS as a scripting language	6
1.3.1	Workspace variables	7
1.3.2	Workspace methods	7
1.3.3	Agendas	9
1.4	Include controlfiles	10
1.5	Test controlfiles	10
1.6	Verbosity levels	10
<b>2</b>	<b>Importing and exporting data</b>	<b>13</b>
2.1	Data formats	13
2.1.1	XML files	13
2.1.2	NetCDF files	13
2.1.3	Gridded fields	13
	Naming convention for grids	13
<b>3</b>	<b>Description of the atmosphere</b>	<b>15</b>
3.1	Altitude coordinates	15
3.2	Atmospheric dimensionality	16
3.3	Atmospheric grids and fields	17
3.4	Geo-location of 1D and 2D	19
3.5	Hydrostatic equilibrium	19
3.6	The reference ellipsoid and the surface	19
3.7	The cloud box	20
3.8	Wind and magnetic vector fields	21

<b>4</b>	<b>Radiative transfer basics</b>	<b>23</b>
4.1	Stokes dimensionality . . . . .	23
4.2	The radiative transfer equation . . . . .	24
4.2.1	Propagation effects . . . . .	24
4.2.2	Absorbing species and particles . . . . .	24
4.2.3	Emission and absorption vectors . . . . .	25
4.2.4	Main cases . . . . .	26
	Clear-sky radiative transfer . . . . .	26
	Radiative transfer with scattering . . . . .	26
<b>5</b>	<b>Complete calculations</b>	<b>27</b>
5.1	Overview . . . . .	27
5.2	Compulsory sensor and data reduction variables . . . . .	29
5.2.1	Sensor position . . . . .	29
5.2.2	Line-of-sight . . . . .	30
5.2.3	Sensor characteristics and data reduction . . . . .	31
5.3	Measurement sequences and blocks . . . . .	31
<b>II</b>	<b>Atmospheric properties</b>	<b>33</b>
<b>6</b>	<b>Gas absorption</b>	<b>35</b>
6.1	Introduction . . . . .	35
6.2	Key physical quantities . . . . .	35
6.3	Agendas . . . . .	36
6.4	Gas absorption in radiative transfer simulations . . . . .	37
6.5	Calculating gas absorption . . . . .	37
6.5.1	Absorption species . . . . .	39
6.5.2	Explicit line-by-line calculations . . . . .	41
6.5.3	Continua and complete absorption models . . . . .	41
6.5.4	Collision-induced absorption . . . . .	43
6.5.5	Zeeman calculations . . . . .	45
6.5.6	Internal line-mixing . . . . .	47
6.5.7	Faraday rotation . . . . .	49
6.5.8	Absorbing particles . . . . .	50
6.5.9	Further input data and parameters for calculating gas absorption . . . . .	51
	Spectral line data . . . . .	51
	Isotopologue ratios . . . . .	51
	Partition functions . . . . .	51
6.6	The gas absorption lookup table . . . . .	51
6.6.1	Introduction . . . . .	51
6.6.2	Lookup table concept . . . . .	52
	Pressure dependence . . . . .	52
	Temperature dependence . . . . .	52
	Trace gas concentration dependence . . . . .	53
	Interpolation . . . . .	53
6.6.3	Workspace variables and methods . . . . .	53
6.6.4	Format of the lookup table . . . . .	54

6.7	Stand-alone gas absorption calculation . . . . .	54
<b>7</b>	<b>Refractive index</b>	<b>57</b>
7.1	Gases . . . . .	58
7.2	Free electrons . . . . .	58
<b>8</b>	<b>Description of clouds</b>	<b>59</b>
8.1	Introduction . . . . .	59
8.2	Single scattering properties . . . . .	59
8.2.1	Coordinate systems . . . . .	59
8.2.2	Scattering datafile structure . . . . .	60
8.2.3	Definition of particle types . . . . .	62
	Macroscopically isotropic and mirror-symmetric scattering media (p20) . . . . .	62
8.3	Particle size distributions . . . . .	64
8.3.1	Mono-disperse particle distribution . . . . .	64
8.3.2	Gamma size distribution . . . . .	64
8.3.3	McFarquhar and Heymsfield parametrization . . . . .	65
8.4	Implementation . . . . .	66
8.4.1	Work space methods and variables . . . . .	66
<b>III</b>	<b>Radiative transfer: clear-sky + general functionality</b>	<b>69</b>
<b>9</b>	<b>Clear-sky radiative transfer</b>	<b>71</b>
9.1	Overall calculation procedure . . . . .	71
9.2	Propagation paths . . . . .	73
9.3	The radiative background . . . . .	73
9.4	Basic radiative transfer variables and expressions . . . . .	75
9.4.1	Unpolarised absorption . . . . .	75
9.4.2	Polarised absorption . . . . .	76
9.4.3	Blackbody and cosmic background radiation . . . . .	77
9.5	Output unit and the $n^2$ -law . . . . .	77
9.6	Single pencil beam calculations . . . . .	78
9.7	Dispersion . . . . .	78
9.8	Auxiliary data . . . . .	79
9.9	Calculation accuracy . . . . .	80
<b>10</b>	<b>Propagation paths</b>	<b>81</b>
10.1	Practical usage . . . . .	81
10.2	Calculation approach . . . . .	82
10.3	Spacing of additional path points . . . . .	83
10.4	Tangent points . . . . .	83
10.5	The propagation path data structure . . . . .	84
10.6	Further reading . . . . .	85

<b>11 Reference ellipsoid and surface properties</b>	<b>87</b>
11.1 The reference ellipsoid . . . . .	87
11.1.1 Ellipsoid models . . . . .	87
11.1.2 Geocentric and geodetic latitudes . . . . .	88
11.2 Surface altitude . . . . .	90
11.3 Surface radiative properties . . . . .	90
11.3.1 Blackbody surface . . . . .	90
11.3.2 Specular reflections . . . . .	90
11.3.3 Lambertian surface . . . . .	91
<b>12 Sensor characteristics</b>	<b>93</b>
12.1 General . . . . .	93
12.2 Some comments . . . . .	94
<b>13 Doppler effects and winds</b>	<b>95</b>
13.1 Winds . . . . .	95
13.2 Planet rotation . . . . .	95
13.3 Sensor velocity . . . . .	96
13.4 Limitations . . . . .	96
13.5 Equations . . . . .	96
<b>14 Faraday rotation</b>	<b>97</b>
14.1 Practical usage . . . . .	97
14.2 Theory . . . . .	97
<b>15 Transmission calculations</b>	<b>99</b>
15.1 Pure transmission calculations . . . . .	99
15.2 Radio link calculations . . . . .	100
15.2.1 Practical usage . . . . .	100
15.2.2 Determination of the radio link path . . . . .	100
15.2.3 Definition of attenuation and loss terms . . . . .	101
15.2.4 Free space loss and sensor characteristics . . . . .	102
15.2.5 Extra path delay . . . . .	103
15.2.6 Bending angle . . . . .	104
15.2.7 Defocusing . . . . .	105
Defocusing, method 1 . . . . .	105
Defocusing, method 2 . . . . .	105
15.2.8 Atmospheric extinction . . . . .	106
<b>16 Clear-sky Jacobians</b>	<b>107</b>
16.1 Introduction . . . . .	108
16.1.1 Perturbations . . . . .	108
16.1.2 Analytical expressions . . . . .	108
16.1.3 Workspace variables and methods . . . . .	108
16.2 Basis functions . . . . .	109
16.2.1 Basis functions for piece-wise linear quantities . . . . .	109
16.2.2 Polynomial basis functions . . . . .	110
16.3 Atmospheric variables, common expressions . . . . .	110
16.3.1 Matrix derivatives . . . . .	110



16.3.2	Separation of terms . . . . .	111
16.3.3	$\partial \mathbf{s} / \partial x_i$ , general case . . . . .	112
16.3.4	Including the surface . . . . .	113
16.3.5	$\partial \mathbf{s} / \partial x_i$ , locally unpolarised absorption . . . . .	113
16.3.6	Limitations . . . . .	113
16.4	Absorption species . . . . .	114
16.4.1	Common practicalities . . . . .	114
16.4.2	Perturbation calculations . . . . .	114
16.4.3	Analytical expressions . . . . .	114
	Unpolarised absorption . . . . .	114
	General case . . . . .	115
16.5	Winds . . . . .	116
16.6	Atmospheric temperatures . . . . .	116
16.6.1	Common practicalities . . . . .	116
16.6.2	Perturbation calculations . . . . .	116
16.6.3	Analytical expressions . . . . .	116
	Unpolarised absorption . . . . .	116
	General case . . . . .	117
	Hydrostatic equilibrium and limitations . . . . .	117
16.7	Sensor pointing . . . . .	118
16.8	Sensor frequencies . . . . .	118
16.9	Polynomial baseline fit . . . . .	119
16.10	Sinusoidal baseline fit . . . . .	119
<b>17</b>	<b>Batch calculations</b> . . . . .	<b>121</b>
17.1	Batch calculations of measurement vector $\mathbf{y}$ . . . . .	121
17.2	Control file examples . . . . .	122
<b>IV</b>	<b>Radiative transfer: dedicated scattering methods</b> . . . . .	<b>123</b>
<b>18</b>	<b>Scattering - DOIT module</b> . . . . .	<b>125</b>
18.1	The discrete ordinate iterative method . . . . .	125
18.1.1	Radiation field . . . . .	125
18.1.2	Vector radiative transfer equation solution . . . . .	126
18.1.3	Scalar radiative transfer equation solution . . . . .	129
18.1.4	Single scattering approximation . . . . .	130
18.2	Sequential update . . . . .	130
18.2.1	Up-looking directions . . . . .	131
18.2.2	Down-looking directions . . . . .	132
18.2.3	Limb directions . . . . .	132
18.3	Numerical Issues . . . . .	133
18.3.1	Grid optimization and interpolation . . . . .	133
	Zenith angle grid optimization . . . . .	133
	Interpolation methods . . . . .	134
	Error estimates . . . . .	135
18.4	Implementation . . . . .	136
18.4.1	1D control file example . . . . .	136

---

18.4.2	DOIT frame . . . . .	136
	The DOIT main agenda . . . . .	138
	Agendas used in <code>doit_i_fieldIterate</code> . . . . .	139
18.4.3	Propagation of the DOIT result towards the sensor . . . . .	141
18.4.4	3D DOIT calculations . . . . .	141
<b>19</b>	<b>Cloud radar simulations</b>	<b>143</b>
19.1	Theory . . . . .	143
19.2	Units . . . . .	144
19.3	Practical usage . . . . .	144
<b>V</b>	<b>Bibliography and Appendices</b>	<b>147</b>
<b>VI</b>	<b>Index</b>	<b>153</b>

**Part I**

**Overview**



# Chapter 1

## Introduction

This section introduces and describes the basic ideas underlying the ARTS program. It also presents some terminology. You should read it if you want to understand how the program works and how it can be used efficiently.

### 1.1 What is ARTS?

The Atmospheric Radiative Transfer Simulator, ARTS, is a software for performing simulations of atmospheric radiative transfer. ARTS is a relatively general and flexible program, where new calculation features can be easily added. Originally, the development of ARTS was initiated to deal with passive mm and sub-mm measurements. The radiation source for such measurements is emission in the atmosphere or by the Earth's surface. Thermal IR radiation is governed by the same basic physical principles and therefore this wavelength region is also well handled in ARTS now. But ARTS contains so far no dedicated methods for scattering of solar radiation and there is therefore a restriction to simulations of long-wave radiation (microwave to thermal IR). However, ARTS can be used for basic studies of lonwave radiation fluxes, as for example in *Buehler et al. [2006]* or *John et al. [2006]*. More lately, some support for handling radio link calculations have been added.

One main application of ARTS should be to perform retrievals for remote sensing data. A special feature of ARTS in this context is its high flexibility when defining observation geometry (including scanning features) and sensor characteristics. Jacobians (weighting functions) are also provided.

There exist two versions of ARTS. This user guide deals with the later of the two versions [*Eriksson et al., 2011*], here denoted as just ARTS. ARTS-1, the first version of ARTS [*Buehler et al., 2005*], can only handle 1D atmospheres with unpolarised radiation and situations where scattering can be neglected. These restrictions have been removed in the current version. A short summary of ARTS's main features is:

**The atmosphere** can be 1D, 2D or 3D. That is, atmospheric variables (temperature, gas concentrations etc.) can be assumed to only vary in the vertical dimension (1D), to

---

#### History

- 110505 Complete revision by Stefan Buehler. Also integrated text from ARTS2 article first submission.
- 2002-10 Written, mainly by Stefan Buehler, some parts by Patrick Eriksson.

have no longitude variation (2D) or vary in all three spatial dimensions (3D).

**The surface** is by default assumed to be spherical. For 2D and 3D, a complete reference ellipsoid is used and the surface can have arbitrary shape.

**Polarisation** is fully described by using the Stokes formalism.

**Scattering** can be considered in several manners. Extinction from scatterers can be included in transmission type calculations. For radiance calculations of thermal emission (in contrast to solar radiation) there are two modules at hand to take the scattering into account: DOIT (Section 18) and MC (*ARTS Theory*, Section 8). The scattering particles are for efficiency reasons confined to a region of the atmosphere denoted as the cloudbox.

**Observation geometry** is free. That is, the forward model can be used to simulate ground-based, down-looking, limb sounding and balloon/aircraft measurements.

**Sensor characteristics** can be incorporated in a flexible and efficient manner.

**Jacobians**, the partial derivatives of simulated measurement with respect to forward model variables, can be provided for a number of variables, where analytical expressions are used as far as possible.

Details are found in later parts of the user guide. Use the table of contents and the index for navigating through the user guide.

## 1.2 Documentation

We know that the ARTS documentation is far from perfect. It is quite complete in some areas, but patchy in others. It also contains bugs and more serious errors. We are struggling to make it as good as possible, but it is ongoing work, and we do not have any direct funding for it. All help from users to extend or correct the documentation is highly appreciated! Having said that, the documentation that already is available for ARTS is described in the following subsections.

### 1.2.1 Guide documents

**ARTS User Guide:** This document.

**ARTS Developer Guide:** Guide for ARTS developers.

**ARTS Theory:** Describes the theoretical basis for some parts of ARTS.

### 1.2.2 Articles

*Buehler et al.* [2005]: General description of the old ARTS version without scattering. Many basic features are still the same, so this article is relevant also for the current ARTS version.

*Eriksson et al.* [2011]: Introduction and overview to ARTS-2.

*Emde et al. [2004]*: Describes the Discrete Ordinate Iterative method (DOIT) for handling scattering.

*Davis et al. [2005]*: Describes the Monte Carlo scattering method.

*Eriksson et al. [2006]*: Describes the calculation approach for the incorporation of sensor characteristics.

*Buehler et al. [2010]*: Describes a method to efficiently handle broadband infrared channels, that is implemented in ARTS.

*Buehler et al. [2011]*: Describes the absorption look-up table approach used inside ARTS.

### 1.2.3 Built-in documentation

ARTS contains built-in documentation for all functions and variables that are directly visible to the user (in ARTS terminology called workspace functions and workspace variables; they are explained in more depth further below). The easiest way to access this documentation is on the web page <http://www.radiativetransfer.org/docserver-stable/>. Alternatively, start ARTS with

```
arts -s
```

or

```
arts --docserver
```

and then point your browser to <http://localhost:9000/>.

This user guide also contains links to the built-in documentation. If you are reading the pdf file on a computer, then names of ARTS objects, such as `f.grid`, will be links to the corresponding entries in the built-in documentation.

### 1.2.4 Test and include controlfiles

ARTS calculations are governed by controlfiles (see below). The ARTS distribution already comes with a large number of controlfiles, which fall into two categories: includes and tests. They are described in more detail below, but already mentioned here as an important source of information for new users. In particular, ARTS already comes with controlfiles to simulate some well-known instruments, such as for example MHS or HIRS.

**FIXME: Control file structure changed, update this section!**

### 1.2.5 Source code documentation

All internal ARTS functions are documented with DOXYGEN at the source code level. This documentation is intended mostly for those who want to do ARTS development work. It can be accessed at <http://www.radiativetransfer.org/misc/arts-doc/doxygen/html/>.

### 1.2.6 Build instructions

Instructions on how to configure and compile the ARTS source code can be found in the file README in the top directory of the ARTS distribution.

```

Arts2 {                               arts-1.14.122
StringCreate(s)                       Executing Arts
StringSet(s,                           {
    "Hello World")                    - StringCreate
Print(s)                                - StringSet
}                                        - Print
                                       Hello World
                                       }
                                       This run took 0.03s (0.03s CPU time)
                                       Everything seems fine. Goodbye.

```

Figure 1.1: Left: A minimal ARTS controlfile example. Right: ARTS output when running this controlfile.

### 1.2.7 Command line parameters

ARTS offers a number of useful command line parameters. In general, there is a short form and a long form for each parameter. The short form consists of a minus sign and a single letter, whereas the long form consists of two minus signs and a descriptive name. To get a full list of available command line parameters, type

```
arts -h
```

or

```
arts --help
```

## 1.3 ARTS as a scripting language

One of the main goals in the ARTS development was to make the program as flexible as possible, so that it can be used for a wide range of applications and new features can be added in a relatively simple manner. As a result, ARTS behaves like a scripting language. An ARTS controlfile contains a sequence of instructions. When ARTS is executed, the controlfile is parsed, and then the instructions are executed sequentially. Controlfile `somefile.arts` is executed by running

```
arts somefile.arts
```

A minimal ARTS controlfile example (the well-known ‘Hello World’ program) is given in Figure 1.1. In this example, the variable `s` is called a *workspace variable*. We use this name to distinguish it from the variables that appear internally in the ARTS source code.

In a similar spirit, the functions `StringCreate`, `StringSet`, and `Print` in the example are called *workspace methods*. We use this name to distinguish them from the functions that appear internally in the ARTS source code. For brevity, we may sometimes drop the workspace qualifier and refer to them just as methods.

ARTS consists roughly of three parts. Firstly, the ARTS core contains the controlfile parser, and the engine that executes the controlfile. This part is quite compact and constitutes only a small fraction of the total source code. Secondly, there is a large collection of workspace methods that can be used to carry out various sub-tasks (at the time of writing approximately 300). Thirdly, there is a large number of predefined workspace variables (at the time of writing more than 200). These predefined variables make it easier to set up controlfiles, since they provide hints on how the different workspace methods fit together.



```

*-----*
Workspace variable = f_grid
-----
The frequency grid for monochromatic pencil beam
calculations.

Usage: Set by the user.

Unit: Hz
-----
Group = Vector
*-----*

```

Figure 1.2: Built-in documentation for variable `f_grid`, obtained by command `'arts -d f_grid'`, or on page [http://www.radiativetransfer.org/docserver-stable/variables/f\\_grid](http://www.radiativetransfer.org/docserver-stable/variables/f_grid).

ARTS has built-in documentation for all workspace methods and variables, which can be accessed as described in Section 1.2.3. In this user guide, just clicking on the name of a variable or method will take you directly to the built-in documentation for that object. Below, we will discuss workspace variables and methods in some more detail and give more examples.

### 1.3.1 Workspace variables

Workspace variables (such as the variable `s` in Figure 1.1) are the variables that are manipulated by the workspace methods during the execution of an ARTS controlfile. Workspace variables belong to different *groups* (Index, String, Vector, Matrix, etc.). The built-in documentation lists all groups, at the time of writing there are approximately 60 of them.

As the example in Figure 1.1 shows, workspace variables can be freely created by the user with methods like `StringCreate`, `VectorCreate`, and so on. Each group has its own create method.

However, in most cases it is not necessary to create new variables in this way, since a lot of variables are predefined in ARTS. The built-in documentation describes all predefined variables. As an example, Figure 1.2 shows the description for the variable `f_grid`, which stores the frequency grid and is used as input by many workspace methods, for example those that calculate absorption coefficients. The built-in documentation also lists all methods that take `f_grid` as input and all methods that produce `f_grid` as output.

### 1.3.2 Workspace methods

As shown in Figure 1.1, names of workspace methods in an ARTS controlfile are followed by their output and input arguments (workspace variables) in parentheses. (`'Print(s)'` prints the content of variable `s`.)

From the methods point of view, arguments can be *output*, *input*, or both, and additionally they can be either *specific* (= referring to a predefined variable) or *generic* (= not referring to a predefined variable). To illustrate this, Figure 1.3 shows the built-in documentation for method `WriteXML`, the most common method to write ARTS variables to a file. The list at the bottom of the documentation shows that `output_file_format` is a specific input argument, and that `v` and `filename` are generic input arguments.

```

*-----*
Workspace method = WriteXML
-----
Writes a workspace variable to an XML file.

This method can write variables of any group.

If the filename is omitted, the variable is written
to <basename>.<variable_name>.xml.

Synopsis:

WriteXML( output_file_format, v, filename )

Authors: Oliver Lemke

Variables:

IN    output_file_format (String): Output file format.
GIN   v (Any): Variable to be saved.
GIN   filename (String, Default: ""): Name of the XML file.
*-----*

```

Figure 1.3: Built-in documentation for method `WriteXML`, obtained by command ‘`arts -d WriteXML`’, or on page <http://www.radiativetransfer.org/docserver-stable/methods/WriteXML>.

What this means is that `output_file_format` already automatically exists as a variable, whereas `v` and `filename` do not. The built-in documentation provides descriptions also of these generic arguments and lists the allowed values.

The predefined variables, combined with specific method arguments, are meant to help in combining methods into meaningful calculations. Predefined variables are typically relevant for more than one method. For example, variable `output_file_format` can be used to change the format of all produced files at the same time. However, the use of a specific variable in the controlfile is not mandatory, so ‘`WriteXML( output_file_format, v, "test.xml" )`’, ‘`WriteXML( "ascii", v, "test.xml" )`’, and ‘`WriteXML( my_format, v, "test.xml" )`’ are all allowed. (But in the last example the variable `my_format` must have been defined before.)

Besides the variable names, the built-in documentation also lists the allowed variable groups (or types). In the example, the groups for workspace variable `v` are ‘Any’, which means that `v` can belong to any of the known groups. The group for `filename` is ‘String’, which means that a string is expected here. Method arguments can be a literal, as in ‘`WriteXML( "ascii", v, "test.xml" )`’, or a variable, as in ‘`WriteXML( "ascii", v, s )`’, where in the latter case variable `s` must be already defined.

The built-in documentation further states that argument `filename` has a default value (in this case the empty string). Because of this, the argument can actually be omitted, so ‘`WriteXML( "ascii", v )`’ will also work.

Alternatively, workspace methods can be called with named arguments. All omitted arguments will be set to their default values. `WriteXML( in=v )` is equivalent to calling `WriteXML( output_file_format, v )`. Note that named arguments can not be

```

*-----*
Workspace variable = propmat_clearsky_agenda
-----*

This agenda calculates absorption coefficients for all gas species
as a function of the given atmospheric state for one point in the
atmosphere. The result is returned in *propmat_clearsky*, the
atmospheric state has to be specified by *rtp_pressure*,
*rtp_temperature*, *rtp_mag*, and *rtp_vmr*.

The methods inside this agenda may require a lot of additional
input variables, such as *f_grid*, *species*, etc.
-----*

Group   = Agenda
Output  = propmat_clearsky
Input   = f_grid, rtp_doppler, rtp_mag, rtp_pressure,
         rtp_temperature, rtp_vmr
*-----*

AgendaSet (                               AgendaSet (
propmat_clearsky_agenda)                   propmat_clearsky_agenda)
{                                           {
  propmat_clearskyInit                     Ignore(rtp_mag)
  propmat_clearskyAddOnTheFly               propmat_clearskyInit
  propmat_clearskyAddZeeman                 propmat_clearskyAddFromLookup
}                                           }

```

Figure 1.4: Top: Built-in documentation for variable `propmat_clearsky_agenda`, obtained by command `'arts -d propmat_clearsky_agenda'`, or on page [http://www.radiativetransfer.org/docserver-stable/agendas/propmat\\_clearsky\\_agenda](http://www.radiativetransfer.org/docserver-stable/agendas/propmat_clearsky_agenda). Bottom left: Controlfile agenda definition for line-by-line absorption calculation. Bottom right: Controlfile agenda definition to extract absorption from a pre-calculated lookup table.

mixed with positional arguments.

One additional rule has to be mentioned here. If all arguments to a method are specific, and the user wants to use all the predefined variables, then the entire argument list (including parentheses) may be omitted.

### 1.3.3 Agendas

Agendas are a special group of workspace variables, which allow to modify how a calculation is performed. A variable of group agenda holds a list of workspace method calls. It can be executed, which means that the method calls it contains are executed one after another.

Figure 1.4 gives an example, for the agenda `propmat_clearsky_agenda`. Several radiative transfer methods use this agenda as input variable. When they need local absorption coefficients for a point in the atmosphere, they execute the agenda with the local pressure, temperature, and trace gas volume mixing ratio values as inputs. The agenda then provides absorption coefficients as output.

The bottom of Figure 1.4 shows two different ways how this agenda could be defined in the controlfile. In the first case a line-by-line absorption calculation is performed when the agenda is executed (every time absorption coefficients are needed). In the second case the

absorption coefficients are extracted from a pre-calculated lookup table.

On invocation, an agenda executes its methods one after the other. The inputs and outputs defined for the agenda must be satisfied by the invoked workspace methods. E.g., if an agenda has `propmat.clearsky` in its list of output workspace variables, at least one workspace method which generates `propmat.clearsky` must be added to the agenda in the controlfile.

## 1.4 Include controlfiles

ARTS controlfiles can *include* other ARTS controlfiles, which is achieved by statements such as `INCLUDE "general.arts"`. This mechanism is used to predefine general default settings, settings for typical applications, and/or settings for the simulation of well-known instruments. A variety of include controlfiles are collected in directory `controlfiles` of the ARTS distribution.

You should normally at least include the file `general.arts`, which contains general default settings. Because giving the full path for every include file is inconvenient, ARTS will look for include files in a special directory. This can be set by the command line option `-I <includepath>`, or by the environment variable `ARTS_INCLUDE_PATH`. If none of these are set, ARTS will assume the include path to point to the `includes` directory in the ARTS distribution. The file `agendas.arts` is also useful, because it predefines agendas with settings suitable for many applications. **FIXME: Revise this section after `general.arts` has been changed.**

## 1.5 Test controlfiles

The directory `controlfiles` in the ARTS distribution contains some test and example controlfiles. You should study them to learn more about how the program works. You can run these controlfiles like this:

```
arts TestAbs.arts
```

This assumes that you are in the directory where the control file resides, and that the `arts` executable is in your path.

Alternatively, you can run a standard set of the test controlfiles by going to the build directory, and say

```
make check
```

This standard set of test is run by us on every automatic build, that means every time a new ARTS version is submitted to the subversion repository. If your ARTS installation is healthy, `make check` should run through without any errors. (See file `README` in the ARTS distribution for detailed instructions on how to build ARTS.)

**FIXME: The tests are now structured differently. Update the text.**

## 1.6 Verbosity levels

The command line parameter

```
arts -r
```

or

```
arts --reporting
```

can be used to set how much output ARTS produces. You can supply a three-digit integer here. Each digit can have a value between 0 and 3.

The last digit determines, how verbose ARTS is in its report file. If it is 0, the report file will be empty, if it is 3 it will be longest.

The middle digit determines, how verbose ARTS is on the screen (stdout). The meaning of the values is exactly as for the report file.

The first digit is special. It determines how much you will see of the output of agendas (other than the main program agenda). Normally, you do not want to see this output, since many agendas are called over and over again in a normal program run.

The agenda verbosity applies in addition to the screen or file verbosity. For example, if you set the reporting level to '123', you will get:

- From the main agenda: Level 1-2 outputs to the screen, and level 1-3 outputs to the report file.
- From all other agendas: Only level 1 outputs to both screen and report file.

As another example, if you set the reporting level to '120' the report file will be empty.

The default setting for ARTS (if you do not use the command line flag) is '010', i.e., only the important messages to the screen, nothing to the report file, and no sub-agenda output.



# Chapter 2

## Importing and exporting data

Sorry, so far just a few words about supported data formats.

**FIXME: Extend this chapter.**

### 2.1 Data formats

#### 2.1.1 XML files

XML is the default file format for exchanging data with ARTS. Two flavors are supported: Plain text and binary. In the plain format all data is stored in the XML file. For binary, the structure of the data is stored in the XML file and the data itself in binary format in a separate file.

#### 2.1.2 NetCDF files

NetCDF input and output is supported for a subset of the data types available in ARTS.

#### 2.1.3 Gridded fields

##### Naming convention for grids

```
% Grid names for GriddedField variables.  
% Keep the description short and on one line.  
% Sort alphabetically.
```

Complex	Complex number "grid" (i.e. exactly 2 elements: real and imaginary)
Frequency	Frequency dimension for spectral dependent fields.
Latitude	Latitude dimension for atmospheric fields (z, T, VMRs, winds, Ne, B, pnd)
Longitude	Longitude dimension for atmospheric fields (z, T, VMRs, winds, Ne, B, pnd)
Pressure	Pressure dimension for atmospheric fields (z, T, VMRs, winds, Ne, B, pnd)

---

#### History

? ?.

```
% Data field names
% mere suggestions and not tested anywhere in ARTS
Temperature      Temperature field
VMR              Volume mixing ratio field
Altitude         Altitude/height field
pnd_field        Particle number density field
```



## Chapter 3

# Description of the atmosphere

This section discusses the model atmosphere: how it is defined, its boundaries and the variables describing the basic properties. One aspect that can cause confusion is that several vertical coordinates must be used (Sec. 3.1). The main vertical coordinate is pressure and atmospheric quantities are defined as a function of pressure (Sec. 3.3), but the effective vertical coordinate from a geometrical perspective (such as the determination of propagation paths) is the radius (Sec. 3.2). Pressures and radii are linked by specifying the geometrical altitudes (`z_field`).

### 3.1 Altitude coordinates

**Pressure** The main altitude coordinate is pressure. This is most clearly manifested by the fact that the vertical atmospheric grid consists of equal-pressure levels. The vertical grid is accordingly denoted as the pressure grid and the corresponding workspace variable is `p_grid`. The choice of having pressure as main altitude coordinate results in that atmospheric quantities are retrieved as a function of pressure.

**Pressure altitude** A basic assumption in ARTS is that atmospheric quantities (temperature, geometric altitude, species VMR etc.) vary linearly with the logarithm of the pressure. This corresponds roughly to assuming a linear variation with altitude.

**Radius** Geometrical altitudes are needed to determine the propagation path through the atmosphere etc. The main geometrical altitude coordinate is the distance to the centre of the coordinate system used, the radius. This is a natural consequence of using a spherical or polar coordinate system. The radius is used inside ARTS for all geometrical calculations.

**Geometrical altitude** The term geometrical altitude signifies here the difference in radius between a point and the reference ellipsoid (Sec. 11.1) along the vector to the centre of the coordinate system (Equation 11.6). This is consistent with the usage of geocentric latitudes (see below). Hence, the altitude is not measured along the local zenith direction.

---

#### History

130219 Revised by Patrick Eriksson.

020315 First version by Patrick Eriksson.

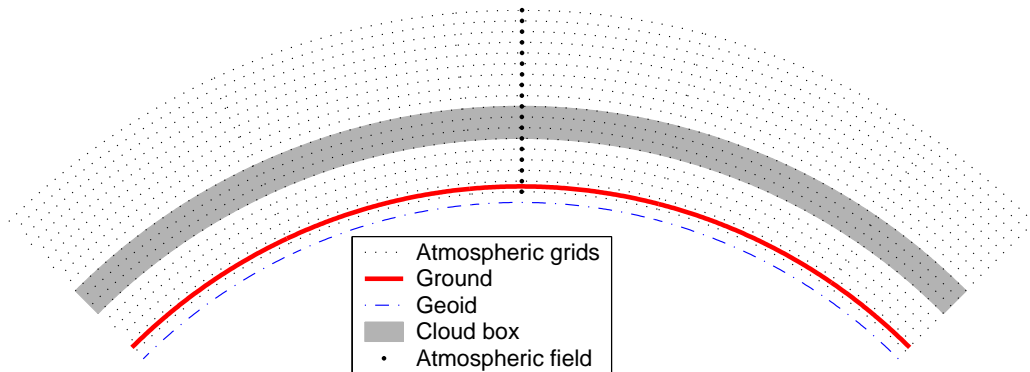


Figure 3.1: Schematic of a 1D atmosphere. The atmosphere is here spherically symmetric. This means that the radius of the ellipsoid, the surface and all the pressure levels are constant around the globe. The fields are specified by a value for each pressure level. The extension of the cloud box is either from the surface up to a pressure level, or between two pressure levels (which is the case shown in the figure). The figure indicates also that the surface must be above the lowermost pressure level. (“Geoid” in the legend should be “Ellipsoid”).

## 3.2 Atmospheric dimensionality

The structure of the modelled atmosphere can be selected to have different degree of complexity, the atmospheric dimensionality. There exist three options, 1D, 2D and 3D, where 1D and 2D can be seen as special cases of 3D. The significance of these different atmospheric dimensionalities and the geometrical coordinate systems used are described below in this section. The atmospheric dimensionality is selected by setting the workspace variable `atmosphere_dim` to a value between 1 and 3. The atmospheric dimensionality is most easily set by the functions `AtmosphereSet1D`, `AtmosphereSet2D` and `AtmosphereSet3D`.

**1D** A 1D atmosphere can be described as being spherically symmetric. The term 1D is used here for simplicity and historical reasons, not because it is a true 1D case (a strictly 1D atmosphere would just extend along a line). A spherical symmetry means that atmospheric fields and the surface extend in all three dimensions, but they have no latitude and longitude variation. This means that, for example, atmospheric fields vary only as a function of altitude and the surface constitutes the surface of a sphere. The radial coordinate is accordingly sufficient when dealing with atmospheric quantities. The latitude and longitude of the sensor are normally of no concern, but when required the sensor is considered to be placed at latitude and longitude zero ( $[\alpha, \beta] = [0, 0]$ ). The sensor is assumed to be directed towards the North pole, corresponding to an azimuth angle of  $0^\circ$ . A 1D atmosphere is shown in Figure 3.1.

**2D** In contrast to the 1D and 3D cases, a 2D atmosphere is only strictly defined inside a plane. More in detail, this case be seen as observations restricted to the plane where the longitude equals  $0^\circ$  or  $180^\circ$ . A polar system, consisting of a radial and an angular coordinate, is applied. The angular coordinate is denoted as latitude, and matches the 3D latitude in the range  $[-90^\circ, +90^\circ]$ , but for 2D there is no lower or upper limit for the latitude coordinate. The 2D case is most likely used for satellite measurements where the atmosphere is observed inside the orbit plane. The 2D “latitude” can then

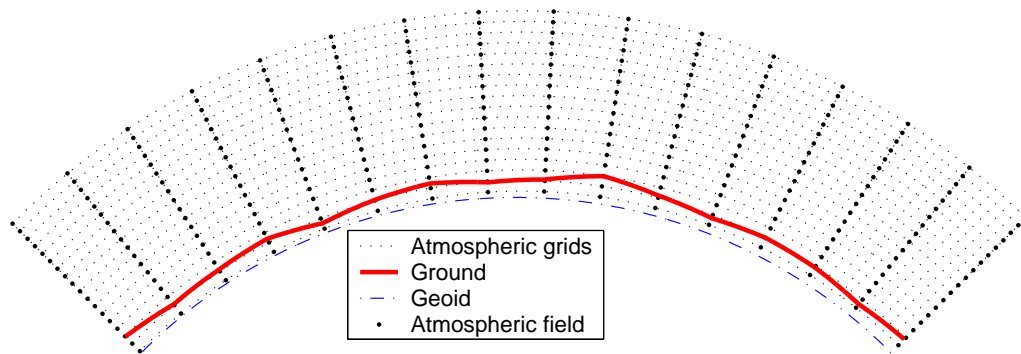


Figure 3.2: Schematic of a 2D atmosphere. The radii (for the surface and the pressure levels) vary here linear between the latitude grid points. The atmospheric fields vary linearly along the pressure levels and the latitude grid points (that is, along the dotted lines). Inside the grid cells, the fields have a bi-linear variation. No cloud box is included in this figure. (“Geoid” in the legend should be “Ellipsoid”.)

be taken as the angular distance along the satellite track. A 2D-latitude of e.g.  $100^\circ$  will then correspond to a 3D-latitude of  $80^\circ$ . The atmosphere is normally treated to be undefined outside the considered plane, but some scattering calculations may treat the surrounding atmosphere in an simplified manner. A 2D atmosphere is shown in Figure 3.2.

**3D** In this, the most general, case, the atmospheric fields vary in all three spatial coordinates, as in a true atmosphere (Figures 3.3). A spherical coordinate system is used where the dimensions are radius ( $r$ ), latitude ( $\alpha$ ) and longitude ( $\beta$ ), and a position is given as  $(r, \alpha, \beta)$ . With other words, the standard way to specify a geographical position is followed. The valid range for latitudes is  $[-90^\circ, +90^\circ]$ , where  $+90^\circ$  corresponds to the North pole etc. Longitudes are counted from the Greenwich meridian with positive values towards the east. Longitudes can have values from  $-360^\circ$  to  $+360^\circ$ . When the difference between the last and first value of the longitude grid is  $360^\circ$  then the whole globe is considered to be covered. The user must ensure that the atmospheric fields for  $\beta$  and  $\beta + 360^\circ$  are equal. If a point of propagation path is found to be outside the range of the longitude grid, this will result in an error if not the whole globe is covered. When possible, the longitude is shifted with  $360^\circ$  in the relevant direction.

### 3.3 Atmospheric grids and fields

As mentioned above, the vertical grid of the atmosphere consists of a set of layers with equal pressure, the pressure grid (**p\_grid**). This grid must of course always be specified. The upper end of the pressure grid gives the practical upper limit of the atmosphere as vacuum is assumed above. With other words, no absorption and refraction take place above the uppermost pressure level.

A latitude grid (**lat\_grid**) must be specified for 2D and 3D. For 2D, the latitudes shall be treated as the angular distance along the orbit track, as described above in Section 3.2. The

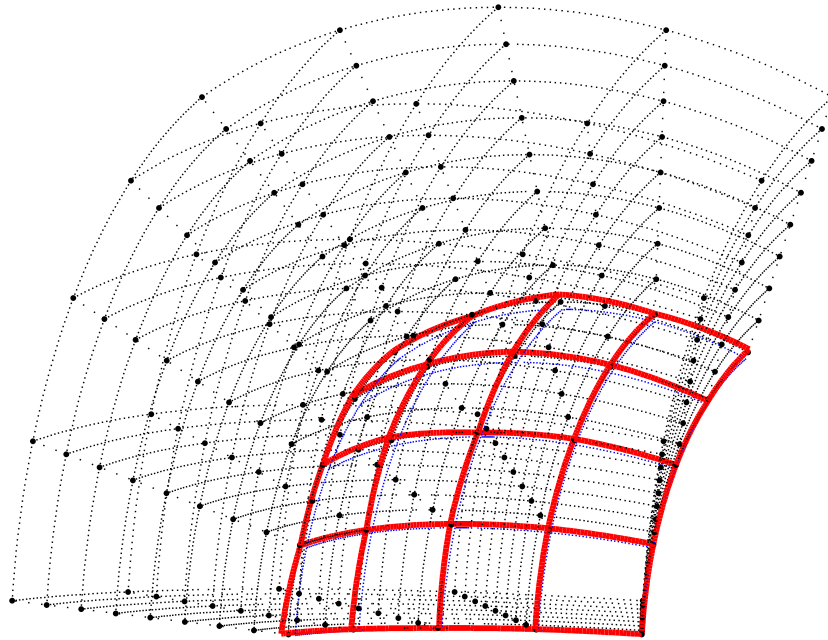


Figure 3.3: Schematic of a 3D atmosphere. Plotting symbols as in Figure 3.2. Radii and fields are here defined to vary linearly along the latitude and longitude grid points. This means that the radius of a pressure level has a bi-linear variation inside the area limited by two latitude and longitude grid values, while the atmospheric fields have a tri-linear variation inside the grid cells.

latitude angle is throughout calculated for the vector going from the centre of the coordinate system to the point of concern. Hence, the latitudes here correspond to the definition of the geocentric latitude, and not geodetic latitudes (Sec. 11.1.1). This is in accordance to the definition of geometric altitudes (Sec. 3.1). For 3D, a longitude grid (`lon_grid`) must also be specified. Valid ranges for latitude and longitude values are given in Section 3.2. If the longitude and latitude grids are not used for the selected atmospheric dimensionality, then the longitude grid (for 1D and 2D) and the latitude grid (for 1D) must be set to be empty.

The atmosphere is treated to be undefined outside the latitude and longitude ranges covered by the grids, if not the whole globe is covered. This results in that a propagation path is not allowed to cross a latitude or longitude end face of the atmosphere, if such exists, it can only enter or leave the atmosphere through the top of the atmosphere (the uppermost pressure level). See further Section 9.2. The volume covered by the grids is denoted as the model atmosphere.

The basic atmospheric quantities are represented by their values at each crossing of the involved grids (indicated by thick dots in Figure 3.2), or for 1D at each pressure level (thick dots in Figure 3.1). This representation is denoted as the field of the quantity. The field must, at least, be specified for the geometric altitude of the pressure levels (`z_field`), the temperature (`t_field`) and considered atmospheric species (`vmr_field`). The content and units of `vmr_field` are discussed in Section 4.2.2.

All the fields are assumed to be piece-wise linear functions vertically (with pressure altitude as the vertical coordinate), and along the latitude and longitude edges of 2D and 3D grid boxes. For points inside 2D and 3D grid boxes, multidimensional linear interpolation is applied (that is, bi-linear interpolation for 2D etc.). Note especially that this is also valid for the field of geometrical altitudes (`z_field`). Fields are rank-3 tensors. For example, the temperature field is  $T = T(P, \alpha, \beta)$ . That means each field is like a book, with one page for each pressure grid point, one row for each latitude grid point, and one column for each longitude grid point. In the 1D case there is just one row and one column on each page. The representation of atmospheric fields, and other quantities, is discussed further in Section 16.2, where the concept of basis functions is introduced. In short, the basis functions give the mapping from the set of discrete values to the continuous representation of the quantity.

### 3.4 Geo-location of 1D and 2D

For 1D and 2D atmospheres, `lat_grid` and `lon_grid` do not contain true geographical positions (they are either empty or `lat_grid` contains transformed data). However, some operations require that the positions is known, and this is handled by `lat_true` and `lon_true`. See the built-in documentation for further information on how to specify these variables.

### 3.5 Hydrostatic equilibrium

There is no general demand that the model atmosphere fulfils hydrostatic equilibrium. That is, `t_field` and `z_field` can be specified independently of each other. On the other hand, ARTS provides means for ensuring that a model atmosphere matches hydrostatic equilibrium by the method `z_fieldFromHSE`. The method considers that gravitation varies with latitude and altitude, and `lat_true` and `lon_true` must be set for 1D and 2D.

Hydrostatic equilibrium gives only constrain for the distance between the pressure levels, not for the absolute geometrical altitudes. For this reason, a “reference point” must be introduced. This is done by setting the pressure of this point by `p_hse` (common for all latitude and longitudes). The geometrical altitudes matching `p_hse` are taken from the original values in `z_field`.

### 3.6 The reference ellipsoid and the surface

Geometrical altitudes are specified as the vertical distance to the reference ellipsoid (`refellipsoid`), discussed further in Section 11.1. The lower boundary of the atmosphere is denoted as the surface. The surface is specified by its geometrical altitude on the latitude and longitude grids. The workspace variable holding these data is called `z_surface`.

It is not allowed that there is an altitude gap between the surface and the lowermost pressure level. That is, the surface pressure must be smaller than the pressure of the lowermost vertical grid level. On the other hand, it is not necessary to match the surface and the first pressure level, the pressure grid can extend below the surface level.

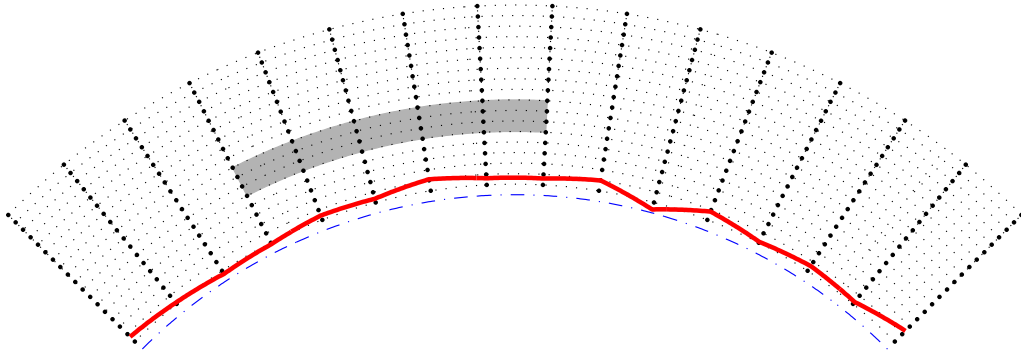


Figure 3.4: A latitudinal, or longitudinal, cross section of a 3D atmosphere. Plotting symbols as in Figure 3.1. Radii and fields inside the cross section match the definitions for 2D. The vertical extension of the cloud box is defined identical for 1D and 3D. The horizontal extension of the cloud box is between two latitude and longitude grid positions, where only one of the dimensions is visible in this figure.

### 3.7 The cloud box

In order to save computational time, calculations involving scattering are limited to a special atmospheric domain. This atmospheric region is denoted as the cloud box. The distribution of scattering matter inside the cloud box is specified by `pnd_field`, see further Section 4.2.2.

The cloud box is defined to be rectangular in the used coordinate system, with limits exactly at points of the involved grids. This means, for example, that the vertical limits of the cloud box are two pressure levels. For 3D, the horizontal extension of the cloud box is between two points of the latitude grid and likewise in the longitude direction (Fig. 3.4). The latitude and longitude limits for the cloud box cannot be placed at the end points of the corresponding grid as it must be possible to calculate the incoming intensity field. The cloud box is activated by setting the variable `cloudbox_on` to 1. The limits of the cloud box are stored in `cloudbox_limits`. It is recommended to use the method `cloudboxOff` when no scattering calculations shall be performed. This method assigns dummy values to all workspace variables not needed when scattering is neglected.

When the radiation entering the cloud box is calculated this is done with the cloud box turned off. This to avoid to end up in the situation that the radiation entering the cloud box depends on the radiation coming out from the cloud box. **It is the task of the user to define the cloud box in such way that the link between the outgoing and ingoing radiation fields of the cloud box can be neglected.** The main point to consider here is radiation reflected by the surface. To be formally correct there should never be a gap between the surface and the cloud box. This is the case as radiation leaving the cloud box can then be reflected back into the cloud box by the surface. If it is considered that the surface is a scattering object it is clear that the surface should in general be part of the cloud box. However, for many cases it can be accepted to have a gap between the surface and the cloud box, with the gain that the cloud box can be made smaller. Such a case is when the surface is treated to act as blackbody, the surface is then not reflecting any radiation. Reflections from the surface can also be neglected if the zenith optical thickness of the atmosphere between the surface and cloud box is sufficiently high.

### 3.8 Wind and magnetic vector fields

The atmospheric fields discussed above are scalar quantities, while some atmospheric variables can be seen as vector fields. However, in ARTS input vector fields are broken down into the zonal, meridional and vertical components and are given as three scalar fields. This division into scalar values is used to allow that one or several of the components easily can be set to zero, which is done by setting the corresponding workspace variable to be empty. Following the standard naming scheme for winds, the components are denoted as

**u** The zonal component. A positive value signifies an Eastward direction.

**v** The meridional component. A positive value signifies a Northward direction.

**w** The vertical component. A positive value signifies an upward direction.

The workspace variables to describe the wind vector field are `wind_u_field`, `wind_v_field` and `wind_w_field`. To clarify the definition of the vector components above, the wind components are defined as follows

$v_u$  A positive wind is defined as air moving from west to east, i.e. towards higher longitudes.

$v_v$  A positive wind is defined as air moving from south to north, i.e. towards higher latitudes.

$v_w$  A positive wind is defined as air moving upwards, i.e. towards higher altitudes.

As described above, one, two or all of these variables can be set to be empty, if the corresponding wind component is zero. Winds affect the radiative transfer by inducing Doppler shifts, see further Chapter 13.

To consider Faraday rotation (Sec. 14) and Zeeman splitting (*ARTS Theory*, Sec. ??), also the magnetic field must be specified. The three component fields are `mag_u_field`, `mag_v_field` and `mag_w_field`. All three components must be specified (but can be set to zero for a part of, or the complete, atmosphere). However, some component can be irrelevant for the calculations. For example, the u-component has no influence on Faraday rotation for 1D and 2D cases. (The internal representation of the magnetic field at a specific point is handled by `rtp_mag`. For this variable the three components are stored together, and thus the local magnetic field is represented as a vector.)





## Chapter 4

# Radiative transfer basics

This chapter introduces some basic radiative transfer nomenclature and equations. The radiative transfer equation is here presented in general terms, while special cases and solutions are discussed in later parts of the document.

### 4.1 Stokes dimensionality

The full polarisation state of radiation can be described by the Stokes vector, and is the formalism applied in ARTS. The vector can be defined in different ways, but it has always four elements. The Stokes vector,  $\mathbf{s}$ , is here written as

$$\mathbf{s} = \begin{bmatrix} I \\ Q \\ U \\ V \end{bmatrix}, \quad (4.1)$$

where the first component ( $I$ ) is the full intensity of the radiation, the second component ( $Q$ ) is the difference between vertical and horizontal polarisation, the third component ( $U$ ) is the difference for  $\pm 45^\circ$  polarisation and the last component ( $V$ ) is the difference between left and right circular polarisation. That is:

$$I = I_v + I_h = I_{+45^\circ} + I_{-45^\circ} = I_{lhc} + I_{rhc}, \quad (4.2)$$

$$Q = I_v - I_h, \quad (4.3)$$

$$U = I_{+45^\circ} - I_{-45^\circ}, \quad (4.4)$$

$$V = I_{lhc} - I_{rhc}, \quad (4.5)$$

where  $I_v$ ,  $I_h$ ,  $I_{+45^\circ}$ , and  $I_{-45^\circ}$  are the intensity of the component linearly polarised at the vertical, horizontal,  $+45^\circ$  and  $-45^\circ$  direction, respectively, and  $I_{rhc}$ , and  $I_{lhc}$  are the intensity for the right- and left-hand circular components. Further details on polarisation and the definition of the Stokes vector are found in *ARTS Theory*, Section 5.

ARTS is a fully polarised forward model, but can be run with a smaller number of Stokes components. The selection is made with the workspace variable `stokes_dim`. For example, gaseous absorption and emission are in general unpolarised, and if not particle

---

#### History

130218 First version by Patrick Eriksson.

and surface scattering have to be considered it is sufficient to only include the first Stokes components in the simulations (ie. `stokes_dim` set to 1). In this case, to include higher order Stokes components results only in slower calculations. Simulations where `stokes_dim` is two or higher are denoted as vector radiative transfer, while scalar radiative transfer refers to the case when only the first Stokes component is considered.

## 4.2 The radiative transfer equation

The radiative transfer problem can only be expressed in a general manner as a differential equation. One version for vector radiative transfer is

$$\frac{ds(\nu, \mathbf{r}, \hat{\mathbf{n}})}{dl} = -\mathbf{K}(\nu, \mathbf{r}, \hat{\mathbf{n}})\mathbf{s}(\nu, \mathbf{r}, \hat{\mathbf{n}}) + \mathbf{j}_e(\nu, \mathbf{r}, \hat{\mathbf{n}}) + \mathbf{j}_s(\nu, \mathbf{r}, \hat{\mathbf{n}}), \quad (4.6)$$

where  $\nu$  is frequency,  $\mathbf{r}$  represents the atmospheric position,  $\hat{\mathbf{n}}$  is the propagation direction (at  $\mathbf{r}$ ),  $l$  is distance along  $\hat{\mathbf{n}}$ ,  $\mathbf{K}$  is the propagation matrix,  $\mathbf{j}_e$  represents the emission at the point, and  $\mathbf{j}_s$  covers the scattering from other directions into the propagation direction.

### 4.2.1 Propagation effects

Three mechanisms contribute to the elements of the propagation matrix: absorption, scattering and magneto-optical effects. Absorption and scattering can together be denoted as extinction, referring to that these two mechanisms result in a decrease of the intensity ( $I$ ). A common name for  $\mathbf{K}$  is also the extinction matrix. The extinction processes also affect the  $Q$ ,  $U$  and  $V$  elements of the Stokes vector. If the degree of polarisation ( $p$ )

$$p = \frac{\sqrt{Q^2 + U^2 + V^2}}{I} \quad (4.7)$$

is kept constant or not depend on symmetry properties of the attenuating media. For example, absorption of atmospheric gases is not changing  $p$  as long as the molecules have no preferred orientation, which is a valid assumption beside when there is a significant Zeeman effect. Non-polarising absorption corresponds to that the propagation matrix can be written as  $\alpha\mathbf{1}$ , where  $\alpha$  is the absorption coefficient and  $\mathbf{1}$  is the identity matrix.

There are also examples on effects that change the polarisation state of the Stokes vector without affecting  $I$ . These effects are caused by an interaction with the magnetic field, and are thus denoted magneto-optical. Ionospheric Faraday rotation can (approximately) be seen as a pure magneto-optical effect, while the Zeeman effect cause both non-isotropic absorption and has magneto-optical aspects.

As Equation 4.6 indicates, there are two source mechanisms that can act to increase the intensity: emission and scattering.

### 4.2.2 Absorbing species and particles

The complexity of the radiative transfer is largely dependent on if scattering must be considered or not. For this reason, ARTS operates with two classes of atmospheric matter:

**Absorbing species** This class covers atmospheric matter for which scattering can be neglected. The set of “species” to consider is described by the workspace variable `abs_species`, and the associated atmospheric fields are gathered into `vmr_field`. As the name indicates, this later variable is mainly containing volume mixing ratio (VMR)

data, but as this unit is not applicable in all cases also other units are accepted. That is, the unit for the fields varies, for gases it is VMR, while particle mass concentrations are given in  $kg/m^3$  and electron density in  $m^{-3}$ .

**Particles** This second class treats all matter causing significant scattering (and likely also adding to the absorption). The amount of scattering matter is given as particle number density fields ( $m^{-3}$ ), denoted as `pnd_field`. The radiative properties of each particle type are stored in `scat_data_array`.

Atmospheric quantities are not hard-coded to belong to any of these matter classes, as the practical division depends on the conditions of the simulations. The general rule is that for the shorter the wavelengths, a higher number of atmospheric constituents must be treated as “particles”. For thermal infrared and microwave calculations, electrons and molecules, and likely also aerosols, can be treated as absorbing species. It can also be possible to place some hydrometeors in this class. For example, non-precipitating liquid clouds can be treated as purely absorbing in the microwave region. Related with the division between absorbing species and particles is:

**Clear-sky** In ARTS, the term “clear-sky” refers to the case when the influence of “particles” can be ignored, and only “absorbing species” are of relevance. Hence, a clear-sky calculation can involve e.g. cloud water droplets, but on the condition that the wavelength is such that scattering can be neglected.

The propagation effects of absorbing species and particles are kept separated. The total propagation matrix is

$$\mathbf{K} = \mathbf{A}_a + \mathbf{K}_p, \quad (4.8)$$

where  $a$  and  $p$  refers to absorbing species and particles, respectively, and the symbol  $\mathbf{A}$  is used for the first term to remind about that the only extinction process covered by this matrix is absorption (but including magneto-optical effects). As workspace variable,  $\mathbf{A}_a$  is denoted as `propmat_clearsky`, obtained by the `propmat_clearsky_agenda` agenda.  $\mathbf{K}_p$  is obtained internally from `scat_data_array`.

### 4.2.3 Emission and absorption vectors

One of the general assumptions in ARTS is that local thermodynamic equilibrium (LTE) can be assumed. For the moment there exists no method in ARTS to handle deviations from LTE, but this can be changed in the future. On the condition of LTE, the emission vector ( $\mathbf{j}_e$ ) in Equation 4.6 can be written as

$$\mathbf{j}_e = B\mathbf{a}, \quad (4.9)$$

where  $B$  is the Planck function (a scalar value), describing blackbody radiation. The related workspace variables are `blackbody_radiation` and `blackbody_radiation_agenda`.

The quantity  $\mathbf{a}$  is denoted as the absorption vector. For clear-sky calculations the absorption vector is given by  $\mathbf{A}_a$ , as in this case the emission vector can be calculated as

$$\mathbf{j}_e = \mathbf{A}_a\mathbf{b}, \quad (4.10)$$

where  $\mathbf{b}$  can be seen as the emission source vector, defined as

$$\mathbf{b} = [B, 0, 0, 0]^T. \quad (4.11)$$

Hence, as only the first element of  $\mathbf{b}$  is non-zero, the absorption vector is in this case equal to the first column of  $\mathbf{A}_a$ . The absorption vector can not be extracted from  $\mathbf{K}_p$  as this propagation matrix covers also scattering and `scat_data_array` must also contain such data.

In summary, the total absorption vector in ARTS is obtained as

$$\mathbf{a} = \mathbf{a}_a + \mathbf{a}_p \quad (4.12)$$

where  $\mathbf{a}_a$  is the first column of  $\mathbf{A}_a$  and  $\mathbf{a}_p$  is the absorption vector due to particles.

#### 4.2.4 Main cases

The two equations below are discussed thoroughly in 6 of *ARTS Theory*. This including that for some conditions also the “n2-law of radiance” must be considered to obtain completely exact results (see also Section 9.5).

The equations below treat a single frequency and a single direction, at a time, and can be said to describe monochromatic pencil beam radiative transfer. For simplicity, the frequency and direction are left out from many of the equations in this user guide.

##### Clear-sky radiative transfer

If we for the moment assume that scattering can be totally neglected, then Equation 4.6 can be simplified to

$$\frac{ds(\nu, \mathbf{r}, \hat{\mathbf{n}})}{dl} = \mathbf{A}_a(\nu, \mathbf{r}, \hat{\mathbf{n}}) [\mathbf{b}(\nu, \mathbf{r}, \hat{\mathbf{n}}) - \mathbf{s}(\nu, \mathbf{r}, \hat{\mathbf{n}})] \quad (= -\mathbf{A}_a \mathbf{s} + B \mathbf{a}_a). \quad (4.13)$$

Cases where Equation 4.13 is valid, are in ARTS denoted as clear-sky radiative transfer (implying LTE if nothing else is stated). The discussion of such radiative transfer calculations is continued in Section 9.

##### Radiative transfer with scattering

Some additional conditions are required to put scattering into the picture. If scattering is of incoherent and elastic nature, the extension of Equation 4.13 is

$$\begin{aligned} \frac{ds(\nu, \mathbf{r}, \hat{\mathbf{n}})}{dl} = & -\mathbf{K}(\nu, \mathbf{r}, \hat{\mathbf{n}}) \mathbf{s}(\nu, \mathbf{r}, \hat{\mathbf{n}}) + B \mathbf{a}_a(\nu, \mathbf{r}, \hat{\mathbf{n}}) + \\ & + \int_{4\pi} \mathbf{Z}(\nu, \mathbf{r}, \hat{\mathbf{n}}, \hat{\mathbf{n}}') \mathbf{s}(\nu, \mathbf{r}, \hat{\mathbf{n}}') d\hat{\mathbf{n}}', \end{aligned} \quad (4.14)$$

where  $\mathbf{Z}$  is the scattering (or phase) matrix. ARTS includes several modules to handle scattering, introduced in the last part of this document.

# Chapter 5

## Complete calculations

This chapter outlines how complete radiative transfer simulations are performed. ARTS is not only performing atmospheric radiative transfer, also sensor characteristics can be considered. As a consequence, the topics of this chapter include the distinction between monochromatic pencil beam and “full” calculations, and how the sensor is introduced.

### 5.1 Overview

An attempt to illustrate a “standard” ARTS calculation is found in Figure 5.1. The figure shows that most calculation tasks are handled by an agenda. For example, `ppath_agenda` has the task of determining the propagation path for the given observation geometry. In principle, the agenda could solve the task by loading data from a file, but most likely it will use some of the dedicated workspace methods. These workspace methods are targeted towards different observation types, for example, radio link calculations require special consideration. Anyhow, the main message here is that by using the agenda concept, a very high degree of flexibility can be achieved and new features can be added fairly simply. On the other hand, the concept requires that the user actually apply methods that make sense for the agenda. The code of ARTS performs some consistency checks of the agenda output, but this can only catch some types of mistakes.

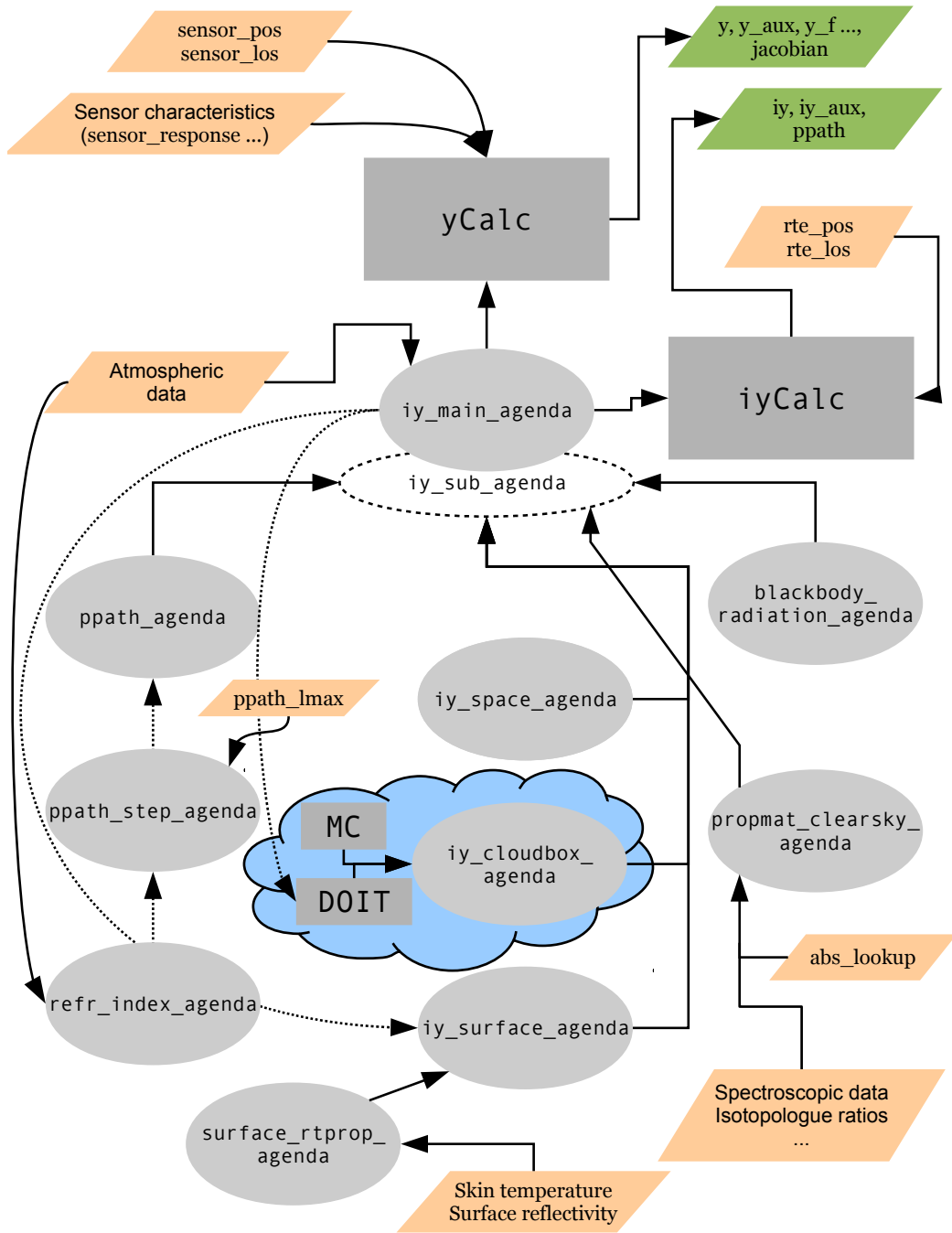
Complete radiative transfer calculations are normally performed by `yCalc`. This method incorporates sensor responses and has the variable `y` as main output. The letter `y` here refers to the measurement vector, `y`, found in the formalism of *Rodgers* [1990, 2000] (see also Sec. 1.3 of *ARTS Theory*). The vector can hold anything from a single value, to a high number of spectra appended. The spectra in the last case can correspond to a limb sounding sequence (hence measured for different zenith angles), or even be measured by different sensors. In any case, the data in `y` contain likely significant impact of different parts of the sensor used, such as the angular weighting by the antenna pattern.

On the other hand, atmospheric radiative transfer is performed for monochromatic frequencies, along pencil beam directions. The outcome of one such calculation is the Stokes vector for each frequency considered, and as workspace variable this quantity is denoted as `iy`. Please, note the distinction to `y`, that can contain information from a number of monochromatic pencil beam calculations, as shown in Section 5.3.

---

#### History

130219 First version by Patrick Eriksson.



(For caption see top of the next page.)

Figure 5.1: A flowchart of a radiative transfer calculation (on previous page), using `yCalc` or `iyCalc`. The figure assumes that `iy_main_agenda` holds `iyEmissionStandard`, that represents the most complex case. Some important input data are shown in orange, and main output are shown in green. The two main methods are plotted as grey boxes, while agendas are shown as ovals. For cases when `iy_sub_agenda` not is defined (the most common situation), the agendas communicate directly with `iy_main_agenda`. For connections between methods and agendas the arrows show the direction of output (calculated) data. Every call of an agenda involves also some input data (settings), but this aspect has been ignored for clarity reasons. Data entering an agenda along a common line indicates mutually independent options. For example, absorption can be calculated "on-the-fly" from basic spectroscopic data or be extracted from a pre-calculated look-up table (see bottom-right corner). The dotted lines indicate that some methods and agendas can make further calls of `iy_main_agenda`.

Further, the term "iy" is not restricted to the final outcome of atmospheric radiative transfer, it is also used to indicate that quantities and operations are of monochromatic pencil beam character. For example, the agenda returning the radiation entering the atmosphere from space is named as `iy_space_agenda` to indicate that the agenda output is directly associated with the calculation of `iy`. If only a single `iy` is of concern, the radiative transfer can be performed by `iyCalc`, having a smaller set of input arguments than `yCalc`.

The output is not restricted to `y` or `iy`, also some auxiliary data can be extracted as described in Section 9.8. In addition, `yCalc` can also provide weighting functions (Chapter 16).

## 5.2 Compulsory sensor and data reduction variables

The instrument real or hypothetical, that detects the simulated radiation is denoted as the sensor. The forward model is constructed in such way that a sensor must exist. For cases when only monochromatic pencil beam radiation is of interest, the positions and directions for which the radiation shall be calculated are given by specifying an imaginary sensor with infinite frequency and angular resolution. The workspace variables for the sensor that always must be specified are `sensor_response`, `sensor_pos`, `sensor_los`, `antenna_dim`, `mblock_za_grid` and `mblock_aa_grid`. These variables are presented separately below.

### 5.2.1 Sensor position

The observation positions of the sensor are stored in `sensor_pos`. This is a matrix where each row corresponds to a sensor position. The number of columns in the matrix equals the atmospheric dimensionality (1 column for 1D etc.). The columns of the matrix (from first to last) are geometrical altitude, latitude and longitude. Accordingly, row  $i$  of `sensor_pos` for a 3D case is  $(z_i, \alpha_i, \beta_i)$ . The sensor position can be set to any value, but the resulting propagation paths (also dependent on `sensor_los`) must be valid with respect to the model atmosphere (see Section 9.2). An obviously incorrect choice is to place the sensor below the surface altitude. If the sensor is placed inside the model atmosphere, any sensor line-of-sight is allowed, this including the cases that the sensor is placed on the surface looking down, and that the sensor is placed inside the cloud box.

One or several spectra can be calculated for each position as described in Section 5.3. The corresponding workspace variable for single pencil beam calculations is `rte_pos`, that is an input argument to e.g. `iy_main_agenda` and `iyCalc`.

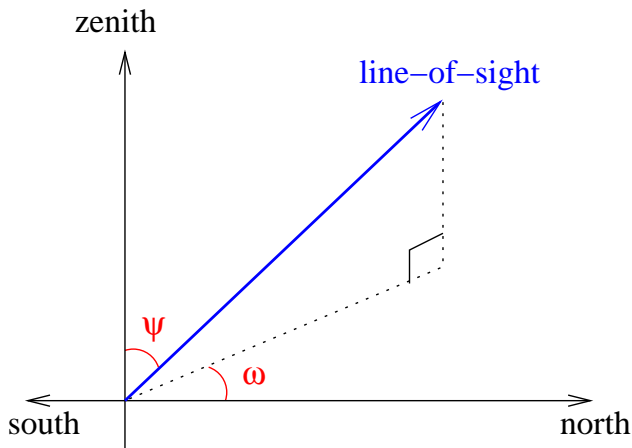


Figure 5.2: Definition of zenith angle,  $\psi$ , and azimuth angle,  $\omega$ , for a line-of-sight. The figure shows a line-of-sight with a negative azimuth angle.

### 5.2.2 Line-of-sight

The viewing direction of the sensor, the line-of-sight, is described by two angles, the zenith angle ( $\psi$ ) and the azimuth angle ( $\omega$ ). The zenith angle exists for all atmospheric dimensionalities, while the azimuth angle is defined only for 3D. The term line-of-sight is not only used in connection with the sensor, it is also used to describe the local propagation direction along the path taken by the observed radiation (Section 9.2). The zenith and azimuth angles are defined in an identical way in both of these contexts (sensor pointing direction; local propagation direction). This is expected as the position of the sensor is the end point of the propagation path. The sensor line-of-sight is the direction the antenna is pointed to receive the radiation. The line-of-sight for propagation paths is defined likewise, it is the direction in which a hypothetical sensor must be placed to receive the radiation along the propagation path at the point of interest. This means that the line-of-sight and the photons are going in opposite directions. As a true sensor has a finite spatial resolution (described by the antenna pattern), theoretically there is an infinite number of line-of-sights associated with the sensor, but in the forward model, spectra are only calculated for a discrete set of directions. If a sensor line-of-sight is mentioned without any comments, it refers to the direction in which the centre of the antenna pattern is directed.

The zenith angle,  $\psi$ , is simply the angle between the line-of-sight and the zenith direction (Figure 5.2). The valid range for 1D and 3D cases is  $[0, 180^\circ]$ . In the case of 2D, zenith angles down to  $-180^\circ$  are also allowed, where the distinction is that positive angles mean a viewing direction towards higher latitudes, and negative angles mean a viewing direction towards lower latitudes. It should be mentioned that the zenith and nadir directions are here defined to be along the line passing the centre of the coordinate system and the point of concern (Section 11.1.1). A nadir observation,  $\psi = 180^\circ$ , is thus a measurement towards the centre of the coordinate system.

The azimuth angle,  $\omega$ , is given with respect to the meridian plane. That is, the plane going through the north and south poles of the coordinate system ( $\alpha = \pm 90^\circ$ ) and the sensor. The valid range is  $[-180^\circ, 180^\circ]$  where angles are counted clockwise;  $0^\circ$  means that the viewing or propagation direction is north-wise and  $+90^\circ$  means that the direction of concern goes eastward. This definition does not work for position on the poles. To cover these special cases, the definition is extended to say that for positions on the poles the azimuth angle equals the longitude along the viewing direction. For example, if standing on



any of the poles and the viewing direction is towards Greenwich, the azimuth angle is  $0^\circ$ .

The sensor line-of-sights are stored in `sensor_los`. This workspace variable is a matrix, where the first column holds zenith angles and the second column is azimuth angles. For 1D and 2D there is only one column in the matrix, while for 3D a row  $i$  of the matrix is  $(\psi_i, \omega_i)$ . The number of rows for `sensor_los` must be the same as for `sensor_pos`. The correspondance to `rte_pos` is `rte_los`.

### 5.2.3 Sensor characteristics and data reduction

The term “sensor characteristics” is used here as a comprehensive term for the response of all sensor parts that affect how the field of monochromatic pencil beam intensities are translated to the recorded spectrum. For example, the antenna pattern, the side-band filtering and response of the spectrometer channels are normally the most important characteristics of a microwave heterodyne radiometer. Any processing of the spectral data that takes place before the retrieval is denoted as data reduction. The most common processing is to represent the original spectra with a smaller set of values, that is, a reduction of the data size. The most common data reduction techniques is binning and Hotelling transformation by an eigenvector expansion.

In ARTS, the influence of sensor characteristics and data reduction is incorporated by transfer matrices. The application of these transfer matrices assumes that each step is a linear operation, which should be the case for the response of the parts of a well designed instrument. Non-linear data reduction could be handled by special workspace methods.

The sensor and data reduction are described as a series of units, each having its own transfer matrix. There is only one compulsory transfer matrix and it is `sensor_response`. There are several workspace variables associated with this transfer matrix where `antenna_dim`, `mblock_za_grid` and `mblock_aa_grid` are the compulsory ones.

The variable `antenna_dim` gives the dimensionality of the antenna pattern, where the options are 1 and 2, standing for 1D and 2D, respectively. A 1D antenna dimensionality means that the azimuth extension of the antenna pattern is neglected, there is only a zenith angle variation of the response. A 2D antenna pattern is converted to a 1D pattern by integrating the azimuth response for each zenith angle. For cases with 1D antenna patterns, `mblock_aa_grid` must be set to be an empty vector.

See further Chapter 12, where inclusion of sensor characteristics is described in .

## 5.3 Measurement sequences and blocks

The series of observations modelled by the simulations is denoted as the measurement sequence. That is, a measurement sequence covers all spectra recorded at all considered sensor positions. A measurement sequence consists of one or several measurement blocks. A measurement block can be treated as a measurement cycle that is repeated, an integer number of times, to form the measurement sequence.

A measurement block covers one or several recorded spectra, depending on the measurement conditions and the atmospheric dimensionality. A block can consist of several spectra when there is no effective motion of the sensor with respect to the atmospheric fields. It should be noted that for 1D cases, a motion along a constant altitude has no influence on the simulated spectra as the same atmospheric fields are seen for a given viewing direction. It is favourable, if possible, to handle all spectra as a single block, instead of using a block

for each sensor position. This is the case as the antenna patterns for the different line-of-sights are normally overlapping and a pencil beam spectrum can be used in connection with several measurement spectra to estimate the intensity field. If a measurement sequence is divided into several blocks even if a single block would be sufficient, pencil beam spectra for basically identical propagation paths can be calculated several times, which of course will increase the computational time. To summarise, for cases when the sensor is not in motion, or with a 1D atmosphere and a sensor not moving vertically, the aim should be to use a single block for the measurement sequence.

If not a single block is used, the standard option should be that the blocks cover one spectrum each. There could exist reasons to select an intermediate solution, to let the extent of the blocks be several spectra (but not the full measurement sequence). This could be the case when the atmospheric dimensionality is 2D or 3D, and the sensor is moving but the movement during some subsequent spectra can be neglected.

The pencil beam spectra for each line-of-sight are appended vertically to form a common vector,  $\mathbf{i}_b$ . Values are put in following the order in `f_grid`. Hence, the frequencies for this vector are

$$\mathbf{i}_b = \begin{bmatrix} \begin{bmatrix} \nu_1 \\ \vdots \\ \nu_n \end{bmatrix} \\ \vdots \\ \begin{bmatrix} \nu_1 \\ \vdots \\ \nu_n \end{bmatrix} \end{bmatrix} \quad (5.1)$$

where  $\nu_i$  is element  $i$  of `f_grid` and  $n$  the length of the same vector. The order of the angles inside `mblock_za_grid` and `mblock_aa_grid` is followed when looping the pencil beam directions, where the azimuth angle direction is the innermost loop. That is, for 2D antenna patterns all azimuth angles are looped for the first zenith angle etc.

The workspace variable `sensor_response` is here denoted as  $\mathbf{H}_b$ . It is applied on each  $\mathbf{i}_b$  and the results are appended vertically, following the order of the positions in `sensor_pos`

$$\mathbf{y} = \begin{bmatrix} \mathbf{H}_b \mathbf{i}_{b,1} \\ \mathbf{H}_b \mathbf{i}_{b,2} \\ \vdots \\ \mathbf{H}_b \mathbf{i}_{b,n} \end{bmatrix} \quad (5.2)$$

where 1 indicates the first sensor position etc.

It should be noted that the compulsory sensor variables give no information about the content of the obtained  $\mathbf{y}$ , as it is not clear which parts and features the block transfer matrix covers. If  $\mathbf{H}_b$  only incorporates the antenna pattern, the result is a set of hypothetical spectra corresponding to a point inside the sensor. On the other hand, if  $\mathbf{H}_b$  includes the whole of the sensor and an eigenvector data reduction, the result is not even a spectrum in traditional way, it is just a column of coefficients with a vague physical meaning.

## **Part II**

# **Atmospheric properties**



# Chapter 6

## Gas absorption

### 6.1 Introduction

When calculating radiative transfer, the local absorption at each point in the atmosphere has to be known. Furthermore, if one also wants to calculate Jacobians, then the partial absorption for different atmospheric components (different absorption species) also has to be known.

This chapter discusses different practical aspects of absorption in ARTS. Sections 6.2 and 6.3 introduce the main physical quantities and the main agendas, respectively. Section 6.4 explains how absorption is handled inside radiative transfer calculations. Section 6.5 discusses how absorption is actually calculated, and how the calculation is set up. Finally, Section 6.6 describes how absorption is stored in a lookup table, and how it is extracted again.

Here in the User Guide we focus on practical aspects of absorption in ARTS. But absorption calculations also have a deep theoretical background, particularly the line-by-line calculations and the continuum models. Some of this background is discussed in *ARTS Theory*, Chapter 2.

### 6.2 Key physical quantities

The scalar gas absorption coefficient  $\alpha$  has units of 1/m. You can think of it as being defined by the Lambert-Beer law

$$I_1 = I_0 e^{-\alpha l}, \tag{6.1}$$

---

#### History

- 2013-06-21 New intro and general revision. Added CIA part. — Stefan Buehler
- 2012-08-28 Updated to `propmat_clearsky` — by Richard Larsson.
- 2011-07-05 Added intro and sections on abs in RT and abs calculation. Also revised lookup table section. First attempt of a complete absorption chapter for ARTS2. — Stefan Buehler
- 2003-03-28 Documentation for `WSM_abs_fieldCalc` extended by Stefan Buehler after comment from Sreerekha T. R..
- 2003-03-10 Lookup tables added by Stefan Buehler.
- 2002-06-04 Restarted for ARTS-1-1 by Stefan Buehler.

Table 6.1: Examples of symbols used in this chapter, the corresponding notation in the ARTS source code and a short description of the quantity.

Here	Unit	In ARTS	Description
$\alpha$	$\text{m}^{-1}$		Scalar gas absorption coefficient
$I$	$\frac{\text{W}}{\text{m}^2 \text{ Hz sr}}$	<code>iy</code>	Intensity
$l$	$\text{m}$		Path length element
$n_i$	$\text{molec}/\text{m}^{-3}$		Number density of species $i$
$\kappa_i$	$\text{m}^2/\text{molec}$	<code>abs_xsec_per_species</code>	Absorption cross-section of absorbing species $i$
$\kappa_{i,j}$	$\text{m}^5/\text{molec}^2$	<code>abs_cia_data</code>	Binary absorption cross-section of absorbing species pair $(i,j)$
$\mathbf{K}$	$\text{m}^{-1} (4 \times 4)$	<code>propmat_clearsky</code>	Clear-sky propagation matrix

where  $I$  is intensity and  $l$  is the distance through a homogeneous medium with absorption coefficient  $\alpha$ .

Absorption is additive, so the total absorption is the sum of the partial absorptions of all absorbers. For an individual absorber, we can define another important quantity, the absorption cross-section  $\kappa_i$ , as

$$\kappa_i = \frac{\alpha_i}{n_i}, \quad (6.2)$$

where subscript  $i$  denotes the absorber and  $n_i$  is the partial number density of that absorber. Absorption cross-sections depend less strongly on pressure than absorption coefficients, and are therefore more suitable for storing in a lookup table.

Some processes create polarized absorption, which is described by a  $4 \times 4$  matrix, in ARTS called propagation matrix (`propmat_clearsky`, already introduced in Section 4.2). This variable is used by the ARTS RT functions to describe absorption. In the absence of polarizing effects it is simply equal to  $\alpha \mathbf{1}_4$ , where  $\mathbf{1}_4$  is the  $4 \times 4$  identity matrix.

Both gases and particles in the atmosphere absorb, and the total absorption is the sum of these two contributions. This chapter only deals with absorption of non-scattering matter, i.e., gas absorption in the first place (but can also include absorption by grey-body particles and polarization changes by electrons).

### 6.3 Agendas

There are two key agendas related to absorption in ARTS: `propmat_clearsky_agenda` and `abs_xsec_agenda`. They fulfill different purposes and complement each other. Agenda `propmat_clearsky_agenda` is called by RT methods when they need absorption (more precisely the clear-sky propagation matrix, as defined above). Hence, this agenda is the interface between the RT part and the absorption part. Is is explained further in the next section.

The other agenda, `abs_xsec_agenda`, is called when absorption is actually calculated (either inside `propmat_clearsky_agenda`, if absorption is handled on-the-fly, or before, when the absorption lookup table is generated). This agenda is just for the scalar gas absorption part and describes in detail the line-by-line absorption calculation and various continua. It

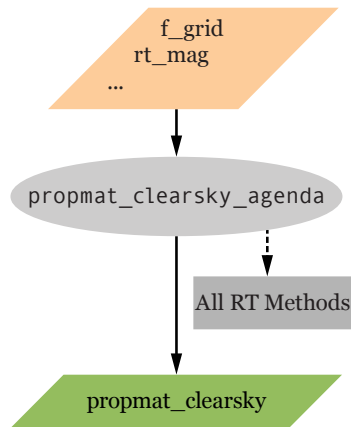


Figure 6.1: An outside view of `propmat_clearsky_agenda`.

is explained further in Section 6.5. You will likely need both of the above agendas for your ARTS RT simulation.

## 6.4 Gas absorption in radiative transfer simulations

The interface between the RT part of ARTS and the absorption part of ARTS is the agenda `propmat_clearsky_agenda` (see Figure 6.1). RT functions execute this agenda whenever they need local absorption matrices. In a typical ARTS run, the agenda will be executed many times over, for different points in the atmosphere. See the built-in documentation for the exact input and output arguments of the agenda. The idea is that input arguments are the local atmospheric conditions (temperature, pressure, trace gas volume mixing ratios, magnetic field, etc.).

The output of the agenda is a single variable, `propmat_clearsky`, a tensor with dimensions of absorption species, frequency, Stokes dimension and Stokes dimension (Stokes dimension of one thus emulates scalar absorption). The physical quantity corresponding to this variable is the clear-sky propagation matrix  $\mathbf{A}_a$  as defined in Equation 4.8. It describes all non-scattering extinction effects, that is, absorption and related polarization effects.

An inside view of `propmat_clearsky_agenda` is given in Figure 6.2. The agenda can contain a number of different workspace methods that in some way or other compute `propmat_clearsky`. See the built-in documentation of the individual methods to learn more. File `agendas.art`, one of the standard include-controlfiles, predefines some typical alternatives how `propmat_clearsky_agenda` can be set for different purposes.

## 6.5 Calculating gas absorption

This section deals with calculating gas absorption matrices in ARTS. This can typically occur in three different contexts: as on-the-fly absorption matrix calculation within the radiative transfer calculation, when preparing a gas absorption lookup table (see Section 6.6), or when the user is only interested in the absorption itself (see Section 6.7).

In all these cases, the same agenda is used to actually calculate absorption: `abs_xsec_agenda`. Outside views of this agenda are shown in Figure 6.2 (as input to `prop-`

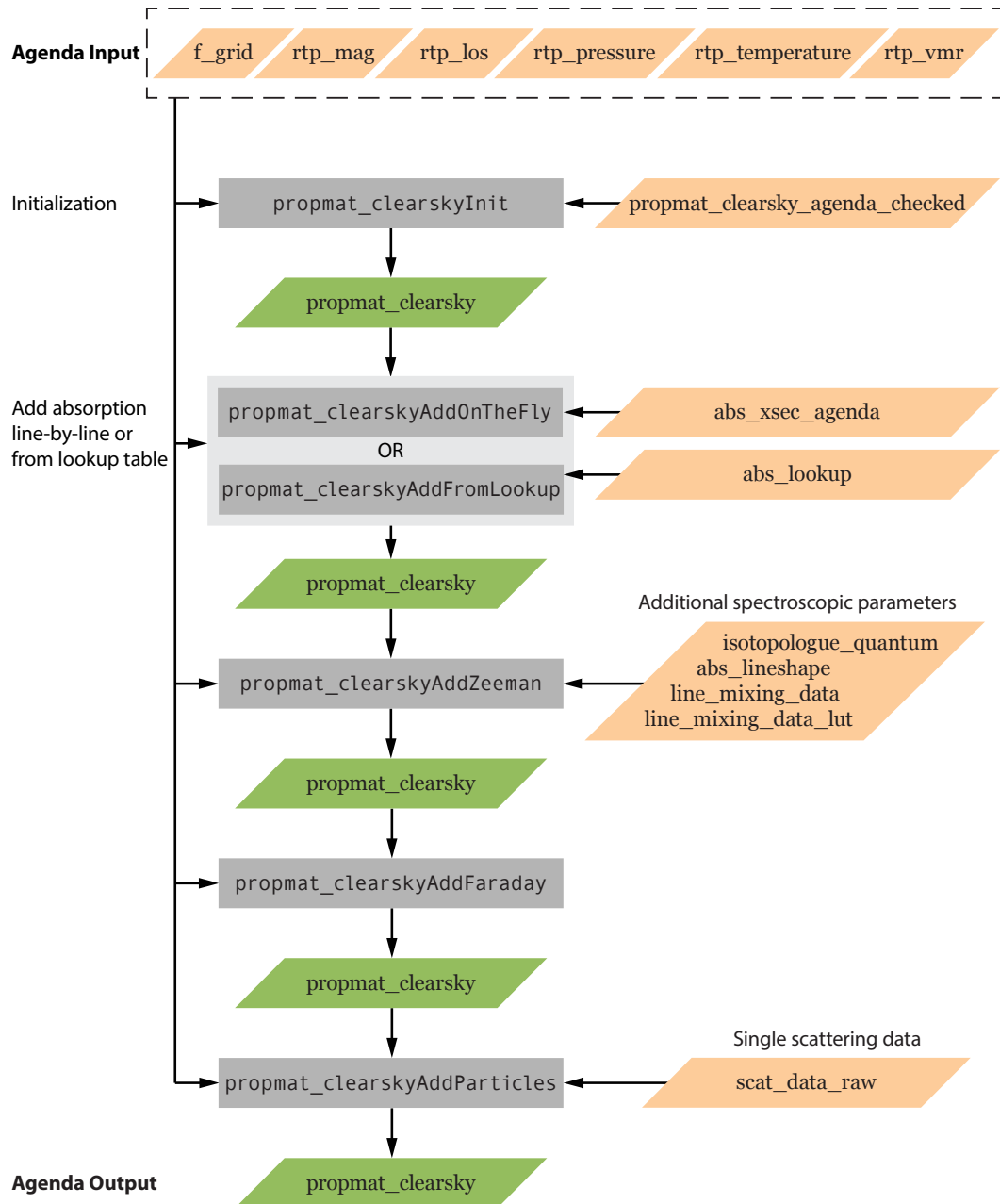


Figure 6.2: An inside view of `propmat_clearsky_agenda`. At the same time, this gives an outside view of `abs_xsec_agenda`, as input to `propmat_clearskyAddOnTheFly` in the context of on-the-fly absorption generation.



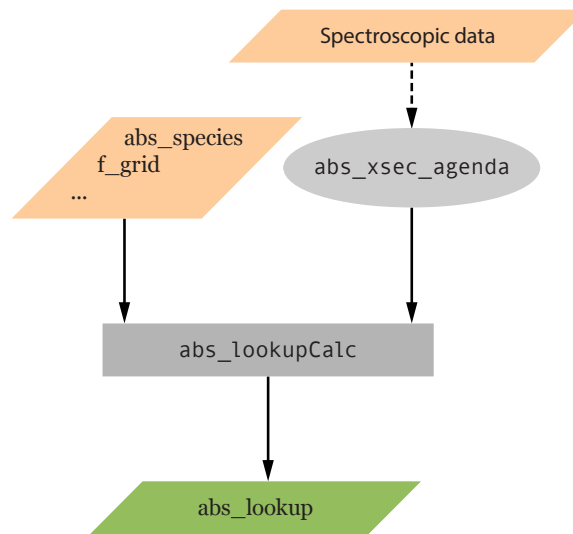


Figure 6.3: An outside view of `abs_xsec_agenda`, in the context of absorption lookup table generation.

`mat_clearskyAddOnTheFly` in the context of on-the-fly absorption generation) and Figure 6.3 (as input to `abs_lookupCalc` in the context of absorption lookup table generation).

An inside view of `abs_xsec_agenda` is given in Figure 6.4. The agenda can contain a number of different workspace methods that in some way or other compute `abs_xsec`. See the built-in documentation of the individual methods to learn more. As for `propmat_clearsky_agenda`, file `agendas.arts` predefines some typical alternatives also for `abs_xsec_agenda`.

### 6.5.1 Absorption species

Absorption is additive, so the total absorption is simply the sum of all partial absorptions. And the partial absorption for gases that have spectral lines can be calculated as a sum over the absorption of each spectral line, plus some more or less empirical continuum terms.

An absorption species in ARTS is an abstract entity that has a partial absorption matrix associated with it, and that usually can be associated with a volume mixing ratio of a corresponding gas (the VMRs are stored in variable `vmr_field`). Total absorption is the sum of the partial absorptions of all absorption species. Absorption species are defined in the ARTS controlfile by special ‘tags’, which are stored in the variable `abs_species`, and set by the method `abs_speciesSet`.

The absorption species tags specify the different considered absorbers, which can be gaseous species but also free electrons and (grey-body) particles. For gaseous species, they also describe the model that should be used to calculate the absorption for each of the species. There are three types of tags, those for explicit line-by-line calculations, those for continua and complete absorption models, and a special Zeeman effect tag. An example of the first kind is `"H2O-18"`, which identifies a particular isotopologue of water vapor. An example of the second kind is `"H2O-ForeignContCKDMT100"`, which identifies a particular continuum model. An example of the third is `"O2-Z"`, which identifies that special Zeeman routines should be used. Tags can be combined, if they refer to the same

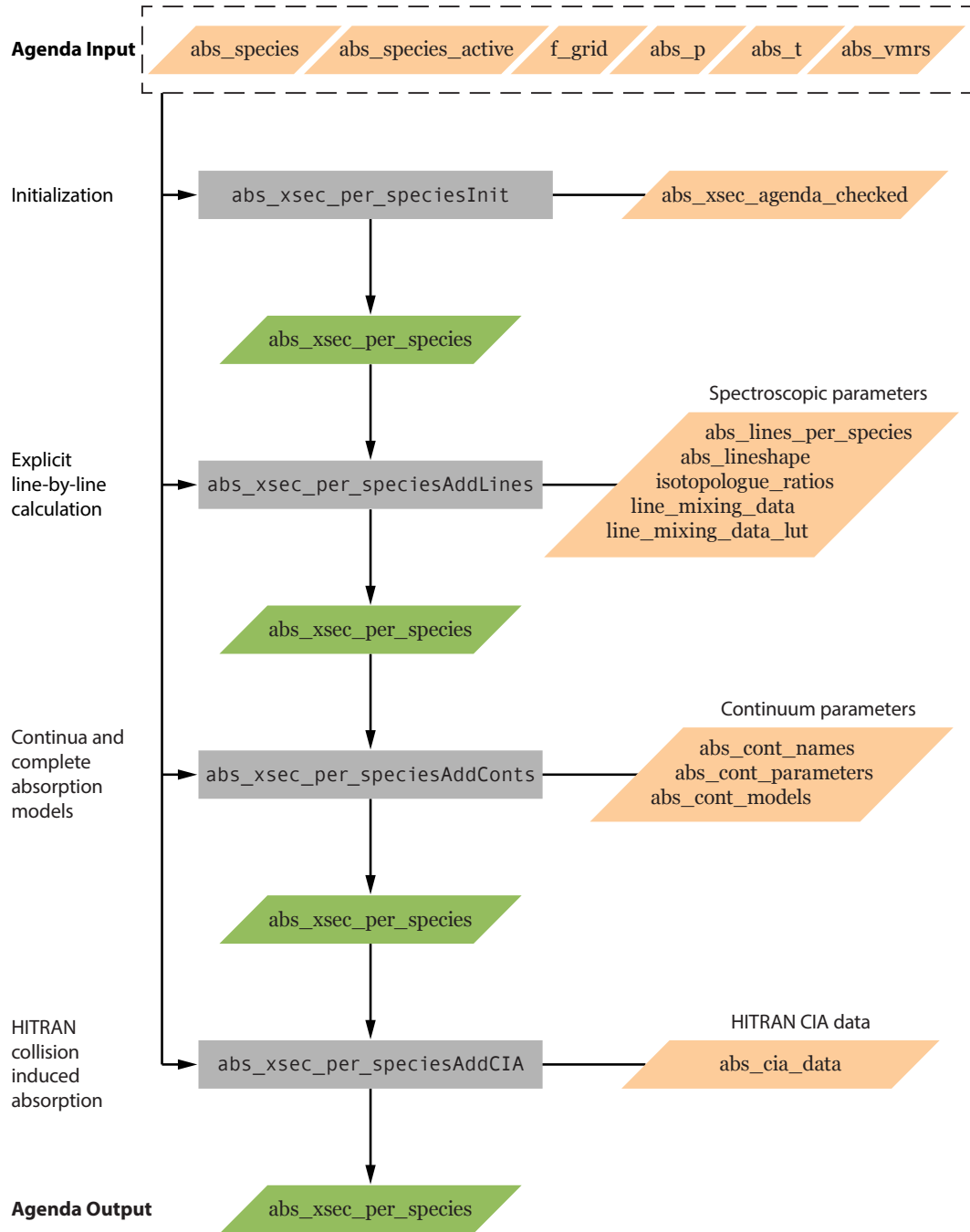


Figure 6.4: An inside view of `abs_xsec_agenda`.

molecule (different isotopologues are allowed). Even continuum tags can be combined with explicit line-by-line tags, if they refer to the same molecule.

It should be noted that isotopologue ratios are taken into account implicitly when line strengths are calculated, so even if you make calculations for individual isotopologues, the VMR numbers in the variable `vmr_field` should not be adjusted for the isotopologue ratio (the isotopologue ratio can be changed instead; see Section 6.5.9). As an example, to make a line-by-line calculation for all ozone isotopologues, you could represent them in different ways by `abs_speciesSet`.

```
a) abs_speciesSet (species=["O3"])
b) abs_speciesSet (species=
    ["O3-666", "O3-668", "O3-686", "O3-667", "O3-676"])
c) abs_speciesSet (species=
    ["O3-666", "O3-668", "O3-686", "O3-667", "O3-676"])
```

Options (a) and (b) are equivalent, you will have one ozone species that represents all isotopologues, and that will be associated with a single VMR field in `vmr_field`. With option (c) you have five different ozone species, so you have to supply five different VMR fields. If those five fields are identical (exactly same numerical values), you will get the same total absorption as with options (a) and (b).

Overall, the tag mechanism allows quite complex absorption setups. The built-in documentation for `abs_speciesSet` gives a detailed explanation of the tag syntax and some examples.

Particularly note, that order of the species list matters as absorption line data is assigned to species in their order within the `abs_species` list and no line record is assigned to more than one species. It is furthermore important to note that there is no ‘intelligence’ in ARTS that checks that the chosen tag combinations make sense, so the user should know what s/he is doing, or follow one of the many examples in the ARTS `controlfiles` directory.

## 6.5.2 Explicit line-by-line calculations

For absorption species with explicit line-by-line calculation the calculation involves the steps summarized in Table 6.2, which contains the steps that are common to all the three contexts in which explicit line-by-line calculations can occur as well as the steps that are specific to each of those cases. The list of variables and methods in the table is not complete. The idea is to give an overview over the important ones and show how they work together. Missing are particularly the input variables that describe the atmospheric conditions, and continuum description variables, which normally do not have to be set by the user anyway.

See the built-in documentation of the various variables and methods for more information. It is on purpose not repeated here, for better maintainability. If you are viewing this pdf file on a computer, just click on a variable or method name to get to the corresponding built-in documentation. Further input data and parameters required (not only) for line-by-line calculations is described in Section 6.5.9.

## 6.5.3 Continua and complete absorption models

ARTS includes many absorption continua and complete absorption models, which are described in *ARTS Theory*, Chapter 2. The common property of all of these is that they do not use the standard ARTS line-by-line calculation mechanism. They may include spectral

#	Step	Variables and Methods
1	Define line shape function(s) to use.	Variable: <code>abs_lineshape</code> . Methods: <code>abs_lineshapeDefine</code> (same shape for all species), <code>abs_lineshape_per_tgDefine</code> (different shapes for different species).
2	Read spectral line data (the order of the first two steps does not matter).	Variable: <code>abs_lines</code> . Methods: <code>abs_linesReadFromArts</code> , <code>abs_linesReadFromSplitArtscat</code> , <code>abs_linesReadFromHitran</code> , <code>abs_linesReadFromHitranPre2004</code> , <code>abs_linesReadFromJpl</code> , <code>abs_linesReadFromMytran2</code> (different methods are for different catalogue formats). For the ARTS internal format, the standard method <code>ReadXML</code> works also, but does not allow to select a frequency range, as the others do.
3	Split line data for different absorption species.	Variable: <code>abs_lines_per_species</code> . Methods: <code>abs_lines_per_speciesCreateFromLines</code> . Alternatively, read lines from different catalogues for different species directly with <code>abs_lines_per_speciesReadFromCatalogues</code> .
4	Optimize line data. (optional)	Variable: <code>abs_lines_per_species</code> . Methods: Add mirror lines for VVW line shape with <code>abs_lines_per_speciesAddMirrorLines</code> (see <i>ARTS Theory</i> , Chapter 2). Remove lines that are outside the line shape cutoff with <code>abs_lines_per_speciesCompact</code> .
<p>The first four steps are preparation, and typically have to be done only once per ARTS run. The fifth step is the actual absorption calculation, which can occur in different contexts.</p>		
5a	Calculate absorption on-the-fly.	Agenda: <code>propmat_clearsky_agenda</code> . Variable: <code>propmat_clearsky</code> , which is initialized in <code>propmat_clearskyInit</code> . Methods: <code>propmat_clearskyAddOnTheFly</code> (the core method for on-the-fly absorption calculation including line-by-line and continuum absorption), <code>propmat_clearskyAddZeeman</code> (see Sec. 6.5.5), <code>propmat_clearskyAddFaraday</code> (see Sec. 6.5.7), <code>propmat_clearskyAddParticles</code> (see Sec. 6.5.8). Alternative: <code>propmat_clearskyAddFromLookup</code> instead of <code>propmat_clearskyAddOnTheFly</code> (extract absorption from pre-calculated lookup table, see Sec. 6.6). Note that the lookup table cannot contain absorption for Zeeman tagged species, Faraday rotation, and particles due to their directional dependencies.
5b	Calculate absorption lookup table.	Variable: <code>abs_lookup</code> . Methods: <code>abs_lookupCalc</code> . Alternative: Load lookup table from file with <code>ReadXML</code> , it then has to be adapted to the current calculation (and checked) with <code>abs_lookupAdapt</code> .
5c	Calculate absorption only (no RT).	Variable: <code>propmat_clearsky_field</code> , <code>abs_coef</code> . Methods, high level: <code>propmat_clearsky_fieldCalc</code> . Methods, low level: <code>abs_xsec_per_speciesInit</code> , <code>abs_xsec_per_speciesAddLines</code> (the core method for the actual line-by-line calculation, used internally by all higher level methods), <code>abs_xsec_per_speciesAddConts</code> (add continua or complete absorption models, see Section 6.5.3), <code>abs_xsec_per_speciesAddCIA</code> (add collision induced absorption, see Section 6.5.4), <code>abs_coefCalcFromXsec</code> (calculate absorption coefficients from absorption cross-sections).

Table 6.2: Steps for line-by-line absorption calculation, and associated ARTS workspace variables and methods.

lines, but then these lines are hardwired into the absorption model itself. Consequently, the first four steps in Table 6.2 are not needed for these models.

The pure continua are intended to be used together with an explicit ARTS line-by-line calculation, the complete models are intended to be used alone. To select a continuum or complete absorption model, simply use the corresponding tag with `abs_speciesSet`. Currently available models are listed in Table 6.3.

The names should be fairly self-explanatory and can be used to find background information on the various models in *ARTS Theory*. The condensate absorption models are a bit special and perhaps need some extra explanation. They are absorption parameterizations by Liebe, and allow the inclusion of condensate in the (rare) cases where scattering is not important. Their general applicability is therefore fairly limited.

The behavior of the continua and complete absorption models can be modified by passing them some additional parameters, stored in the variables `abs_cont_names`, `abs_cont_models`, and `abs_cont_parameters`. Basically, `abs_cont_names` identifies the model, `abs_cont_models` contains switches that select different behavior (for example taking only the lines, or only the continuum part of a complete model), and `abs_cont_parameters` can contain numerical parameters.

Yes, the nomenclature for these additional continuum parameters, particularly `abs_cont_models`, is confusing. However, most users will never have to deal with these variables explicitly. They are set to default values in the include file `continua.arts`. Users should therefore always include this file at the start of their controlfiles with

```
INCLUDE "continua.arts"
```

Unless you work on continuum model development or verification, you should never have to modify these default settings.

The core method to calculate continua and complete absorption models is `abs_xsec_per_speciesAddConts`. Users normally do not have to call this method explicitly, since it is used implicitly by higher level methods, such as `propmat_clearskyAddOnTheFly` and `propmat_clearsky_fieldCalc`.

#### 6.5.4 Collision-induced absorption

Collisions of centro-symmetric molecules, e.g., O<sub>2</sub>, N<sub>2</sub>, H<sub>2</sub>, CO<sub>2</sub>, and CH<sub>4</sub>, possessing no permanent electric dipole create a transient dipole, which causes so-called collision-induced absorption (CIA). Absorption strength of CIA is characterized by its dependency on the molecular density of both molecular species involved in the collision.

Recently, the well-known HITRAN spectral line catalogue has started to offer also tabulated binary absorption cross-sections for CIA. This is described in detail in *Richard et al. [2012]*, and also in the documentation that comes with the data themselves.

Binary absorption cross-sections  $\kappa_{i,j}$  have to be multiplied with the number densities of both involved molecular species to yield absorption coefficients:

$$\alpha_{i,j} = \kappa_{i,j} n_i n_j, \quad (6.3)$$

where  $i$  and  $j$  denote the two different absorbing species. As a consequence,  $\kappa_{i,j}$  has units of  $\text{m}^5/\text{molec}^2$  in ARTS (the original HITRAN units are different).

Using CIA in ARTS is easy. First of all, include one or more CIA tags in your absorption species list (`abs_species`). All valid tags are listed in Table 6.4. Secondly, read in WSV `abs_cia_data`, which contains the tabulated binary absorption cross-sections, from a file.

Class	Tag name
Water vapor continua	H2O-SelfContStandardType
	H2O-ForeignContStandardType
	H2O-ForeignContMaTippingType
	H2O-ContMPM93
	H2O-SelfContCKDMT100
	H2O-ForeignContCKDMT100
	H2O-SelfContCKD222
	H2O-ForeignContCKD222
	H2O-SelfContCKD242
	H2O-ForeignContCKD242
	H2O-SelfContCKD24
	H2O-ForeignContCKD24
H2O-ForeignContATM01	
Complete water vapor models	H2O-CP98
	H2O-MPM87
	H2O-MPM89
	H2O-MPM93
	H2O-PWR98
Carbon dioxide continua	CO2-CKD241
	CO2-CKDMT100
	CO2-SelfContPWR93
	CO2-ForeignContPWR93
	CO2-SelfContHo66
CO2-ForeignContHo66	
Oxygen continua	O2-CIAfunCKDMT100
	O2-v0v0CKDMT100
	O2-v1v0CKDMT100
	O2-SelfContStandardType
	O2-SelfContMPM93
O2-SelfContPWR93	
Complete oxygen models	O2-PWR98
	O2-PWR93
	O2-PWR88
	O2-MPM93
	O2-MPM92
	O2-MPM89
	O2-MPM87
	O2-MPM85
	O2-TRE05
Nitrogen continua	N2-SelfContMPM93
	N2-SelfContPWR93
	N2-SelfContStandardType
	N2-SelfContBorysow
	N2-CIArotCKDMT100
	N2-CIAfunCKDMT100
	N2-DryContATM01
Condensate absorption models	liquidcloud-MPM93
	icecloud-MPM93
	rain-MPM93

Table 6.3: ARTS continua and complete absorption models. The molecular species can be inferred from the start of the tag name. See *ARTS Theory*, Chapter 2 for more information on the various models.

This will usually be the file `hitran_cia2012_adapted.xml.gz`, which is included in the `arts-xml-data`, but the original HITRAN data files can also be read. Finally, use WSM `abs_xsec_per_speciesAddCIA` in `abs_xsec_agenda` to add the CIA absorption. For usage examples, look in directory `controlfiles/artscomponents/cia` that is part of the ARTS distribution.

Figure 6.5 shows all CIA continua that are currently available in ARTS (left) and separately the ones that are relevant for Earth’s atmosphere (right). The valid frequency and temperature ranges for these data, as available in ARTS, are listed in Table 6.4. Outside the covered frequency ranges, the binary absorption cross-sections are set to zero, while exceeding the valid temperature range will produce NaN values and eventually trigger a runtime error.

To make the HITRAN data work in ARTS, some modifications were necessary, specifically:

**N<sub>2</sub>-N<sub>2</sub>:** The two high-frequency datasets were merged into one.

**O<sub>2</sub>-O<sub>2</sub>:** Three apparently separate datasets that really belong together were merged. UV/Vis dataset were removed.

**CO<sub>2</sub>-CO<sub>2</sub>:** Caveat: This is only the self continuum of CO<sub>2</sub>. The CO<sub>2</sub>-air continuum has strong features above 250 cm<sup>-1</sup> that are present in CKD.MT (also available in ARTS as one of the continuum and full absorption models), but are missing here. Furthermore, *Richard et al.* [2012] point out that for molecules with more than two atoms further mechanisms affecting CIA exist, which are not covered by the simple models used. They hence state that “these data should be used very carefully”. Conclusion: No changes, but use with care.

Also note that no data exists at frequencies below 30 GHz (1 cm<sup>-1</sup>) though some significant absorption is still present at the limiting frequency. For those low frequencies, the CO<sub>2</sub>-SelfContPWR93 continuum (see Table 6.3) can be used as an alternative (we estimated that to be valid at least up to about 100 GHz, but deviating significantly above 500 GHz).

**O<sub>2</sub>-N<sub>2</sub>, O<sub>2</sub>-CO<sub>2</sub>:** These UV/Vis-only datasets were removed.

### 6.5.5 Zeeman calculations

The Zeeman effect is calculated in the method `propmat_clearskyAddZeeman`. If this method is included in the `propmat_clearsky_agenda`, then species with the tag “-z” will be calculated as Zeeman species. If the method is not included, then these species will simply be ignored. Note that the order within the tag string is important: the Zeeman tag must directly follow the molecular species tag. That is, `O2-Z-66` will be counted as Zeeman splitting on the O<sup>16</sup>O<sup>16</sup> molecule, whereas `O2-66-Z` will not work the same way, or even at all.

The physics and internal workings of the Zeeman calculations follow the scheme presented in *Larsson et al.* [submitted 2013]

In order to calculate Zeeman splitting, additional line parameters that are not readily available in, e.g., HITRAN are necessary. These include  $g_s$  [-], the relative Landé factor, and  $S$  [-], the molecular total spin. These variables must therefore be read to the WSM `isotopologue_quantum`. This variable is of type `SpeciesAuxData`, and a file providing that kind of data would, e.g., look like:

Table 6.4: Absorption species tags, frequency ranges, and temperature ranges for HITRAN CIA data as implemented in ARTS. (These data contain some modifications from the original HITRAN data, which are described in the text.)

CIA tag	Spectral range [ $\text{cm}^{-1}$ ]	Temp range [K]	No. of datasets
N2-CIA-N2-0	0.02 – 554.00	40.00 – 400.00	10
N2-CIA-N2-1	1850.00 – 3000.09	228.20 – 362.50	10
N2-CIA-H2-0	0.02 – 1886.00	40.00 – 400.00	10
N2-CIA-CH4-0	0.02 – 1379.00	40.00 – 400.00	10
H2-CIA-H2-0	20.00 – 10000.00	200.00 – 3000.00	113
H2-CIA-He-0	20.00 – 20000.00	200.00 – 9900.00	334
H2-CIA-CH4-0	0.02 – 1946.00	40.00 – 400.00	10
H2-CIA-H-0	100.00 – 10000.00	1000.00 – 2500.00	4
He-CIA-H-0	50.00 – 11000.00	1500.00 – 10000.00	10
O2-CIA-O2-0	1150.00 – 1950.00	193.40 – 353.40	15
CO2-CIA-CO2-0	1.00 – 250.00	200.00 – 800.00	7
CH4-CIA-CH4-0	0.02 – 990.00	40.00 – 400.00	10
CH4-CIA-Ar-0	1.00 – 697.00	70.00 – 296.00	5

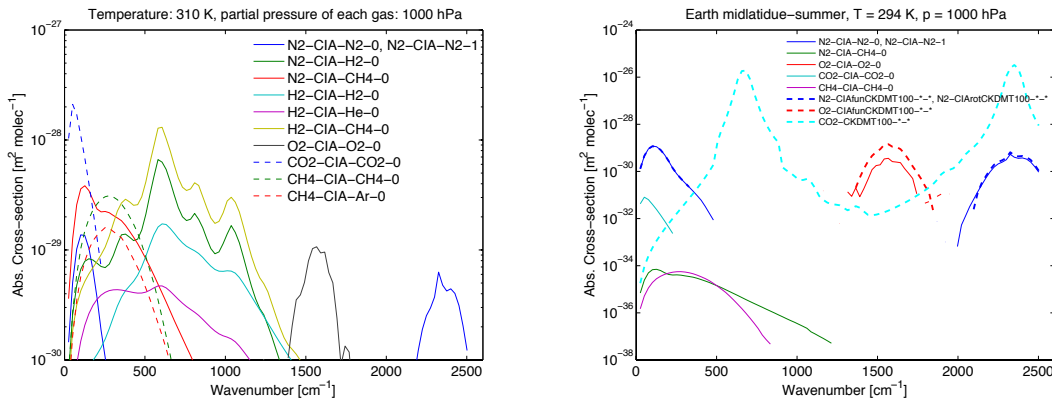


Figure 6.5: Left: All HITRAN CIA continua that are implemented in ARTS (each gas here has a partial pressure of 1000 hPa). Right: Only the ones that are relevant for Earth (for Earth surface conditions).



```
<arts format="ascii" version="1">
  <SpeciesAuxData version="1" nelem="1" nparam="3">
    @ O2-66 2.002064 1 1
  </SpeciesAuxData>
</arts>
```

In this example, @ indicates the beginning of a new data record, O2-66 specifies what isotopologue is associated with the data, the number 2.002064 is the relative Landé factor, and the molecule got  $S = 1$ . The last value indicates what Hund case is used in the calculations. For oxygen, Hund case b is used, indicated by the number "1". Presently, Hund case a, indicated by number "0" also works for some molecules. It is up to the user to assure the correct quantum numbers for each case are set properly. The supported molecules in ARTS so far for Zeeman calculations are

- O<sub>2</sub>, case b
- NO, case a/b
- OH, case a
- ClO, case a
- HO<sub>2</sub>, case b
- NO<sub>2</sub>, case b

but only O<sub>2</sub> is tested beyond initial modeling results.

Beside the additional line parameters, it is also necessary to input the magnetic field into the model. This can be done following:

```
GriddedField3Create(B)
  ReadXML(B, "B_1comp.xml.gz")
  GriddedFieldLatLonRegrid( B, lat_grid, lon_grid, B )
  GriddedFieldPRegrid( B, p_grid, B )
  FieldFromGriddedField( mag_w_field, p_grid, lat_grid,
                        lon_grid, B )
```

where B\_1comp.xml.gz contains the (atmospheric) profile or field for one components of the magnetic field. Input needs to be provided for each non-zero magnetic field component separately into the respective WSVs `mag_w_field`, `mag_v_field`, and `mag_u_field`. For more information on magnetic field format in ARTS see Section 3.8.

Lastly, it is necessary to take phase effects into account when calculating the Zeeman effect. It is therefore important that `abs_lineshape` is chosen such that it allows for this information to be provided. One suitable line shape can be defined through

```
abs_lineshapeDefine( abs_lineshape, "Faddeeva_Algorithm_916",
                    "VVH", 750e9 )
```

### 6.5.6 Internal line-mixing

For first- and second-ordered line-mixing there exists an explicit tag to read and match line-mixing parameters to individual lines. This can be accessed through the tags "O2-LM\_2NDORDER" or "O2-Z-LM\_2NDORDER", if you want to calculate line-mixing

with the Zeeman effect. In order to match the data to specific lines, a set of calls are necessary by the user. First of all, after `abs.lines` have been created, line mixing needs to be initialized through `line_mixing_dataInit`. After this, it is important to pass an `ArrayOfLineMixingRecord` containing the line-mixing data into `line_mixing_dataMatch`, which will match the data in the `Array*` by quantum numbers to lines in `abs.lines`. If this is done properly, line-mixing will be applied at a lower level.

Example flow for code calculating a single Zeeman line with O<sub>2</sub> line-mixing spectrum in the background:

```
# Define your atmospheric species,
abs_speciesSet (species=["O2-Z-66-LM_2NDORDER-53.0469e9-53.0869e9",
    "O2-66-LM_2NDORDER", "O2"])

# read from a line database,
abs_linesReadFromHitran(filename="HITRAN08.par",
    fmin=40e9, fmax=120e9)

# and create the lines.
abs_lines_per_speciesCreateFromLines

# Initiate the line-mixing
line_mixing_dataInit

# Create a way to temporally store line-mixing data.
ArrayOfLineMixingRecordCreate(lm_o2)
ReadXML(lm_o2, "o2_v1_0_band_40-120_GHz.xml")

# Finally match the line-mixing data with the species you
are interested in.
line_mixing_dataMatch(
    species_tag="O2-66-LM_2NDORDER",
    line_mixing_records=lm_o2)
line_mixing_dataMatch(
    species_tag="O2-Z-66-LM_2NDORDER-53.0469e9-53.0869e9",
    line_mixing_records=lm_o2)
```

There is future plans for more methods to allow internal line-mixing for different molecules, but at the time of writing the second order line-mixing method for the oxygen molecule is the only included method. As a consequence, first order line-mixing also works for oxygen. For details on the second order line-mixing method see *Makarov et al.* [2011]. To be fully accurate, the method should work with the correct input data for other molecules as well.

Example of correct input data:

```
<?xml version="1.0"?>
<arts format="ascii" version="1">
<Array type="LineMixingRecord" nelem="38">
<LineMixingRecord>
<SpeciesTag>"O2-66-*-*"</SpeciesTag>
<QuantumNumberRecord>
<Upper><QuantumNumbers nelem="3">
    J 1/1 N 1/1 v1 0/1
</QuantumNumbers></Upper>
<Lower><QuantumNumbers nelem="3">
```

```

    J 2/1 N 1/1 v1 0/1
</QuantumNumbers></Lower>
</QuantumNumberRecord>
<Vector nelem="10">
2.65e-06
-1.32e-07
-8.35e-12
8.43e-13
0.000545
0.00017
300
0.8
1.6
1.6
</Vector>
</LineMixingRecord>
</Array>
</arts>

```

The format of the above data is thusly: SpeciesTag, QuantumNumberRecord, Vector, The above input will cause the O2-66-\*\*\* line with upper quantum numbers  $J = 1$ ,  $N = 1$  and  $\nu_1 = 0$  and with lower quantum numbers  $J = 2$ ,  $N = 1$  and  $\nu_1 = 0$  to match. If this is the only input file, the described line is the only line experiencing line-mixing in your calculations. If there were more lines in the file, these would also experience line-mixing. In order of appearance in the vector, its format is first order zeroth phase correction [ $\text{Pa}^{-1}$ ], first order first phase correction [ $\text{Pa}^{-1}$ ], second order zeroth absorption correction [ $\text{Pa}^{-2}$ ], second order first absorption correction [ $\text{Pa}^{-2}$ ], second order zeroth line-center correction [ $\text{Hz Pa}^{-2}$ ], second order first line-center correction [ $\text{Hz Pa}^{-2}$ ], standard temperature for corrections [K], first order phase temperature correction exponential term [-], second order absorption temperature correction exponential term [-], and second order line-center temperature correction exponential term [-]. The format of the vector is fixed according to necessary information found in *Makarov et al.* [2011], the naming scheme of the variables above can also be understood from the same work.

First order line mixing, as per the MPM/PWR complete oxygen models, can be achieved with the correct input by letting the second order terms be nil.

*Warning:* There appears to be some errors in the quantum number encoding in HITRAN04 and HITRAN08 that makes the line mixing module wrong. The newer HITRAN2012 has fixed these issues.

### 6.5.7 Faraday rotation

Faraday rotation is a change of polarization state of radiation in interaction with (free) electrons in presence of a static magnetic field. For further details on theory and usage in ARTS see Section 14. Here we only give a short summary how to setup the calculation of Faraday contribution to the absorption (or better: propagation) matrix `propmat_clearsky`.

First, to include Faraday rotation effects `propmat_clearskyAddFaraday` must be included in the `propmat_clearsky_agenda`. Second, a species tag "free\_electrons" needs to be contained in `abs_species`. Correspondingly, a field of electron densities is required in `vmr_field`.

For usage examples, check `controlfiles/artscomponents/faraday` that is part of the ARTS distribution.

### 6.5.8 Absorbing particles

As pointed out before, this chapter deals with absorption by non-scattering matter. In first place this refers to gases, while particles (aerosols, clouds, precipitation) are considered to (also) scatter radiation and are handled differently (see Chapters 8 and 18). However, when particles are small compared to the wavelength of the radiation they act as broadband grey-body absorbers and can be treated similarly to continuum absorption by gases.

This is reflected in ARTS providing a few continuum models for condensed matter (see Tab. 6.3), which essentially are particles, too. It is tedious, though, to implement those kind of particle continua for a wide range of different base materials as become of interest when being interested in other than the Earth's atmosphere.

In the ARTS scattering modules, particles are represented by single scattering property data (`scat_data_array`) and particle concentrations (particle number density fields `pnd_field`). The single scattering data originate from scattering theory programs (e.g., Mie theory, T-matrix model, Discrete Dipole Approximation) and their preparation typically requires significant efforts. Comprehensive data for hydrometeors in the Earth atmosphere, but also clouds, dust and the like for other planets is available from the `arts-xml-data` package. It is appealing to apply this data in non-scattering calculations (e.g. at low frequencies, where the scattering contribution is negligible) in a consistent manner. The ARTS method for that is `propmat_clearskyAddParticles` and its application is described in the following.

To consider grey-body particle absorption, the user has to include `propmat_clearskyAddParticles` in the `propmat_clearsky_agenda`. Furthermore, for each particle type (see Section 8.1 for how a particle type is defined) a "particles" tag needs to be added to `abs_species`, the corresponding concentration field to be added to `vmr_field`, and its single scattering data have to be added as an element to `scat_data_array`. This can be done each-by-each using `ReadXML` and `Append` methods, but a dedicated method `ParticleType2abs_speciesAdd` is available performing these three steps for one particle type at once. `ParticleType2abs_speciesAdd` adds the concentration field to `vmr_field_raw`, i.e., the particle concentration fields can be converted to the internal atmospheric grids together with the gas concentration fields using, e.g., `AtmFieldsCalc`. Note that `ParticleType2abs_speciesAdd` is essentially doing the same as `ParticleTypeAdd`, but for non-scattering instead for scattering-in-cloudbox cases (where in non-scattering setups the concentration data is stored together with gas concentrations in `vmr_field`, while for scattering setups it is stored separately in `pnd_field`), and that for the single scattering data and concentration fields the exact same data can be applied.

Beside being able to re-use particle data from scattering cases, this method is also advantageous compared to the particles-as-continuum-models implementations as it allows for directional dependent absorption and for polarization effects that occur, e.g., with non-spherical particles.

Be aware that both `propmat_clearskyAddParticles` and the scattering methods use `scat_data_array` to store the particle single scattering data. Hence, it is straight-forward that these methods can not be applied simultaneously. In one ARTS run, all particles are handled either as scattering entities (when using the scattering modules) or as grey-body absorbers (when applying `propmat_clearskyAddParticles`). Trying to use both in parallel results in a runtime error.

See the built-in documentation of the individual methods for further information. **FIXME: add a usage example to `controlfiles/artscomponents`.**

## 6.5.9 Further input data and parameters for calculating gas absorption

### Spectral line data

Important input to the line-by-line calculations is the spectral line data, usually provided by spectroscopic catalogues. ARTS has its own format for the spectral line data, but is also capable of handling data from other catalogues like HITRAN (both pre- and post-2004 formats) and JPL (see Table 6.2, step 2). Section 2.1.2 of *ARTS Theory* contains more information on the internal format of the spectral line data. It also contains theoretical background for the calculation itself.

### Isotopologue ratios

Isotopologue ratios (mostly) from HITRAN and valid for Earth atmosphere are stored in ARTS source code. These data are necessary for working with HITRAN data (as HITRAN line strengths are weighted with isotopologue abundance). However, it is convenient for the user to be able to change isotopologue ratio values, e.g., when modeling absorption in other planets' atmospheres.

The WSV `isotopologue_ratios` holds the isotopologue ratios applied in the absorption calculation. They have to be set by the user. It is possible to apply the ARTS built-in values mentioned above using `isotopologue_ratiosInitFromBuiltin`. Alternatively, they can be read from file using `ReadXML`. For easy manipulation, the user might initialize `isotopologue_ratios` from built-in data, write the `isotopologue_ratios` structure to file using `WriteXML`, modify the data accordingly, and read in the manipulated file. Files with isotopologue ratios for a couple of planetary atmospheres are provided with the `arts-xml-data` package.

It shall be noted, that only isotopologue ratios of the species used in the absorption calculation need to be given. Reading in from file resets the full list of isotopologue ratios (i.e., the values for all absorption species known to ARTS) with species not given in the input data set to NaN.

### Partition functions

Partition functions are currently still hard-coded into ARTS. That is, no settings related to those have to be or can be done on the user level. For more information on theoretical background as well as the source and implementation in ARTS see Section 2.1.4 of *ARTS Theory*.

## 6.6 The gas absorption lookup table

### 6.6.1 Introduction

Calculating gas absorption matrix spectra in a line by line way is quite an expensive thing to do. Sometimes contributions from thousands or ten thousands of lines have to be summed up. To make matters worse, this has to be done over and over again for each point in the atmosphere.

Actually, the absorption matrix depends not directly on position, but on the atmospheric state variables:

- Pressure

- Temperature
- Concentrations of absorbing matter (i.e., gases, absorbing particles, free electrons)
- Magnetic field

The basic idea of the lookup table is to pre-calculate absorption for discrete combinations of these variables, and then use interpolation to extract absorption for the actual atmospheric state. Due to the nature of the Zeeman and Faraday effects (also particle absorption), particularly due to their directional dependence, those are not implemented in the lookup table. Thus, we can ignore the magnetic field.

The lookup table concept and implementation is described only very briefly here in the user guide. Much more details and validation results can be found in *Buehler et al.* [2011].

### 6.6.2 Lookup table concept

The fundamental law of Beer<sup>1</sup> states that extinction is proportional to the intensity of radiation, and to the amount of absorbing substance:

$$\frac{dI}{dl} = -I \sum_i \kappa_i n_i = -I \sum_i \alpha_i = -I \alpha_{\text{total}} \quad (6.4)$$

where the meaning of the symbols is defined in Table 6.1.

As one can see from the above equation, a large part of the pressure dependence of  $\alpha_i$  comes from  $n_i$ . (If one assumes constant volume mixing ratio of species  $i$ , then  $n_i$  is proportional to the total pressure according to the ideal gas law.) Therefore, the lookup table should store  $\kappa$ , rather than  $\alpha$ . We then have to worry only about the dependence of  $\kappa$  on the atmospheric state variables.

#### Pressure dependence

The pressure dependence is the most important dependence of  $\kappa$ . It comes from the fact that the width of the line shape functions is governed by pressure broadening. We have to store the  $\kappa_i$  on some pressure grid and interpolate if we need them for intermediate values.

#### Temperature dependence

This is the next effect to take into account. Both the line widths and the line intensities depend on temperature. Of course, only certain combinations of pressure and temperature occur in the Earth's atmosphere. Hence, storing the  $\kappa_i$  in a two dimensional table as a function of pressure and temperature would waste a lot of memory (and computation time). Instead, they are stored for a reference temperature and set of temperature perturbations for each pressure level. E.g., if the set of perturbations is  $[-10, 0, +10]$ , then the  $\kappa_i$  would be stored for three different temperatures for each pressure level:  $[T_R(p) - 10 \text{ K}, T_R(p), T_R(p) + 10 \text{ K}]$ , where  $T_R(p)$  is the reference temperature for each pressure level.

<sup>1</sup>According to C. Melsheimer, Beer's law is: 'The taller the glass, the darker the brew, the less the amount of light that comes through'. He might have been quoting someone else, there, but I do not know whom.

### Trace gas concentration dependence

This is a second order effect. The width of the line depends not only on total pressure, but also on the partial pressure of one or more trace gases. In theory this is always the case, because the broadening is different for each combination of collision partners. However, in practice trace gas concentrations in the Earth's atmosphere are normally so low that this can be safely neglected. An important exception is water vapor in the lower troposphere, which can reach quite high volume mixing ratios. Therefore, the effect of water vapor mixing ratio on water vapor absorption (self broadening), as well as on oxygen absorption (for example according to the parameterization by *Rosenkranz [1993]*) may not be negligible.

This is handled by storing water vapor perturbations. In contrast to the temperature case, the water vapor perturbations are multiplicative, not additive. Hence, if the set of perturbations is  $[0, 1, 10]$ , then the  $\kappa_i$  would be stored for three different H<sub>2</sub>O VMRs for each pressure/temperature grid point:  $[0, \text{VMR}_R(p, T), 10 * \text{VMR}_R(p, T)]$ , where  $\text{VMR}_R(p, T)$  is the reference water vapor VMR for each pressure/temperature grid point.

### Interpolation

The interpolation scheme is quite important for the accuracy of the lookup table. In particular, higher order interpolation gives considerably better accuracy for the same table grid spacing. The interpolation orders in the ARTS implementation of the lookup table can be chosen by the user. The settings that are recommended, and set as defaults in file `general.arts`, are quite high interpolation orders of 5, 7, and 5 for pressure, temperature, and water vapor, respectively. Such high orders are only appropriate because the function to be interpolated (the  $\kappa_i$ ) is very smooth.

### 6.6.3 Workspace variables and methods

The gas absorption lookup table is implemented by the class `GasAbsLookup`, which resides in the files `gas_abs_lookup.cc` and `gas_abs_lookup.h`.

The lookup table itself is stored in the workspace variable `abs.lookup`. It can be generated with the method `abs.lookupCalc`. ARTS also includes some methods that automatically set input parameters for `abs.lookupCalc`, such as grid ranges and reference profiles of pressure, temperature, and trace gas concentrations. These methods are `abs.lookupSetup`, `abs.lookupSetupBatch`, and `abs.lookupSetupWide`. The first two will take into account the actual atmospheric state, or set of atmospheric states, for the calculation. The third alternative simply sets up a table that should cover most reasonable atmospheric conditions. *Buehler et al. [2011]* as well as the built-in documentation contains more information on these setup methods.

Alternatively, the table can be loaded from a file with `ReadXML`. After loading, the method `abs.lookupAdapt` has to be called. It will make sure that the lookup table agrees exactly with your calculation. For example, it has to check that the frequencies that you want to use are included in the set of frequencies for which the table has been calculated. There is no interpolation in frequency. This is on purpose, because the gas absorption spectrum is the quantity that changes most rapidly as a function of frequency. Frequency interpolation here could be quite dangerous. The `abs.lookupAdapt` method also checks that all used species (apart from Zeeman, Faraday, and particle species) are present in the table, reduces the table to the used species, and sorts the table species data in exactly the same

way that they occur in your calculation. It sets the variable `abs.lookup.is_adapted` to flag that the table is now ok.

When the table has been successfully adapted, one can extract absorption matrices with the method `propmat_clearskyAddFromLookup`. This will extract *absorption matrices*, i.e., the cross-sections stored in the table are not only interpolated to the desired atmospheric conditions, but are also multiplied with the partial number density of the present absorbers.

The `propmat_clearskyAddFromLookup` method is meant to be used inside the agenda `propmat_clearsky_agenda`, which is applied in several places where absorption matrices are needed, both inside the scattering box and outside.

#### 6.6.4 Format of the lookup table

Usually the user does not need to bother with it, as ARTS provides methods to create, read and write, and extract data from the lookup table. However, sometimes one desires to analyze, e.g., the absorption cross-section data calculated and stored in the lookup table. Therefore we give a short description of the format of the absorption lookup table here. More detailed information can be found in the source code, where the `GasAbsLookup` class is implemented – specifically in `gas_abs_lookup.h`.

The absorption lookup table is a compound type variable comprising of (in this order; variable type of each entry shown in parantheses)

- **species:** an array of the species tags the lookup table is valid for (`ArrayOfArrayOfSpeciesTag`)
- **nonlinear\_species:** an array indicating the species that require non-linear treatment (`ArrayOfIndex`)
- **f\_grid:** the frequency grid (`Vector`)
- **p\_grid:** the pressure grid (`Vector`)
- **vmrs\_ref:** the reference profiles of volume mixing ratios (VMRs) for all species associated with the pressure (`Matrix`; dimension: [number of species, number of pressure levels])
- **t\_ref:** the reference temperature profile associated with the pressure grid (`Vector`)
- **t\_pert:** the temperature perturbations (`Vector`)
- **nls\_pert:** the VMR perturbations of the non-linear species in terms of fractional units of the reference VMRs (`Vector`)
- **xsec:** the absorption cross-sections (`Tensor4`; dimension: [number of temperature perturbations, number of species (and non-linear species perturbations), number of frequencies, number of pressure levels])

### 6.7 Stand-alone gas absorption calculation

Within the RT calculations, gas absorption is calculated or extracted locally, i.e., for a specific point in the atmosphere or in other words for a specific set of pressure, temperature, and trace gas VMR. However, sometimes it is of interest to explicitly calculate and output



absorption, e.g., for testing and validating modules of the absorption calculation, for model comparisons, for plotting and analyzing absorption coefficients, etc. Table 6.2, step 5c lists high- and low-level workspace methods for this purpose. In particular, the method `prop-mat_clearsky_fieldCalc` provides the absorption matrices, i.e., polarized absorption coefficients, per species tag group for an entire atmospheric scenario and the complete frequency grid.



## Chapter 7

# Refractive index

**FIXME:** Write a proper introduction. Comment on that this is not the complex refractive index, also covering absorption. ...

Refractive index (here restricted to the real part of the refractive index, which is basically a complex quantity with the imaginary part expressing absorption) describes several effects of matter on propagation of electromagnetic waves. This particularly includes changes of the propagation speed of electromagnetic waves, which leads to a delay of the signal as well as a change of the propagation direction, a bending of the propagation path. The latter is commonly called refraction.

Several components in the atmosphere contribute to refraction, hence to the refractive index: the gas mixture (“air”), solid and liquid constituents (clouds, precipitation, aerosols), and electrons. ARTS includes mechanisms for deriving the contributions from gases and electrons with the available methods described in the Sections below. ARTS does not consider refraction by solid and liquid particle as their refractive index is not known to ARTS (when scattering is considered, ARTS gets their single scattering properties as input, see Chapter 8). However, the contribution of solid and liquid constituents to the refractive index is commonly neglected in radiative transfer models and is expected to have only small effects.

Refractivity ( $N$ ) describes the deviation of the refractive index of a medium  $n$  from the vacuum refractive index ( $n_{\text{vacuum}} = 1$ ):  $N = n - 1$ . Contributions of the different components to refractivity are additive. Therefore, all ARTS methods that provide refractive index, calculate refractivity and sum it up with the input refractive index.

Within ARTS, refractive index is required for calculations of refracted propagation paths and related parameters (e.g., deriving viewing angle for a given tangent altitude). **FIXME: for more?**

Whenever refractive index is required, e.g., at each point along a propagation path, it is evaluated according to the mechanism specified by `refr_index_air_agenda`. `refr_index_air_agenda` provides both the monochromatic refractive index `refr_index_air`, in the following denoted as  $n$ , as well as the group refractive index `refr_index_air_group`, denoted as  $n_g$ . `refr_index_air` differs from `refr_index_air_group` in case of dispersion, which e.g. leads to diverging propagation paths at different frequencies.

**FIXME:** Describe where each variable is used. Expand ...

---

### History

120918 Started (Patrick Eriksson).

## 7.1 Gases

For calculating the contribution to the refractive index from atmospheric gases, the following workspace methods are currently available in ARTS: `refr_index_airMWgeneral`, `refr_index_airThayer` and `refr_index_airIR`. All of them are non-dispersive, i.e., monochromatic and group refractive index are identical. They are supposed to be applied as alternatives, not in addition to each other.

`refr_index_airMWgeneral` provides refractivity due to different gas mixtures as occurring in planetary atmospheres and is valid in the microwave spectral region. It uses the methodology introduced by *Newell and Baird* [1965] for calculating refractivity of the gas mixture at actual pressure and temperature conditions based on the refractivity of the individual gases at reference conditions. Reference refractivities from *Newell and Baird* [1965] are available for N<sub>2</sub>, O<sub>2</sub>, CO<sub>2</sub>, H<sub>2</sub>, and He. Additionally, reference refractivity for H<sub>2</sub>O has been derived from H<sub>2</sub>O contribution as described by `refr_index_airThayer` (see below) for a reference temperature of  $T_0=273.15$  K<sup>1</sup>. Any mixture of these gases can be taken into account. The missing contribution from further gases is roughly accounted for by normalising the calculated refractivity from the six reference gases to a volume mixing ratio of 1. More details on the applied formulas are given in Section 4.1.1 of *ARTS Theory*.

`refr_index_airThayer` calculates the microwave “air” refractivity in the Earth’s atmosphere taking into account refractivity of “dry air” and water vapour. All other gases are assumed to have a negligible contribution. More details are given in Section 4.1.2 of *ARTS Theory*.

`refr_index_airIR` derives the infrared “air” refractivity in the Earth’s atmosphere considering only refractivity of “dry air”. More details are given in Section 4.1.3 of *ARTS Theory*.

## 7.2 Free electrons

Free electrons, as exist in the ionosphere, affect propagating radio waves in several ways. Free electrons will have an impact of the propagation speed of radio waves, hence a signal can be delayed and refracted. This section considers only the refraction effect (neglecting influences of any magnetic field). For effects on polarisation state of the waves in presence of a static magnetic field, i.e., Faraday rotation, see Section 14.

`refr_index_airFreeElectrons` derives this contribution of free electrons to the refractive index. The method is only valid when the radiative transfer frequency is large enough (at least twice the plasma frequency). Information on theoretical background and details on the applied formulas are provided in Section 4.2 of *ARTS Theory*.

---

<sup>1</sup>Reducing the `refr_index_airThayer` approach to inverse temperature proportionality as applied by `refr_index_airMWgeneral` causes significant deviations from H<sub>2</sub>O refractivity from `refr_index_airThayer`. However, they are smaller than when refraction by H<sub>2</sub>O is not accounted for.

# Chapter 8

## Description of clouds

### 8.1 Introduction

In the Earth's atmosphere we find liquid water clouds consisting of approximately spherical water droplets and cirrus clouds consisting of ice particles of diverse shapes and sizes. We also find different kinds of aerosols. In order to take into account this variety, the model allows to define several *particle types*. A particle type is either a specified particle or a specified particle distribution, for example a particle ensemble following a gamma size distribution. The particles can be completely randomly oriented, azimuthally randomly oriented or arbitrarily oriented. For each particle type being a part of the modeled cloud field, a data file containing the single scattering properties ( $\langle \mathbf{K}_i \rangle$ ,  $\langle \mathbf{a}_i \rangle$ , and  $\langle \mathbf{Z}_i \rangle$ ), and the appropriate particle number density field is required. The particle number density fields are stored as `GField3`, including the field stored in a three-dimensional tensor and also the appropriate atmospheric grids (pressure, latitude and longitude grid). For each grid point in the cloud box the single scattering properties are averaged using the particle number density fields. In the scattering database the single scattering properties are not always stored in the same coordinate system. For instance for randomly oriented particles it makes sense to store the single scattering properties in the so-called scattering frame in order to reduce memory requirements. The following section describes in detail the `SingleScatteringData` class. The consequent section describes how to realize different kinds of size distributions in the ARTS frame by defining appropriate particle number density fields.

### 8.2 Single scattering properties

#### 8.2.1 Coordinate systems: The laboratory frame and the scattering frame

For radiative transfer calculations we need a coordinate system to describe the direction of propagation. For this purpose we use the laboratory frame, which is also shown in *ARTS Theory*, Figure 6.1. The z-axis corresponds to the local zenith direction and the x-axis points towards the north-pole. The propagation direction is described by the local zenith angle  $\theta$  and the local azimuth angle  $\phi$ . This coordinate system is the most appropriate frame to describe the propagation direction and the polarization state of the radiation. However, in

---

#### History

050913 Created and written by Claudia Emde

order to describe scattering of radiation by a particle or a particle ensemble, it makes sense to define another coordinate system taking into consideration the symmetries of the particle or the scattering medium, as one gets much simpler expressions for the single scattering properties. For macroscopically isotropic and mirror-symmetric scattering media it is convenient to use the scattering frame, in which the incidence direction is parallel to the z-axis and the x-axis coincides with the scattering plane, that is, the plane through the unit vectors  $\hat{\mathbf{n}}^{\text{inc}}$  and  $\hat{\mathbf{n}}^{\text{sca}}$ . The scattering frame is illustrated in Figure 8.1. For symmetry reasons the single scattering properties defined with respect to the scattering frame can only depend on the scattering angle  $\Theta$ ,

$$\Theta = \arccos(\hat{\mathbf{n}}^{\text{inc}} \cdot \hat{\mathbf{n}}^{\text{sca}}), \quad (8.1)$$

between the incident and the scattering direction.

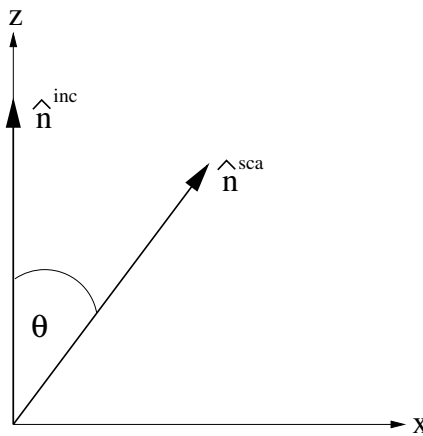


Figure 8.1: Illustration of the scattering frame. The z-axis coincides with the incident direction  $\hat{\mathbf{n}}^{\text{inc}}$ . The scattering angle  $\Theta$  is the angle between  $\hat{\mathbf{n}}^{\text{inc}}$  and  $\hat{\mathbf{n}}^{\text{sca}}$ .

## 8.2.2 Scattering datafile structure

The single scattering properties are pre-calculated, for example by using the T-matrix code by *Mishchenko et al.* [2002], and stored in data-files. Different methods for the calculation of single scattering properties are reviewed in *Emde* [2005].

The format of the scattering database allows space reduction due to symmetry for certain special cases, e.g. random orientation or horizontal alignment. The file format is XML. The data is stored in a class called `SingleScatteringData`, which resides in the files `optproperties.h`. The class consists of the following fields (compare also Table 8.2.2):

- *enum* ptype: An attribute which contains information about the data type, which is the classification of the kind of hydrometeor species (randomly oriented, general case ...). This attribute is needed in the radiative transfer function to be able to extract the physical phase matrix, the physical extinction matrix and the physical absorption vector from the data.

Possible values of ptype are:

```

PARTICLE_TYPE_GENERAL = 10
PARTICLE_TYPE_MACROS_ISO = 20
PARTICLE_TYPE_HORIZONTAL = 30

```

A more detailed description of the different cases is given below.

- *String* `description`: Here the particle type should be specified explicitly. We can have the case randomly oriented particles, but furthermore we also have to specify the exact particle properties (i.e. size and shape distribution). This can be a longer text describing how the scattering properties were generated. It should be formatted for direct printout to screen or file.
- *Vector* `f_grid`: Frequency grid [Unit: Hz].
- *Vector* `T_grid`: Temperature grid [Unit: K].
- *Vector* `za_grid`:
  1. `p10`, `p30`: Zenith angle grid (Range:  $0.0^\circ \leq za \leq 180.0^\circ$ ).
  2. `p20`: Scattering angle grid (Range:  $0.0^\circ \leq za \leq 180.0^\circ$ ).
- *Vector* `aa_grid`: Azimuth angle grid.
  1. `p10`: Range:  $-180.0^\circ \leq aa \leq 180.0^\circ$
  2. `p20`: Not needed, since optical properties depend only on scattering angle (dummy grid).
  3. `p30`: Only half of the grid is required (Range:  $0.0^\circ \leq aa \leq 180.0^\circ$ )

The angular grids have to satisfy the following conditions:

- They have to be equidistant.
- The value of the data must be the same for the first and the last grid-point. This condition is required for the integration routine.
- If we only have to store a part of the grid, for example `za_grid` only from  $0^\circ$  to  $90^\circ$ , these two values ( $0^\circ$ ,  $90^\circ$ ) must be grid-points.
- *Tensor7* `pha_mat_data`: Phase matrix data  $\langle \mathbf{Z} \rangle$  [Unit:  $\text{m}^2$ ]. The dimensions of the data array are:
 

```
[frequency temperature za_sca aa_sca za_inc aa_inc
matrix_element]
```

The order of matrix elements depends on the chosen case. For most cases we do not need all matrix elements (see description of cases below).
- *Tensor5* `ext_mat_data`: Extinction matrix data  $\langle \mathbf{K} \rangle$  [Unit:  $\text{m}^2$ ]. The dimensions are:

```
[frequency temperature za_inc aa_inc matrix_element]
```

Again, the order of matrix elements depends on the chosen case.

Table 8.1: Structure of single scattering data files

Symbol	Type	Dimensions	Description
	enum		specification of particle type
	String		short description of particle type
$\nu$	Vector	$(\nu)$	frequency grid
$T$	Vector	$(T)$	temperature grid
$\psi$	Vector	$(\psi)$	zenith angle grid
$\omega$	Vector	$(\omega)$	azimuth angle grid
$\langle \mathbf{Z} \rangle$	Tensor7	$(\nu, T, \psi, \omega, \psi', \omega', i)$	phase matrix
$\langle \mathbf{K} \rangle$	Tensor5	$(\nu, T, \psi, \omega, i)$	extinction matrix
$\langle \mathbf{a} \rangle$	Tensor5	$(\nu, T, \psi, \omega, i)$	absorption vector

- *Tensor5* `abs_vec_data`: Absorption vector data  $\langle \mathbf{a} \rangle$  [Unit:  $\text{m}^2$ ].

The absorption vector is also precalculated. It could be calculated from extinction matrix and phase matrix. But this calculation takes long computation time, as it requires an angular integration over the phase matrix. For the cases with symmetries (e.g., random orientation) the data files will not become too large even if we store additionally the absorption vector. The dimensions are:

```
[frequency temperature za_inc aa_inc vector.element]
```

### 8.2.3 Definition of particle types

#### Macroscopically isotropic and mirror-symmetric scattering media (p20)

For macroscopically isotropic and mirror-symmetric scattering media (totally randomly oriented particles) the optical properties are calculated in the so-called scattering frame as shown in Figure 8.1. In this coordinate system the z-axis corresponds to the incident direction and the xz-plane coincides with the scattering plane. Using this frame only the scattering angle, which is the angle between incident and scattered direction is needed. Furthermore the number of matrix elements of both matrices, phase matrix and extinction matrix, can be reduced (see *Mishchenko et al.* [2002], p.90). To calculate the particle optical properties it is convenient to use Mishchenko's T-matrix code for randomly oriented particles [*Mishchenko and Travis*, 1998] which returns the averaged phase matrix and extinction matrix. The only drawback is that the single scattering data has to be transformed from the particle frame representation to the laboratory frame representation. These transformations are described in the appendix of *Emde* [2005].

Only six elements of the transformed phase matrix, which is commonly called scattering matrix  $\mathbf{F}$ , are different. Therefore the size of `pha_mat_data` is:

```
[N_f N_T N_za_sca 1 1 1 6]
```

The order of the matrix elements is as follows:  $F11, F12, F22, F33, F34, F44$

The extinction matrix is in this case diagonal and independent of direction and polarization. That means that we need to store only one element for each frequency. Hence the size of `ext_mat_data` is



```
[N_f N_T 1 1 1]
```

The absorption vector is also direction and polarization independent. Therefore the size of `abs_vec_data` for this case is the same as `ext_mat_data`:

```
[N_f N_T 1 1 1]
```

**Horizontally aligned plates and columns (p30)** For particle distributions of horizontally aligned plates and columns that are oriented randomly in the azimuth the angular dimension can be reduced by one, if we rotate the coordinate system appropriately. For this case we use the T-matrix code for single particles in fixed orientation and average phase matrix and extinction matrix manually like in the general case.

The phase matrix (and also extinction matrix and absorption vector) become independent of the incident azimuth angle in this frame. Furthermore, regarding the symmetry of this case, it can be shown that for the scattered directions we need only half of the angular grids, as the two halves must contain the same data. `pha_mat_data` therefore has the following size:

```
[N_f N_T N_za_sca N_aa_sca N_za_inc/2+1 1 16]
```

We store `za_sca` for all grid points from  $0^\circ$  to  $180^\circ$ , `aa_sca` from  $0^\circ$  to  $180^\circ$ , and `za_inc` from  $0^\circ$  to  $90^\circ$ . This means that the zenith angle grid has to include  $90^\circ$  as grid-point. The order of the matrix elements is the same as in the general case. For this case it can be shown that the extinction matrix has only three elements  $K_{jj}$ ,  $K_{12}(=K_{21})$ , and  $K_{34}(=-K_{43})$ . Because of azimuthal symmetry, it can not depend on the azimuth angle. Hence the size of `ext_mat_data` is

```
[N_f N_T N_za/2+1 1 3]
```

The absorption coefficient vector has only two elements  $a_1$  and  $a_2$ . This means that the size of `abs_vec_data` is

```
[N_f N_T N_za/2+1 1 2]
```

**General case (p10)** If there are no symmetries at all we have to store all 16 elements of the phase matrix. The average phase matrix has to be generated from all individual phase matrices of the particles in the distribution outside ARTS. The individual phase matrices are calculated using Mishchenko's T-matrix code for single particles in fixed orientation [*Mishchenko, 2000*]. We have to store all elements for all angles in the grids. The size of `pha_mat_data` is therefore:

```
[N_f N_T N_za_sca N_aa_sca N_za_inc N_aa_inc 16]
```

The matrix elements have to be stored in the following order:  $Z_{11}$ ,  $Z_{12}$ ,  $Z_{13}$ ,  $Z_{14}$ ,  $Z_{21}$ ,  $Z_{22}$ , ... Seven extinction matrix elements are independent (cp. *Mishchenko et al. [2002]*, p.55). The elements being equal for single particles should still be equal for a distribution as we get the total extinction just by adding. Here we need only the incoming grids, so the size of `ext_mat_data` is:

```
[N_f N_T N_za_inc N_aa_inc 7]
```

The absorption vector in general has four components (cp. Equation (2.186) in *Mishchenko et al. [2002]*). The size of `abs_vec_data` is accordingly:

```
[N_f N_T N_za_inc N_aa_inc 4]
```

**Generating single scattering properties** It is very convenient to use the Python module PyARTS, which has been developed especially for ARTS and which is freely available at

<http://www.radiativetransfer.org/tools/>. This module can be used to generate single scattering properties for horizontally aligned as well as for randomly oriented particles in the ARTS data-file-format. PyARTS has been developed by C. Davis, who has implemented the Monte Carlo scattering algorithm in ARTS (see *ARTS Theory*, Section 8). The ATMLAB package includes functions to generate single scattering properties for spherical particles (Mie-Theory).

### 8.3 Representation of the particle size distribution

The particle size has an important impact on the scattering and absorption properties of cloud particles as shown for instance in [Emde *et al.*, 2004]. Clouds contain a whole range of different particle sizes, which can be described by a size distribution giving the number of particles per unit volume per unit radius interval as a function of radius. It is most convenient to parameterize the size distribution by analytical functions, because in this case optical properties can be calculated much faster than for arbitrary size distributions. The T-matrix code for randomly oriented particles includes several types of analytical size distributions, e.g., the gamma distribution or the log-normal distribution. This section presents the size distribution parameterizations, which were used for the ARTS simulations included in this thesis.

#### 8.3.1 Mono-disperse particle distribution

The most simple assumption is, that all particles in the cloud have the same size. In order to study scattering effects like polarization or the influence of particle shape, it makes sense to use this most simple assumption, because one can exclude effects resulting from the particle size distribution itself.

Along with the single scattering properties we need the particle number density field, which specifies the number of particles per cubic meter at each grid point, for ARTS scattering simulations. For a given *IMC* and mono-disperse particles the particle number density  $n^p$  is simply

$$n^p(IMC, r) = \frac{IMC}{m} = \frac{IMC}{V\rho} = \frac{3}{4\pi} \frac{IMC}{\rho r^3}, \quad (8.2)$$

where  $m$  is the mass of a particle,  $r$  is its equal volume sphere radius,  $\rho$  is its density, and  $V$  is its volume.

#### 8.3.2 Gamma size distribution

A commonly used distribution for radiative transfer modeling in cirrus clouds is the *gamma distribution*

$$n(r) = ar^\alpha \exp(-br). \quad (8.3)$$

The dimensionless parameter  $\alpha$  describes the width of the distribution. The other two parameters can be linked to the effective radius  $R_{eff}$  and the ice mass content *IMC* as follows:

$$b = \frac{\alpha+3}{R_{eff}}, \quad (8.4)$$

$$a = \frac{IMC}{4/3\pi\rho b^{-(\alpha+4)}\Gamma[\alpha+4]}, \quad (8.5)$$

where  $\rho$  is the density of the scattering medium and  $\Gamma$  is the gamma function. For cirrus clouds  $\rho$  corresponds to the bulk density of ice, which is approximately  $917 \text{ kg/m}^3$ .

Generally, the effective radius  $R_{eff}$  is defined as the average radius weighted by the particle cross-section

$$R_{eff} = \frac{1}{\langle A \rangle} \int_{r_{min}}^{r_{max}} A(r) r n(r) dr, \quad (8.6)$$

where  $A$  is the area of the geometric projection of a particle. The minimal and maximal particle sizes in the distribution are given by  $r_{min}$  and  $r_{max}$  respectively. In the case of spherical particles  $A = \pi r^2$ . The average area of the geometric projection per particle  $\langle A \rangle$  is given by

$$\langle A \rangle = \frac{\int_{r_{min}}^{r_{max}} A(r) n(r) dr}{\int_{r_{min}}^{r_{max}} n(r) dr}. \quad (8.7)$$

The question is how well a gamma distribution can represent the true particle size distribution in radiative transfer calculations. This question is investigated by *Evans et al. [1998]*. The authors come to the conclusion that a gamma distribution represents the distribution of realistic clouds quite well, provided that the parameters  $R_{eff}$ ,  $IMC$  and  $\alpha$  are chosen correctly. They show that setting  $\alpha = 1$  and calculating only  $R_{eff}$  gave an agreement within 15% in 90% of the considered measurements obtained during the First ISCCP Regional Experiment (FIRE). Therefore, for all calculations including gamma size distributions for ice particles,  $\alpha = 1$  was assumed.

The particle number density for size distributions is obtained by integration of the distribution function over all sizes:

$$n^p(IMC, R_{eff}) = \int_0^\infty n(r) dr \quad (8.8)$$

$$= \int_0^\infty a r^\alpha \exp(-br) dr = a \frac{\Gamma(\alpha+1)}{b^{\alpha+1}}. \quad (8.9)$$

After setting  $\alpha = 1$ , inserting Equation 8.5 and some simple algebra we obtain

$$n^p(IMC, R_{eff}) = \frac{2 IMC}{\pi \rho R_{eff}^3}. \quad (8.10)$$

Comparing Equation 8.2 and 8.10, we see that the particle number density for mono-disperse particles with a particle size of  $R$  is smaller than the particle number density for gamma distributed particles with  $R_{eff} = R$ . The reason is that in the gamma distribution most particles are smaller than  $R_{eff}$ .

### 8.3.3 Ice particle size parameterization by McFarquhar and Heymsfield

A more realistic parameterization of tropical cirrus ice crystal size distributions was derived by *McFarquhar and Heymsfield [1997]*, who derived the size distribution as a function of temperature and  $IMC$ . The parameterization was made based on observations during the Central Equatorial Pacific Experiment (CEPEX). Smaller ice crystals with an equal volume sphere radius of less than  $50 \mu m$  are parametrized as a sum of first-order gamma functions:

$$n(r) = \frac{12 \cdot IMC_{<50} \alpha_{<50}^5}{\pi \rho \Gamma(5)} \exp(-2\alpha_{<50} r), \quad (8.11)$$

where  $\alpha_{<50}$  is a parameter of the distribution, and  $IMC_{<50}$  is the mass of all crystals smaller than  $50 \mu m$  in the observed size distribution. Large ice crystals are represented better by a log-normal function

$$n(r) = \frac{3 \cdot IMC_{>50}}{\pi^{3/2} \rho \sqrt{2} \exp(3\mu_{>50} + (9/2)\sigma_{>50}^2) r \sigma_{>50} r_0^3} \cdot \exp \left[ -\frac{1}{2} \left( \frac{\log \frac{2r}{r_0} - \mu_{>50}}{\sigma_{>50}} \right)^2 \right], \quad (8.12)$$

where  $IMC_{>50}$  is the mass of all ice crystals greater than  $50 \mu m$  in the observed size distribution,  $r_0 = 1 \mu m$  is a parameter used to ensure that the equation does not depend on the choice of unit for  $r$ ,  $\sigma_{>50}$  is the geometric standard deviation of the distribution, and  $\mu_{>50}$  is the location of the mode of the log-normal distribution. The fitted parameters of the distribution can be looked up in the article by *McFarquhar and Heymsfield [1997]*. The particle number density field is obtained by numerical integration over a discrete set of size bins. This parameterization of particle size has been implemented in the PyARTS package, which was introduced in Section 8.2.2. Using PyARTS one can calculate the size distributions, the corresponding single scattering properties and the particle number density fields for given  $IMC$  and temperature.

## 8.4 Implementation

The workspace methods related to the description of clouds in ARTS are implemented in the file `m_cloudbox.cc`. Work space methods related to the optical properties of the clouds are implemented in the file `m_optproperties.cc`. The coordinate system transformations described above reside in the file `optproperties.cc`.

### 8.4.1 Work space methods and variables

The following controlfile section illustrates how a simple cloud can be included in an ARTS calculation.

First we have to define the cloudbox region, i.e. the region where scattering objects are found. To do this we use the method `cloudboxSetManuallyAltitude`:

```
cloudboxSetManuallyAltitude( cloudbox_on, cloudbox_limits,
                             atmosphere_dim, p_grid,
                             lat_grid, lon_grid,
                             8000, 120000,
                             0, 0, 0, 0 )
```

If we want to do a simulation for a cirrus cloud at an altitude from 9 to 11 km the cloudbox limits can be set to 8 and 12 km. The latitude and longitude limits are set to an arbitrary value for a 1D calculation. For 3D calculations they are also needed. Alternatively one can use the method `cloudboxSetManually`, where one has to provide pressure instead of altitude limits.

Now we have to specify the cloud particles inside the scattering region:

```
# Initialisation
ParticleTypeInit
# Only one particle type is added in this example
```

```

ParticleTypeAdd( scat_data_array, pnd_field_raw,
                 atmosphere_dim, f_grid, p_grid,
                 lat_grid, lon_grid, cloudbox_limits,
                 "ssd_sphere_50um_p20.xml",
                 "pnd_sphere_50um_p20.xml" )

```

In the workspace method **ParticleTypeAdd** the single scattering properties for one particle type are read. The generic input `filename_scat_data` must be set to the filename of a datafile including scattering data (class `SingleScatteringData`) in xml-format. The generic input `filename_pnd_field` must contain the filename of the corresponding particle number density field in xml-format (class `GField3`). If the cloud is composed of several different particle types **ParticleTypeAdd** can be used repeatedly for all particle types, for instance one could add to the randomly oriented spherical particles above horizontally aligned cylindrical particles:

```

ParticleTypeAdd( scat_data_array, pnd_field_raw,
                 atmosphere_dim, f_grid, p_grid,
                 lat_grid, lon_grid, cloudbox_limits,
                 "ssd_cylinder_30um_p30.xml",
                 "pnd_cylinder_30um_p30.xml" )

```

Alternatively it is possible to use the method **ParticleTypeAddAll**, which is convenient to generate a size distribution using several size bins. In this case one needs to define one particle type for each size bin. For many size bins the control file becomes very lengthy if one uses **ParticleTypeAdd** repeatedly. **ParticleTypeAddAll** requires as input an array of string including all filenames of the single scattering data files and the variable `pnd_field_raw` which includes the particle number density fields for all particle types. Using this function, one has to make sure that the order of the filenames containing the single scattering data corresponds to the order of the particle number density fields in `pnd_field_raw`. After reading the data the workspace variable `pnd_field` is calculated using `pnd_fieldCalc`:

```

# Calculate the particle number density field
pnd_fieldCalc

```

The definition of the single scattering data along with the corresponding particle number density fields is common in both scattering modules, the DOIT module described in Chapter 18 and the Monte Carlo module described in *ARTS Theory*, Chapter 8.



## **Part III**

# **Radiative transfer: clear-sky + general functionality**





## Chapter 9

# Clear-sky radiative transfer

This section discusses variables and the approach used to handle the actual radiative transfer calculations. This includes how effects caused by the sensor and surface are incorporated. Measurements of thermal emission in absence of particle scattering are used as example, and the basic theory for such simulations is also covered. The first ARTS version was developed for emission measurements, and such observations remain the standard case in ARTS.

A basic assumption for this chapter is thus that there is no particle scattering. This is denoted as clear-sky calculations. Scattering is restricted to the “cloud box” (Sec. 3.7). In short, the more demanding calculations are restricted to a smaller domain of the model atmosphere, and the radiative transfer in that domain is mainly treated by dedicated workspace methods. For pure transmission measurements (where scattering into the line-of-sight is neglected), see Chapter 15. This chapter discusses only the direct radiative transfer, partial derivatives (i.e. the Jacobian or weighting functions) are discussed in Section 16.

Absorption by atmospheric gases does normally not depend on polarisation but exceptions exist, where Zeeman splitting is one example. Both polarised and unpolarised absorption is handled. Even if the gaseous absorption in itself is unpolarised, the expressions to apply must allow that polarisation signals from the surface and the cloud box are correctly propagated to the sensor.

For an introduction to a complete radiative transfer calculations, see Chapter 5. For example, the content of this chapter corresponds roughly to the flowchart displayed in Figure 5.1, outlining a standard radiative transfer emission calculation. In fact, this chapter can be seen as a direct continuation of Chapter 5.

### 9.1 Overall calculation procedure

The structure handling complete radiative transfer calculations is fixed, where the main workspace method is denoted as `yCalc` (Fig. 5.1). That is, most ARTS control files include

---

#### History

- 130220 Revised after parts moved to a new chapter (Patrick Eriksson).
- 120831 Added flowchart and sections on polarised absorption, `iyCalc`, auxiliary data and dispersion (Patrick Eriksson).
- 110611 Extended and general revision (Patrick Eriksson).
- 050613 First complete version by Patrick Eriksson.

---

**Algorithm 1** Outline of the overall clear sky radiative transfer calculations (**yCalc**).

---

allocate memory for the matrix **y** (Equation 5.2)  
 allocate memory for the matrix  $\mathbf{i}_b$  (Equation 5.1)  
**for all** sensor positions **do**  
   **for all** pencil beam directions of the block **do** (Section 5.3)  
     call **iy\_main\_agenda**, giving  $\mathbf{i}_y$  (Algorithm 2)  
     copy  $\mathbf{i}_y$  to correct part of  $\mathbf{i}_b$   
   **end for**  
 put the product  $\mathbf{H}_b \mathbf{i}_b$  in correct part of **y**  
**end for**

---

**Algorithm 2** The main operations for methods to be part of **iy\_main\_agenda**.

---

determine the propagation path by **p\_path\_agenda** (Section 9.2)  
 determine the radiation at the start of the propagation path (Section 9.3)  
 perform radiative transfer along the propagation path (Section 9.4)  
 unit conversion of  $\mathbf{i}_y$  following **iy\_unit** (Section 9.5)

---

a call of **yCalc** and this section outlines this method and the associated main variables.

The calculation approach fits with the formalism presented in Sections 1.1-1.2 of *ARTS Theory*, where the separation between atmospheric radiative transfer and inclusion of sensor effects shall be noted especially, and a similar nomenclature is used here:

**y** : Complete measurement vector. In addition to atmospheric radiative transfer, the vector can include effects by sensor characteristics and data reduction operations. The corresponding workspace variable is **y**.

$\mathbf{i}_b$  : Monochromatic pencil beam data for a measurement block. The definition of a measurement block is found in Section 5.3. This vector is only affected by atmospheric radiative transfer. As workspace variable denoted as **iyb**, but can be considered as a pure internal variable and should not be of concern for the user.

$\mathbf{i}_y$  : Monochromatic data for one line-of-sight, i.e. a single pencil beam calculation. The corresponding workspace variable is **iy**. ( $\mathbf{i}_b$  consists of one or several  $\mathbf{i}_y$  appended.)

$\mathbf{H}_b$  : The complete sensor response matrix, for a measurement block. Can include data reduction. The corresponding workspace variable is **sensor\_response**.

The **yCalc** method is outlined in Algorithm 1. For further details of each calculation step, see the indicated equation or section. In summary, **yCalc** appends data from different pencil beam calculations and applies the sensor response matrix ( $\mathbf{H}_b$ ). The actual radiative transfer calculations are not part of **yCalc**.

Atmospheric radiative transfer is solved for each pencil beam direction (line-of-sight) separately. It is the task of **iy\_main\_agenda** (Algorithm 2) to perform a single clear sky radiative transfer calculation. This agenda, in its turn, makes us of other agendas, such as **p\_path\_agenda**. All methods developed for **iy\_main\_agenda** adapt automatically to the value of **stokes\_dim**.

That is, **yCalc** is a common method, independent of the details of the radiative transfer. For example, **yCalc** is used both if emission measurements or pure transmission data are simulated, that choice is made inside **iy\_main\_agenda**. The three following sections describes the main calculation steps of **iy\_main\_agenda**, in the order they are executed.

## 9.2 Propagation paths

A pencil beam path through the atmosphere to reach a position along a specific line-of-sight is denoted as the propagation path. Propagation paths are described by a set of points on the path, and the distance along the path between the points. These quantities, and a number of auxiliary variables, are stored together in a structure described in Section 10.5. The path points are primarily placed at the crossings of the path with the atmospheric grids (`p_grid`, `lat_grid` and `lon_grid`). A path point is also placed at the sensor if it is placed inside the atmosphere. Points of surface reflections are also included if such exist. More points can also be added to the propagation path, for example, by setting an upper limit for the distance along the path between the points. This is achieved by the variable `ppath.lmax`, see further Sections 9.9 and 10.1.

The propagation paths are determined basically by starting at the sensor and following the path backwards by some ray tracing technique. If the sensor is placed above the model atmosphere, geometrical calculations are used (as there is no refraction in space) to find the crossing between the path and the top of the atmosphere where the ray tracing then starts. Paths are tracked backwards until the top of the atmosphere or to an intersection with the cloud box or the surface. The propagation path (or paths) before a surface reflection is calculated when determining the up-welling radiation from the surface (Section 11.3). Example on propagation paths are shown in Figures 9.1 and 9.2.

Not all propagation paths are allowed for 2D and 3D. In short, the paths can only enter and leave the model atmosphere at the top of the atmosphere, as the atmospheric fields are treated to be undefined outside the covered latitude and longitude ranges.

Controlled by `ppath_step_agenda`, propagation paths can be calculated purely geometrically or considering refraction. When considering refraction, the refractive index is determined at each point along the path according to `refr_index_air_agenda`. Details about different methods applicable within `refr_index_air_agenda` are given in Chapter 7.

If nothing else is stated, it is assumed that all frequency components share a single propagation path. Another way to express this assumption is that dispersion is neglected. See Section 9.7 for how to consider dispersion. In the non-dispersive case, the propagation path is valid for average of the first and last element in `f_grid`, as this is the frequency given to `refr_index_air_agenda`.

Propagation paths can be calculated separately by the method `ppathCalc`, but for standard calculations the propagation paths are calculated internally by `yCalc`. Methods and variables to control the path calculations are discussed in Section 10.1.

## 9.3 The radiative background

The radiative intensity at the starting point of the path, and in the direction of the line-of-sight at that point, is denoted as the radiative background. Four possible radiative backgrounds exist:

**Space** When the propagation path starts at the top of the atmosphere, space is the radiative background. The normal case should be to set the radiation at the top of the atmosphere to be cosmic background radiation. An exception is when the sensor is directed towards the sun. The radiative background at the top of the atmosphere is determined by `iy_space_agenda`. If a propagation path is totally outside the model

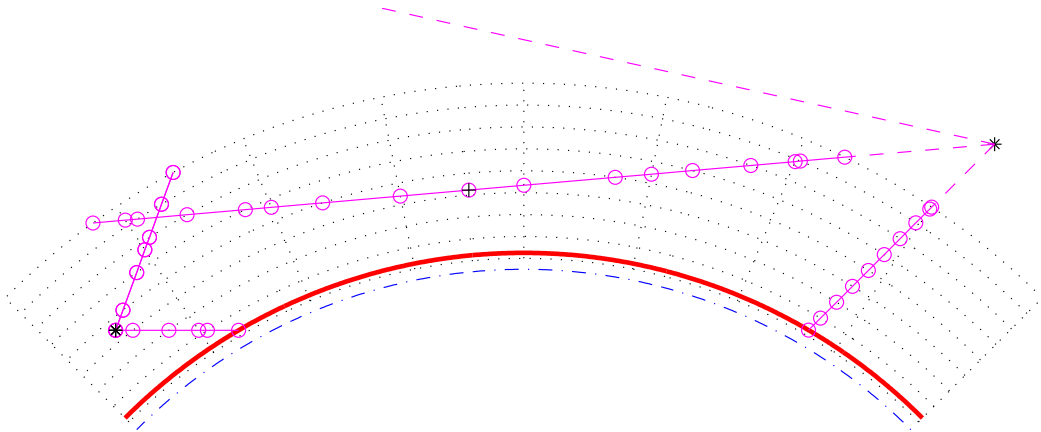


Figure 9.1: Examples on allowed propagation paths for a 2D atmosphere. The atmosphere is plotted as in Figure 3.2 beside that the points for the atmospheric fields are not emphasised. The position of the sensor is indicated by an asterisk (\*), the points defining the paths are plotted as circles ( $\circ$ ), joined by a solid line. The part of the path outside the atmosphere, not included in the path structure, is shown by a dashed line. Path points corresponding to a tangent point are marked by an extra plus sign ( $\oplus$ ); but note that these no longer are explicitly included as path point (in contrast to ARTS-2.0 and earlier). The shown paths include the minimum set of definition points. There exists also the possibility to add points inside the grid cells, for example, to ensure that the distance between the path points does not exceed a specified limit.

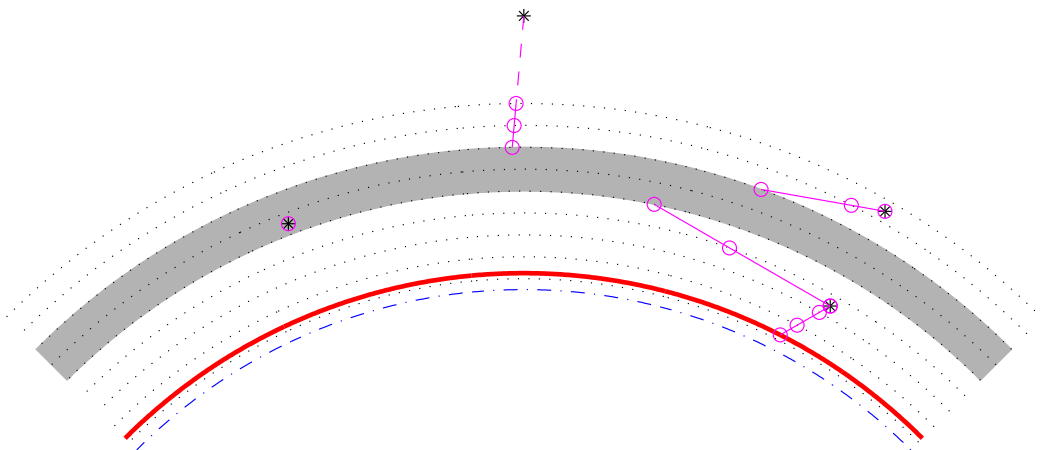


Figure 9.2: Examples on allowed propagation paths for a 1D atmosphere with an activated cloud box. Plotting symbols as in Figure 9.1. When the sensor is placed inside the cloud box, the path is defined with a single point, to know for which position and line-of-sight the intensity field of the cloud box shall be interpolated.

atmosphere, the observed monochromatic pencil beam intensity ( $i_y$  in Algorithm 1) equals the output of `iy_space_agenda`.

**The surface** The sum of surface emission and radiation reflected by the surface is the radiative background when the propagation path intersects with the surface. It is the task of `iy_surface_agenda` to return this up-welling radiation from the surface, see further Chapter 11.

**Surface of cloud box** For cases when the propagation path enters the cloud box the radiative background is the intensities leaving the cloud box. This radiation is obtained by `iy_cloudbox_agenda`.

**Interior of cloud box** If the sensor is situated inside the cloud box, there is basically no propagation path. The radiative background, and also the final spectrum, equals the internal intensity field of the cloud box at the position of the sensor, in the direction of the sensor line-of-sight. This case is also handled by `iy_cloudbox_agenda`.

It should be noted that except for the first case above, the determination of the radiative background involves further radiative transfer calculations. For example, in the case of surface reflection, the down-welling radiation could be determined by a new call of `iy_main_agenda` and the radiative background for that calculation is then space or the cloud box. The intensity field entering the cloud box is in some cases calculated by calls of `iy_main_agenda` (with cloud box deactivated) and the radiative background for these calculations is then space or the surface. This results in that space is normally the ultimate radiative background for the calculations. The exception is for propagation paths that intersects with the surface, and the surface is treated to act as a blackbody. For such cases, the propagation path effectively starts at the surface.

## 9.4 Basic radiative transfer variables and expressions

This section describes how the core radiative transfer equation is solved practically in ARTS. As mentioned, in this chapter focus is put on emission measurements. Local thermodynamic equilibrium (LTE) is throughout assumed. The equation to solve is Equation 4.13:

$$\frac{ds}{dl} = \mathbf{A}_a [\mathbf{b} - \mathbf{s}] = -\mathbf{A}_a \mathbf{s} + B \mathbf{a}_a, \quad (9.1)$$

where the involved quantities are defined and discussed in Section 4.2.

### 9.4.1 Unpolarised absorption

Let's start with the simpler case of non-polarised absorption (that is, the absorption is independent of polarisation state). For unpolarised absorption the matrix  $\mathbf{A}_a$  is diagonal, with all diagonal elements equal, and only the first of the elements of  $\mathbf{a}_a$  is non-zero.

The radiative transfer equation above can be solved in many ways, and with different level of refinement. The standard approach in ARTS is to solve the radiative transfer from one point of the propagation path to next. For the first Stokes element the following expression is applied (compare *ARTS Theory*, Equation 6.55)

$$I_{i+1} = I_i e^{-\tau_i} + \bar{B}_i (1 - e^{-\tau_i}), \quad (9.2)$$

with

$$\bar{B}_i = (B(T_i) + B(T_{i+1}))/2, \quad (9.3)$$

$$\tau_i = \Delta l_i(\alpha_i + \alpha_{i+1})/2, \quad (9.4)$$

where  $I_i$ ,  $T_i$  and  $\alpha_i$  are the radiance, temperature and absorption coefficient, respectively, at point  $i$  of the propagation path, and  $\Delta l_i$  is the distance along the path between point  $i$  and  $i + 1$ . That is,  $\bar{B}_i$  is an average of the Planck function at the path step end points, and the absorption is assumed to vary linearly between the two points. The start value of  $I$  is governed by the radiative background (Section 9.3).

A consequence of unpolarised absorption is that also the emission is unpolarised, and the emission term vanishes for higher Stokes elements. Accordingly, the expression for the second Stokes component is

$$Q_{i+1}(\nu) = Q_i(\nu)e^{-\tau_i}. \quad (9.5)$$

The third and fourth Stokes component are handled likewise. The expressions above are implemented in the workspace method `iyEmissionStandard`, intended to be part of `iy_main_agenda`.

An alternative way to perform the calculations for the first Stokes element would be

$$I = \sum_i t_{i+1} \bar{B}_i (1 - e^{-\tau_i}), \quad (9.6)$$

where  $I$  is the final intensity and  $t_i$  is the transmission between the sensor and point  $i$ . This calculation approach is not used as it fits poorer with the calculation of weighting functions ( $I_i$  must be known, Section 16). However, the calculation of weighting functions is simplified if  $\mathbf{T}_i$  is at hand, and this quantity is also tracked by `iyEmissionStandard`.

## 9.4.2 Polarised absorption

The overall calculation procedure is the same with polarised absorption, the only difference is the radiative transfer expression applied. The calculations for the different Stokes components can here not be separated, and matrix-vector notation is required:

$$\mathbf{s}_{i+1} = e^{-\Delta l_i \bar{\mathbf{K}}_i} \mathbf{s}_i + (\mathbf{1} - e^{-\Delta l_i \bar{\mathbf{K}}_i}) \bar{\mathbf{b}}_i, \quad (9.7)$$

where  $\mathbf{1}$  is the identity matrix. The  $\mathbf{K}$  and  $\mathbf{b}$  at point  $i$  and  $i + 1$  are averaged (element-wise) to give  $\bar{\mathbf{K}}$  and  $\bar{\mathbf{b}}$ , respectively, in line with Equation 9.4. The calculation of the transmission matrix,

$$\mathbf{T}_i = e^{-\Delta l_i \bar{\mathbf{K}}_i}, \quad (9.8)$$

involves a matrix exponential. This calculation step is handled for simpler cases with analytical expressions, while for more complex cases the Padé approximation (*ARTS Developer Guide*, Section 7.3) is applied. Only the first element of  $\bar{\mathbf{b}}$  is non-zero, and only the first column of the matrix corresponding to the term  $(\mathbf{1} - e^{-\Delta l_i \bar{\mathbf{K}}_i})$  is of interest.

### 9.4.3 Blackbody and cosmic background radiation

The term  $B$  is set by `blackbody_radiation_agenda`. The setting of this agenda basically determines the unit of the final outcome of Eq. 9.2, see further Sec. 9.5. For radiance calculations, the standard workspace method to use inside `blackbody_radiation_agenda` is `blackbody_radiationPlanck`. The Planck function is in this method, and in ARTS generally, defined as

$$B(T) = \frac{2h\nu^3}{c^2(\exp(h\nu/k_bT) - 1)} \quad (9.9)$$

where  $h$  is the Planck constant,  $c$  the speed of light and  $k_b$  the Boltzmann constant. This expression gives the total power, per unit frequency per unit area per solid angle. (The Planck function can also be defined as a function of wavelength.) The expression in Equation 9.9 deviates from the exact definition (see Eq. 6.16 in *ARTS Theory*) as it includes  $c$  instead of the local propagation speed ( $v$ ). The reason for this is the n<sup>2</sup>-law of radiance, discussed in the section below.

As long as cosmic background radiation is the only type of non-telluric radiation that has to be considered, the standard method for inclusion in `iy_space_agenda` is `MatrixCBR` (together with some calls of `Ignore`). Please, note that `blackbody_radiation_agenda` and `iy_space_agenda`, as well as `iy_surface_agenda`, must be defined in a consistent manner (that they use the same unit for  $B$ ).

## 9.5 Output unit and the n<sup>2</sup>-law

First of all, it should be noticed that ARTS does not enforce any fixed unit for calculated spectra ( $y$ ), it depends on the calculation set-up. For example, if emission is considered, or if just transmissions are calculated.

The primary unit for emission data (radiance) is [W/(Hz·m<sup>2</sup>·sr)]. The emission intensity corresponds directly with the definition of the Planck function (Eq. 9.9). Conversion to other units is selected by the `iy_unit` workspace variable. The standard manner is to apply the unit conversion as part of the calculations performed inside `yCalc`. See the built-in documentation of the workspace method you have selected for `iy_main_agenda` for comments on practical aspects and available output units. The most extensive support for conversion to other units is provided by `iyEmissionStandard`, while other methods have no support at all (ie. they ignore `iy_unit`). It is also possible to change the unit as a post-processing step by `yApplyUnit` (or `iyApplyUnit`), but some restrictions apply and there are no automatic checks if the input data have correct unit. Further considerations and expressions for the unit conversion are discussed in the ARTS-2 journal paper [Eriksson *et al.*, 2011, Sec. 5.7].

The n<sup>2</sup>-law of radiance is introduced in Section 6.5 of *ARTS Theory*. As shown in that section, the main impact of the law is handled by consistently using the vacuum speed in the definition of the Planck radiation law, as done inside ARTS (Eq. 9.9). This suffices if the sensor is placed in space (where the refractive index is 1), or if you use brightness temperatures. Remaining cases are also handled exactly if `iyEmissionStandard` is used. For those remaining cases, radiance data shall be scaled with the refractive index squared at the observation position. For Earth, the maximum value of this factor is about 0.1 %, and can anyhow normally be neglected.

In summary, there is normally no need for you as an user to consider the n<sup>2</sup>-law. The exception is if you extract radiance data for a point inside an atmosphere, and the refractive index deviates significantly from 1 at this point.

## 9.6 Single pencil beam calculations

The text above assumes that `yCalc` is used. This method can always be used, but `yCalc` is not mandatory if the simulations only deal with monochromatic data for a single line-of-sight. In this case, it could be more handy to use `iyCalc`, which basically is a direct call of `iy_main_agenda`. A reason for selecting `iyCalc` is that a larger set of auxiliary quantities can be extracted (Sec. 9.8).

On the input side, the main difference when using `iyCalc` is that the observation position and line-of-sight are specified by `rte_pos` and `rte_los` (instead of `sensor_pos` and `sensor_los`). The calculated radiances are returned as the matrix `iy` (instead of the vector `y`). No automatic unit conversion is made inside `iyCalc`. This is instead handled separately by `iyApplyUnit`.

## 9.7 Dispersion

The clear-sky radiative transfer methods handle all frequencies in `f_grid` in parallel, for efficiency reasons. One consequence of this feature is that only a single propagation path is calculated, that is assumed to be common for all frequencies. With other words, dispersion is not considered. This is in general an acceptable simplification, but exceptions exist where one example is radiative transfer through the ionosphere at frequencies approaching the “plasma frequency”.

When dispersion is expected to give a significant impact on the results, ARTS offers a general solution. Dispersion can be handled by setting `iy_main_agenda` as:

```
AgendaSet ( iy_main_agenda ) {
    iyLoopFrequencies
}
```

The radiative transfer method you put in `iy_main_agenda` for non-dispersive calculations are now moved to `iy_sub_agenda`. For example, if `iyEmissionStandard` is the method of your choice:

```
AgendaSet ( iy_sub_agenda ) {
    iyEmissionStandard
}
```

The approach is simple, `iyLoopFrequencies` calls `iy_sub_agenda` for each single frequency in `f_grid` and appends the output. With some details, `iyLoopFrequencies` performs a loop over the `f_grid`, creates an internal `f_grid` of length 1 holding the frequency of concern and calls `iy_sub_agenda` with this length-1 frequency grid. This has the result that a propagation path is calculated for each frequency component.

Some more steps are required to correctly include dispersion. A basic demand is that `ppath_agenda` considers refraction. Further, `refr_index_air_agenda` must provide a dispersive refractive index. Most methods aimed for `refr_index_air_agenda` give a refractive index that does not varies with frequency. An example on the opposite is `refr_index_airFreeElectrons`. If a method with dispersive refractive index is used for non-dispersive calculations, it receives the mean of the first and last element in `f_grid` (as already commented above).

A limitation of `iyLoopFrequencies` is that it can not be combined with auxiliary data of along-the-path character (Sec. 9.8)



## 9.8 Auxiliary data

The core output of the radiative calculations is **y** (**iy** if **iyCalc** is used, jacobians discussed in Sec. 16), but different auxiliary data can be extracted. First of all, **yCalc** outputs automatically **y\_f**, **y\_pol**, **y\_pos** and **y\_los**. These data give information about the frequency, polarisation, sensor position and sensor bore-sight, respectively, corresponding to each value in **y**. The content of the variables are governed by the sensor settings and the order calculated radiances are stored (discussed in Sec. 5.3).

A more general mechanism for extracting auxiliary data is controlled by the **iy\_aux\_vars** workspace variable. This mechanism is most useful together with **iyCalc**, and for the moment we assume that this method is used (limitations for **yCalc** are discussed below). The quantities that can be extracted differ, see the built-in documentation for the options for each workspace method of concern, e.g.:

```
arts -d iyEmissionStandard
```

The options for this particular method (**iyEmissionStandard**) can be divided into different groups (more variables will/can be added):

**Atmosphere, along-the-path** The pressure, temperature and volume mixing ratios along the propagation path.

**Attenuation, along-the-path** Total and species specific absorption coefficients along the propagation path.

**Radiative properties, along-the-path** The radiance at each propagation path point.

**Overall radiative properties** The total (clear-sky) optical depth along the path and flag giving the radiative background.

“Along-the-path” means that data are provided for each point of the propagation path. The path is described by **ppath**, that is also returned by **iy\_main\_agenda**. The **ppath** variable contains the information needed to geo-position, for example, “along-the path temperatures”.

Example on setting of **iy\_aux\_vars** (again valid for **iyEmissionStandard**):

```
ArrayOfStringSet( iy_aux_vars,
  [ "Temperature",
    "VMR, species 0",
    "Absorption, summed",
    "Absorption, species 0",
    "Absorption, species 2",
    "iy",
    "Optical depth" ] )
```

The data are outputted in a single variable, **iy\_aux**. This variable is an array of Tensor4. All dimensions are used when storing e.g. the propagation matrix along the path (for all frequencies of **f\_grid**). For other types of quantities, one or several dimensions are set to have length 1. See the built-in documentation for further details, such as the order of the data dimensions.

Storage of quantities of “along-the-path” type assumes that there exists a common propagation path. This is necessarily not the case for calculations by **yCalc**. This is the case as a calculation considering an antenna response includes radiative transfer along several propagation paths. The points of these paths do not end up on common altitude grid, neither

are at a fixed distance from the sensor. In fact, the number of points of the paths will likely differ. For this reason, `yCalc` will issue an error if you in `iy_aux_vars` include a quantity of “along-the-path” character.

The same applies to dispersion calculations (here the propagation path differs already between the frequencies), and also `iyLoopFrequencies` gives also an error if “along-the-path” auxiliary data are selected.

To simplify the practical usage this mechanism to extract auxiliary data, `iyEmissionStandard` also accepts some other variable, related to particle properties, but do not trigger any calculations. The corresponding elements of `iy_aux` can at a later stage be filled with `iy_auxFillParticleVariables`. This feature can be useful for checking if any particles are found along the propagation path, to determine if scattering calculations are required.

## 9.9 Calculation accuracy

The accuracy of the calculations depends on many factors. For many factors, such as spectroscopic parameters, there is nothing else to do than using best available data. On the other hand, for other factors there is a trade-off between accuracy and speed. More accurate calculations require normally also more computer memory. All different grids and the propagation path step length fall into this category of accuracy factors. It could be worth discussing the selection of atmospheric grids and the path step length as there can be some confusion about how that affects the accuracy.

The main purpose of the atmospheric grids (`p_grid`, `lat_grid` and `lon_grid`) is to build up the mesh on which the atmospheric fields are defined. This means that the spacing of these grids shall be selected having the representation of the atmospheric fields in mind. That is, the spacing shall be fine enough that the atmospheric field is sufficiently well approximated by the piece-wise (multi-)linear representation between the grid crossings. The result is that a finer spacing must be used to represent correctly atmospheric fields with a lot of structure, while the grids can have fewer points when the atmospheric fields are smooth.

The accuracy when performing the actual radiative transfer calculations depends on the refinement of the expressions used and the discretisation of the propagation path. If Equation 9.2 is used, the underlying assumption is that the Planck function and the absorption vary linearly along the propagation path step. These assumptions are of course less violated if the path step length is made small. An upper limit of the path step length is set by `ppath_lmax`. In many cases it should suffice to just include path points at the crossings of the atmospheric grids (`ppath_lmax ≤ 0`). An exception can be limb sounding where the path step length can be very long around the tangent point, but a limit of about 25 km should suffice normally. See also Section 10.3.

# Chapter 10

## Propagation paths

A propagation path is the name given in ARTS to the way the radiation travels to reach the sensor for a specified line-of-sight. Propagation paths are introduced in Section 9.2 and this section provides further details. For a general usage of ARTS, it should suffice to read Section 10.1. The remaining sub-sections deal with more low-level aspects of the calculations, and are of interest only if you want to understand the finer details of ARTS. The actual equations applied are found in Chapter 7 of *ARTS Theory*.

### 10.1 Practical usage

The overall calculation approach for finding the propagation path is specified by `ppath_agenda`. The standard choice for this agenda is `ppathStepByStep`, applying `ppath_step_agenda` repeatedly in order to trace the path backwards, starting at the sensor. This set-up is assumed throughout this chapter. A slightly different selection of workspace methods is required for radio link calculations, see further Section 15.2.

The exact ray tracing algorithm to be applied for the calculation of propagation path is selected through `ppath_step_agenda` (see further Section 9.2). The fastest calculations are obtained if refraction is neglected, denoted as geometrical calculations. The workspace method to apply if this assumption can be made is `ppath_stepGeometric`.

The main consideration for using `ppath_stepGeometric` is to select a value for `ppath_lmax`. This variable controls to some extent the calculation accuracy, as described in Section 9.9. This variable sets the maximum distance between points of the propagation path. Set this variable to e.g. -1 if you don't want to apply such a length criterion.

A straightforward, but inefficient, treatment of refraction is provided by `ppath_stepRefractionBasic`. This method divides the propagation path into a series of geometrical ray tracing steps. The size of the ray tracing steps is selected by `ppath_lraytrace`. This variable affects only the ray tracing part, the distance between points of the propagation path actually returned is controlled by `ppath_lmax` as above. At each ray tracing step, the refractive index is evaluated according to the specification of `refr_index_air_agenda`. Several methods to determine refractive index are available (see Chapter 7).

---

#### History

120202 Revised and parts moved to *ARTS Theory* (Patrick Eriksson).  
030310 First complete version written by Patrick Eriksson.

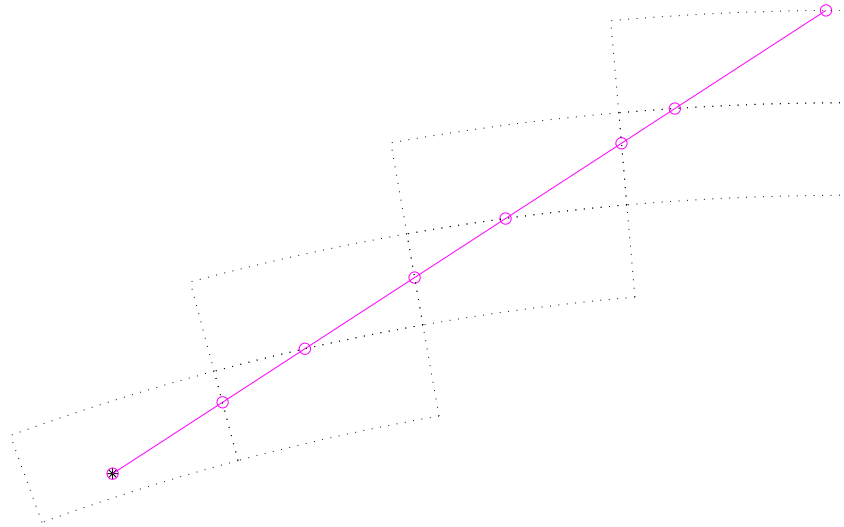


Figure 10.1: Tracking of propagation paths. For legend, see Figure 10.2. The figure tries to visualize how the calculations of propagation paths are performed from one grid cell to next. In this example, the calculations start directly at the sensor position (\*) as it placed inside the model atmosphere. The circles give the points defining the propagation path. Path points are always included at the crossings of the grid cell boundaries. Such a point is then used as the starting point for the calculations inside the next grid cell.

## 10.2 Calculation approach

The propagation paths are calculated in steps, as outlined in Section 9.2. The path steps are normally from one crossing of the atmospheric grids to next. To introduce propagation paths steps was necessary to handle the iterative solution for scattering inside the cloud box, as made clear from Figure 18.2.

A full propagation path is stored in the workspace variable `p_path`, that is of the type `P_path` (see Section 10.5). The paths are determined by calculating a number of path steps. A path step is the path from a point to the next crossing of either the pressure, latitude or longitude grid (Figure 10.1). There is one exception to this definition of a path step, and that is when there is an intersection with the surface, which ends the propagation path at that point. The starting point for the calculation of a path step is normally a grid crossing point, but can also be an arbitrary point inside the atmosphere, such as the sensor position. The path steps are stored in the workspace variable `p_path_step`, that is of the same type as `p_path`.

Propagation paths are calculated with the internal function `p_path_calc`. The communication between this method and `p_path_step_agenda` is handled by `p_path_step`. That variable is used both as input and output to `p_path_step_agenda`. The agenda gets back `p_path_step` as returned to `p_path_calc` and the last path point hold by the structure is accordingly the starting point for the new calculations. If a total propagation path shall be determined, the agenda is called repeatedly until the starting point of the propagation path is found.

The path is determined by starting at the end point and moving backwards to the starting point. The calculations are initiated by filling `p_path_step` with the practical end point of the path. This is either the position of the sensor (true or hypothetical), or some point at the top

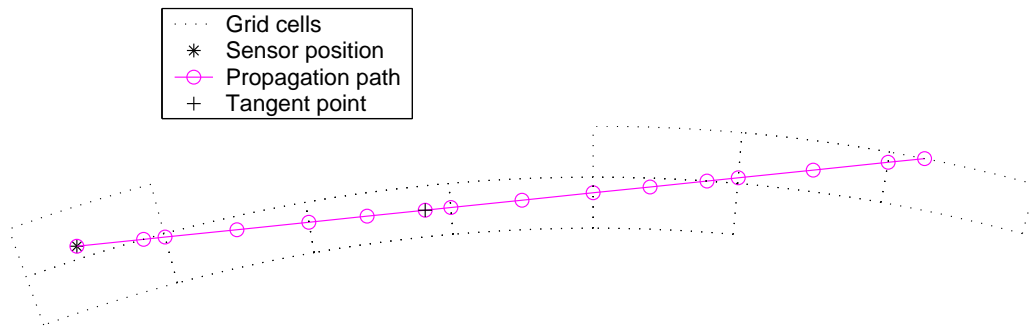


Figure 10.2: As Figure 10.1, but with a length criterion for the distance between the points defining the path. Note: Tangent points are no longer included automatically.

of the atmosphere (determined by geometrical calculations starting at the sensor).

The agenda performs only calculations to next crossing of a grid, all other tasks are performed by `ppath_calc`, with one exception. If there is an intersection with the surface, the calculations stop at this point. This is flagged by setting the background field of `ppath_step`. Beside this, `ppath_calc` checks if the starting point of the calculations is inside the cloud box or below the surface level, and check if the last point of the path has been reached.

### 10.3 Spacing of additional path points

The strategy when considering `ppath_lmax` differs somewhat between the workspace methods. For pure geometrical calculations, the points are spaced evenly inside the grid box. That is, the points are separated with the same distance ( $\leq$  `ppath_lmax`).

When refraction is considered, the ray tracing moves forward in steps following `ppath_lraytrace`. When another step of this size would result in a distance  $>$  `ppath_lmax`, the present point is added to `ppath_step`. A consequence of this is that additional points are likely not evenly spaced. The distance between most points will be `ppath_lraytrace` times an integer value, but the distance between the last additional point and the grid border can be any number ( $\leq$  `ppath_lmax`). If `ppath_step` is set to be negative, no additional points are included, as for geometrical calculations.

As points are always included in the propagation paths at the crossings of the atmospheric grids, making these grids finer will give shorter path steps. However, it is neither good practise or efficient to use the atmospheric grids to control the accuracy of the radiative transfer calculations. An upper limit on the step length (`ppath_lmax`) shall be applied for this purpose.

### 10.4 Tangent points

The term “tangent point” refers to the point of a limb sounding path with the lowest altitude. For 1D cases this definition is clear, but for 2D and 3D calculations there are complications. First of all, there are two different possible definitions: the point having the lowest radius (ie. distance to the planets centre) or the point with the lowest altitude (ie. vertical distance to the reference ellipsoid). The later is the more important with respect to optical thickness

of the path, but the point of the highest pressure would be an even more relevant definition in this context. Another complication is that with refraction there can in principle exist more than one tangent point.

Up to ARTS-2.0 minimum-radius tangent points were added as extra points to the propagation paths (a reminiscent from ARTS-1), but this feature has now been removed following the discussion in the paragraph above. However, many internal functions make use of the concept of tangent point (as the minimum-radius one). The altitude-based tangent point for a propagation path can be determined with the method `TangentPointExtract`.

## 10.5 The propagation path data structure

A propagation path is represented by a structure of type `Ppath`. This structure holds also auxiliary variables to facilitate the radiative transfer calculations and to speed up the interpolation. The fields of `Ppath` are as follows:

**dim** [Index] The atmospheric dimensionality. This field shall always be equal to the workspace variable `atmosphere_dim`.

**np** [Index] Number of positions to define the propagation path through the atmosphere. Allowed values are  $\geq 1$ . The number of rows of `pos` and `los`, and the length of `z`, `gp_p`, `gp_lat` and `gp_lon`, shall be equal to `np`. The length of `l_step` is `np - 1`. If `np ≤ 1`, the observed spectrum is identical to the radiative background. For cases where the sensor is placed inside the model atmosphere and `np = 1`, the stored position is identical to the sensor position and that position can be used to determinate the radiative background (see below).

**constant** [Numeric] The propagation path constant. It is defined as the product:  $rn \sin(\psi)$  (see Chapter 7.4.1 of *ARTS Theory*), at the position of the sensor. This is a true constant for the path just for 1D atmospheres, but can be useful also in other cases. For example, it equals the impact parameter normally used to define limb radio occultations. This field is initiated -1, to indicate that the constant is not yet set.

**background** [String] The radiative background for the propagation path. The possible options for this field are 'space', 'surface', 'cloud box interior' and 'cloud box level', where the source of radiation should be clear the content of the strings.

**start\_pos** [Vector] The practical start position of the propagation path. This vector equals in general the last row of `pos`. The exception is radio link calculations where the transmitter is placed above the model atmosphere, where this field gives the position of the transmitter.

**start\_los** [Vector] Line-of-sight at start point of propagation path. Set and used in the same way as `start_pos`.

**start\_lstep** [Numeric] The distance between `start_pos` and the last position in `pos`. This value is zero, except for a transmitter placed above the top-of-the-atmosphere. Hence, this length corresponds to propagation in free space (`n=1`).

**end\_pos** [Vector] The end position of the propagation path. If the point is placed inside the atmosphere, this field is redundant as it is equal to the first row of `pos`, but identifies the sensor position for observations from space.

- end\_los** [Vector] The line-of-sight at the end point of the propagation path. Provides additional information if the sensor is placed above the top-of-the-atmosphere, and gives then the observation direction of the sensor.
- end\_lstep** [Numeric] The distance between `end_pos` and the first position in `pos`. This value is non-zero just if the sensor is placed above the top-of-the-atmosphere. Hence, this length corresponds to propagation in free space ( $n=1$ ).
- pos** [Matrix] The position of the propagation path points inside the atmosphere. This matrix has `np` rows and up to 3 columns. Each row holds a position where column 1 is the radius, column 2 the latitude and column 3 the longitude (cf. Section 5.2.1). The number of columns for 1D and 2D is 2, while for 3D it is 3. The latitudes are stored for 1D cases as these can be of interest for some applications and are useful if the propagation path shall be plotted. The latitudes for 1D give the angular distance to the sensor (see further Section 3.2). The propagation path is stored in reversed order, that is, the position with index 0 is the path point closest to the sensor (and equals `start_pos` if it is inside the atmosphere).
- los** [Matrix] The line-of-sight of the propagation path at each point. The number of rows of the matrix is `np`. For 1D and 2D, the matrix has a single column holding the zenith angle. For 3D there is an additional column giving the azimuth angle. The zenith and azimuth angles are defined in Section 5.2.2. If the radiative background is the cloud box, the last position (in `pos`) and line-of-sight give the relevant information needed when extracting the radiative background from the cloud box intensity field.
- r** [Vector] The radius for each path position. The length of this vector is accordingly `np`. This is a help variable for plotting and similar purposes.
- lstep** [Vector] The length along the propagation path between the positions in `pos`. The first value is the length between the first and second point etc.
- nreal** [Vector] The real part of the refractive index at each path position. This index corresponds to the phase velocity.
- ngroup** [Vector] The group index of refraction. This index corresponds to the group velocity.
- gp\_p** [ArrayOfGridPos] Index position with respect to the pressure grid. The structure for grid positions is described in *ARTS Developer Guide*, Section 5.4.
- gp\_lat** [ArrayOfGridPos] As `gp_p` but with respect to the latitude grid.
- gp\_lon** [ArrayOfGridPos] As `gp_p` but with respect to the longitude grid.

## 10.6 Further reading

The implementation, calculation approaches and the numerical expressions used are discussed in Chapter 7 of *ARTS Theory*.





# Chapter 11

## Reference ellipsoid and surface properties

### 11.1 The reference ellipsoid

The ellipsoid is an imaginary surface used as a reference when specifying the surface altitude and the altitude of pressure levels. As the name indicates, this reference surface is defined as an ellipsoid. The reference ellipsoid should normally be set to some global geodetic datum, such as WGS-84. Inside ARTS, the ellipsoid is represented as a vector denoted as `refellipsoid`. This vector must have length two, where the two elements are equatorial radius ( $r_e$ ) and eccentricity ( $e$ ), respectively.

#### 11.1.1 Ellipsoid models

A geodetic datum is based on a reference ellipsoid. The ellipsoid is rotationally symmetric around the north-south axis. That is, the ellipsoid radius has no longitude variation, it is only a function of latitude. The ellipsoid is described by an equatorial radius,  $r_e$ , and a polar radius,  $r_p$ . These radii are indicated in Figure 11.1. The definition of the ellipsoid used in ARTS is based on  $r_e$  and the eccentricity,  $e$ :

$$e = \sqrt{1 - r_e^2/r_p^2}. \quad (11.1)$$

Workspace methods to set the reference ellipsoid for a particular planet include `refellipsoidEarth`, `refellipsoidMars` and `refellipsoidMars`.

The radius of the ellipsoid for a given (geocentric) latitude,  $\alpha$ , is

$$r_{\odot}(\alpha) = \sqrt{\frac{r_e^2 r_p^2}{r_e^2 \sin^2 \alpha + r_p^2 \cos^2 \alpha}} = \frac{r_p}{\sqrt{\sin^2 \alpha + (1 - e^2) \cos^2 \alpha}} \quad (11.2)$$

The radius given by Equation 11.2 can be directly applied for 3D atmospheres. For 2D cases, the ellipsoid data must be adopted. The assumption inside ARTS is that the 2D plane goes through the North and South poles. The polar radius to apply should then match

---

#### History

120224 Extended and revised (Patrick Eriksson).

050613 First version finished by Patrick Eriksson.

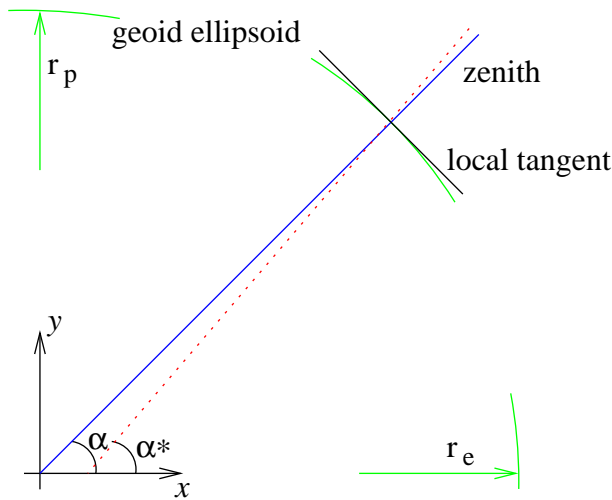


Figure 11.1: Definition of the ellipsoid radii,  $r_e$  and  $r_p$ , geocentric latitude,  $\alpha$ , and geodetic latitude,  $\alpha^*$ . The dotted line is the normal to the local tangent of the ellipsoid. The zenith and nadir directions, and geometrical altitudes, are here defined to follow the solid line.

the real ellipsoid radius at the highest latitude inside the satellite orbit plane. The method `refellipsoidOrbitPlane` performs this operation.

Further, for 1D cases the reference ellipsoid is by definition a sphere and the radius of this sphere shall be selected in such way that it represents the local shape of a reference ellipsoid. This is achieved with `refellipsoidForAzimuth`, that sets  $r_e$  to the local radius of curvature of the ellipsoid and  $e$  to zero. The curvature radius differs from the local radius except at the equator and an east-west direction. For example, at the equator and a north-south direction, the curvature radius is smaller than the local radius, while at the poles (for all directions) it is greater (see further Figure 11.2). The curvature radius,  $r_c$ , of an ellipsoid is [Rodgers, 2000]

$$r_c = \frac{1}{r_{ns}^{-1} \cos^2 \alpha + r_{ew}^{-1} \sin^2 \alpha} \quad (11.3)$$

where  $r_{ns}$  and  $r_{ew}$  are the north-south and east-west curvature radius, respectively,

$$r_{ns} = r_e^2 r_p^2 (r_e^2 \cos^2 \omega + r_p^2 \sin^2 \omega)^{-\frac{3}{2}} \quad (11.4)$$

$$r_{ew} = r_e^2 (r_e^2 \cos^2 \omega + r_p^2 \sin^2 \omega)^{-\frac{1}{2}} \quad (11.5)$$

The azimuth angle,  $\omega$ , is defined in Section 5.2.2. The latitude and azimuth angle to apply in Equations 11.3–11.5 shall rather be valid for a middle point of the propagation paths (such as some tangent point), instead of the sensor position.

### 11.1.2 Geocentric and geodetic latitudes

The fact that Earth is an ellipsoid instead of a sphere, opens up for the two different definitions of the latitude. The geocentric latitude, which is the one used here, is the angle between the equatorial plane and the vector from the coordinate system centre to the position of concern. The geodetic latitude is also defined with respect to the equatorial plane, but the angle to the normal to the reference ellipsoid is considered here, as shown in Figure 11.1. It could be mentioned that a geocentric latitude does not depend on the ellipsoid used, while the geodetic latitudes change if another reference ellipsoid is selected. For Earth, the largest difference between geocentric and geodetic latitude is found at mid-latitudes, where it reaches 12 arc-minutes. There are yet no methods in ARTS for conversion of data between geodetic and geocentric latitudes.

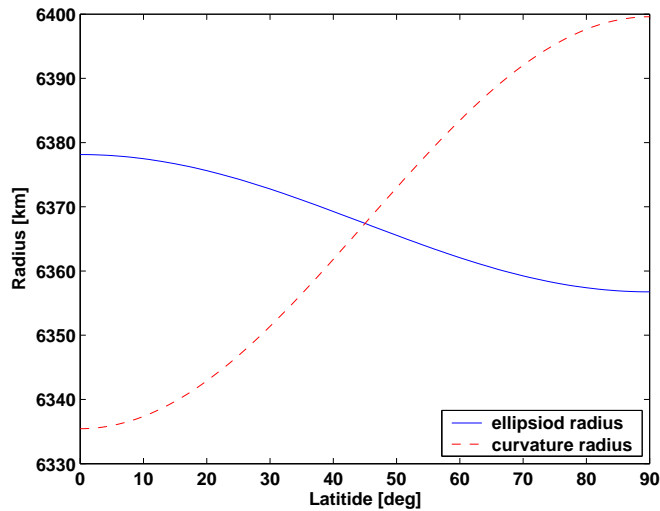


Figure 11.2: The ellipsoid radius ( $r_{\odot}$ ) and curvature radius ( $r_c$ ) for the WGS-84 reference ellipsoid. The curvature radii are valid for the north-south direction.

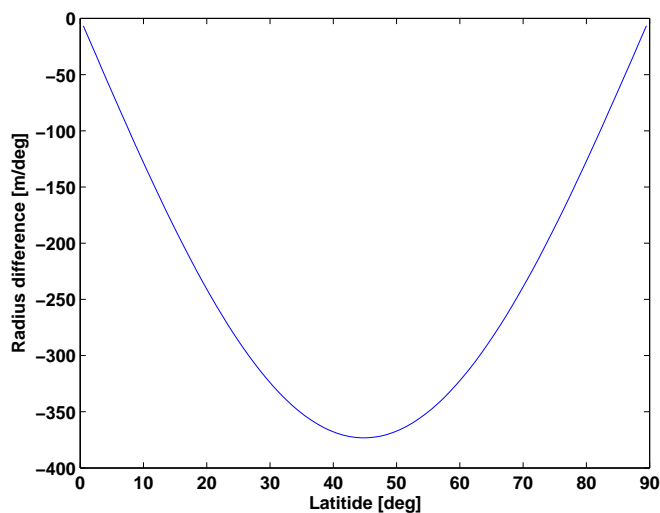


Figure 11.3: The change of the WGS-84 ellipsoid radius for  $1^\circ$  latitude differences.

## 11.2 Surface altitude

The surface altitude,  $z_g$ , is given as the geometrical altitude above the reference ellipsoid. The radius for the surface is accordingly

$$r_s = r_{\odot} + z_s \quad (11.6)$$

As also mentioned in Section 3.6, a gap between the surface and the lowermost pressure level is not allowed.

The ARTS variable for the surface altitude (`z_surface`) is a matrix. For 1D, the surface constitutes a sphere by definition (as the ellipsoid), while for 2D and 3D any shape is allowed and a rough model of the surface topography can be made.

## 11.3 Surface radiative properties

If there is an interception of the propagation path by the surface, emission and scattering by the surface must be considered. This is the task of `iy_surface_agenda`. The standard method for this agenda is `iySurfaceRtpropAgenda` (in fact, the only option implemented so far) and the rest of this section outlines how this workspace method works. The upwelling radiation from the surface can be written as (Figure 11.4)

$$I_a^u = I_e + \sum_l \mathbf{R}_l I_l^d \quad (11.7)$$

where  $I$  indicates the Stokes vector for one frequency,  $I_a^u$  is the total upward travelling intensity from the surface along the propagation path,  $I_e$  is the emission from the surface,  $I_l^d$  is the downward travelling intensity reaching the surface along direction  $l$ , and  $\mathbf{R}_l$  is the reflection coefficient matrix from direction  $l$  to the present propagation path. The emission from the surface  $I_e$  is stored in `surface_emission`, the directions  $l$  for which downward travelling intensities are given by `surface_los`, and the reflection coefficients ( $\mathbf{R}$ ) are stored in `surface_rmatrix`.

Some special cases are discussed below. Section 6.8 of *ARTS Theory* provides the theoretical background.

### 11.3.1 Blackbody surface

If the surface can be assumed to act as a blackbody, the workspace method `surfaceBlackbody` can be used. This method sets `surface_emission` to  $[B, 0, 0, 0]^T$ , and `surface_los` and `surface_rmatrix` to be empty.

### 11.3.2 Specular reflections

Several methods to incorporate a flat surface exist, including `surfaceFlatRefractiveIndex` and `surfaceFlatScalarReflectivity`. The methods differ in how the dielectric properties of the surface are given, and if these are constant or not with frequency.

In the case of specular reflections, `surface_los` has the length 1. The specular direction is calculated by the internal function `surface_specular_los`<sup>1</sup>. Equations 6.72-6.74 in *ARTS Theory* give the values of `surface_rmatrix` and `surface_emission`.

<sup>1</sup>Any tilt of the surface is neglected when determining the specular direction. If there would be any need to consider surface tilt, almost complete code for this task existed in `surface_specular_los` but was removed in version 1-1-876. The code can be obtained by e.g. checking out version 1-1-875.

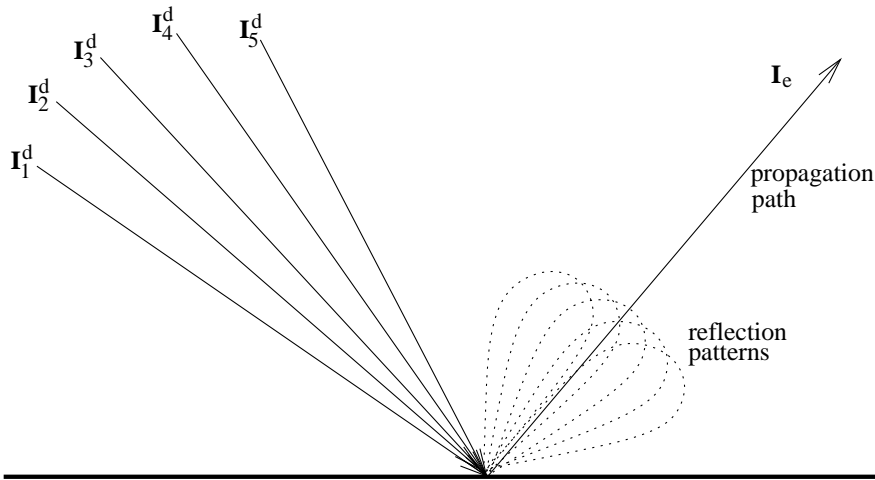


Figure 11.4: Schematic of Equation 11.7.

### 11.3.3 Lambertian surface

A basic treatment of Lambertian surfaces is provided by the method `surfaceLambertianSimple`. This method assumes that the down-welling radiation has no azimuthal dependency, which fits the assumptions for 1D atmospheres. The number of angles to apply in `surface_los` is selected by the user.

For a Lambertian surface the reflected radiation is unpolarised (thus independent of the polarisation of the down-welling radiation). That is, each `surface_rmatrix` has the structure:

$$\mathbf{R} = \begin{bmatrix} w & 0 & 0 & 0 \\ 0 & 0 & 0 & 0 \\ 0 & 0 & 0 & 0 \\ 0 & 0 & 0 & 0 \end{bmatrix}. \quad (11.8)$$

When determining the “weight”  $w$  above, the method assumes that the down-welling radiance ( $I$ ) is constant inside each zenith angle range:  $[\theta_a, \theta_b]$ . Hence,  $w$  equals (cf. Equation 6.75 of *ARTS Theory*)

$$w = \int_{\theta_a}^{\theta_b} \int_{\phi_a}^{\phi_b} \cos(\theta) f(\theta, \phi, \theta_1, \phi_1) \sin(\theta) d\phi d\theta, \quad (11.9)$$

that gives

$$w = \frac{r_d}{2} [\cos(2\theta_a) - \cos(2\theta_b)]. \quad (11.10)$$

Thus, this value is a combination of the surface reflectivity and an solid angle weight.

The emission (`surface_emission`) becomes:

$$\mathbf{b} = \begin{bmatrix} r_d B \\ 0 \\ 0 \\ 0 \end{bmatrix}. \quad (11.11)$$



# Chapter 12

## Sensor characteristics

A sensor model is needed because a practical instrument gives consistently spectra deviating from the hypothetical monochromatic pencil beam spectra provided by the atmospheric part of the forward model. For a radio (heterodyne) instrument, the most influential sensor parts are the antenna, the mixer, the sideband filter and the spectrometer. The response (as a function of frequency, zenith angle ...) of such instrument parts is here denoted as the sensor characteristics.

The treatment of sensor variables is introduced in Section 5.2. As described in that section, the position and line-of-sight (`sensor_pos` and `sensor_los`) are treated separately, while remaining sensor characteristics are summarised by a “response matrix” denoted as `sensor_response`. This matrix is applied following Equation 5.2. The purpose of this section is to describe how data on sensor characteristics are inputted to obtain a `sensor_response` that matches your particular instrument.

The implementation follows closely *Eriksson et al. [2006]*. That article provides also a more careful description of the approach of applying a response matrix, and the equations used to convert different type of characteristics to response values. As a user of ARTS, the main practical issue is to understand the different file formats used for the different sensor parts. For the moment, this is only described mainly through the on-line documentation.

### 12.1 General

In principle, a sensor must always be specified. However, if this shall be a hypothetical sensor just providing the monochromatic pencil beam data coming out of the atmospheric radiative transfer calculations, use `sensorOff` (`sensor_response` is in this case just an identity matrix).

For other cases, the definition of the sensor characteristics is initiated by calling `sensor_responseInit`. The natural order to call the main functions for the different sensor parts should be to follow the radiation through the instrument. That is, the antenna should normally be the first part to consider. If the order can be changed depends on the conditions. For example, for a double side-band receiver the antenna must be considered before the mixer, if the antenna response differs between the two bands. If the same antenna response

---

#### History

110826 A simple version by Patrick Eriksson.

can be assumed for both bands, the same result is obtained even if the mixer is introduced before the antenna.

Each response is defined for some grid. All responses are assumed to be zero outside the range covered by the grid, even if the end values deviate from zero. A positive aspect of this definition is that it is possible to define true “rectangular” responses. This is achieved by setting the end points of the grid where the response drops to zero.

The sensor parts are normally associated with some loss of power, and sensor contains also some amplification device. In general, it is not needed to consider these aspects, as such effects are cancelled out by the calibration process. The sensor should then be modelled as having no losses, which is ensured by setting `sensor_norm` to 1. The different responses are then normalised in an appropriate manner. With `sensor_norm` set to 0, all normalisation issues must be handled when defining the response files.

## 12.2 Some comments

Some text removed from other chapters, to be integrated into this chapter:

For each sensor position, a number of monochromatic pencil beam spectra are calculated. The monochromatic frequencies are given by `f_grid`. The pencil beam directions are obtained by summing the sensor line-of-sight angles (`sensor_los`) for the position and the values of `mblock_za_grid` and `mblock_aa_grid`. For example, pencil beam zenith angle  $i$  is calculated as

$$\psi_i = \psi_0 + \Delta\psi_i \quad (12.1)$$

where  $\psi_0$  is the sensor line-of-sight for the position of concern and  $\Delta\psi_i$  is value  $i$  of `mblock_za_grid`. With other words, `mblock_za_grid` and `mblock_aa_grid` give the grid (relative to the sensor line-of-sight) for the calculation of the intensity field that will be weighted with the antenna response.

As the sensor line-of-sight and block grid values are just added, there is an ambiguity of the line-of-sight. It is possible to apply a constant off-set to the line-of-sights, if the block grids are corrected accordingly. For example, if the simulations deal with limb sounding and a 1D atmosphere, where normally a single block should be used despite a number of spectra are recorded, it could be practical to set the line-of-sight to the viewing direction of the uppermost or lowermost spectrum, and the zenith angles in `mblock_za_grid` will not be centred around zero which is the case when the “true” line-of-sight is used.



# Chapter 13

## Doppler effects and winds

The default assumption in ARTS can be expressed as the atmosphere is assumed to be static and the observation platform is static during each measurement, while any relative movement between the atmosphere and the sensor will cause Doppler effects. ARTS handles three sources to Doppler shifts: winds, rotation of the planet and sensor velocity.

### 13.1 Winds

Atmospheric transport is not considered by ARTS, but winds can still be of importance due to the Doppler effect they can cause. This effect is most significant at high altitudes where the line shape is narrow, and a frequency shift of absorption and emission is most easily discerned.

The workspace variables to specify winds are `wind_u_field`, `wind_v_field` and `wind_w_field`, below denoted as  $v_u$ ,  $v_v$  and  $v_w$ , respectively. The user need to set all these three variables. It is allowed, for all three wind components, to set the variable to be empty, which is shorthand for saying that the wind is zero throughout the atmosphere (Sec. 3.8). Otherwise, the size of the variable is required to match the atmospheric grids.

No further input is required, a Doppler shift is added as soon as any of the winds is non-zero (exceptions discussed in Sec. 13.4). For clarity, even though a setting of `wind_u_field` always is demanded, this wind component has no effect on Doppler shifts for 1D and 2D calculations, as the wind moves at an angle of  $90^\circ$  from the observation plane (Sec. 3.8).

### 13.2 Planet rotation

ARTS applies an Earth-Centred, Earth-Fixed, (ECEF) coordinate system. This implies that a ground-based receiver follows the planet's rotation. On the other hand, if e.g. the sensor is placed on another planet, or is in a transit orbit, the rotation of the observed planet will cause Doppler effects. This is treated in ARTS by a short-cut, the rotational movement can be translated to an imaginary wind by the method `wind_u_fieldIncludePlanetRotation`.

---

#### History

- 130223 Restructured to include effects beside winds (PE).
- 121218 First version by Patrick Eriksson.

### 13.3 Sensor velocity

The feature is not yet fully implemented, but a rudimentary inclusion of the sensor's velocity can be made by the `rte_alonglos_v` workspace variable. The variable shall be set to the sensor velocity component along the viewing direction. For the moment, this velocity is assumed to be the same for all pencil beam calculations.

### 13.4 Limitations

For efficiency reasons, when extracting particle extinction (absorption and scattering) the mean Doppler shift along the propagation path is applied (but the shift varies with frequency). This allows to at least include larger shifts caused by e.g. satellite velocity. The smaller shifts (due to winds) are here of less importance as the particle extinction is quite smooth with frequency.

The above is valid for transmission type calculations. Doppler shifts are so far totally neglected inside the DOIT and MC scattering modules.

### 13.5 Equations

The main equations for deriving the Doppler shift from the winds are given in this section. The total wind,  $v$ , is

$$v = \sqrt{v_u^2 + v_v^2 + v_w^2}. \quad (13.1)$$

The zenith angle of the wind direction is

$$\psi_v = \arccos(v_w/v), \quad (13.2)$$

and the azimuth angle is

$$\omega_v = \arctan(v_u/v_v). \quad (\text{implemented by the atan2 function}) \quad (13.3)$$

The cosine of the angle between the wind vector and the line-of-sight is

$$\cos \gamma = \cos \psi_v \cos \psi_l + \sin \psi_v \sin \psi_l \cos(\omega_v - \omega_l), \quad (13.4)$$

where  $\psi_l$  and  $\omega_l$  are the angles of the line-of-sight.

Finally, as the winds do not reach relativistic values, the Doppler shift can be calculated as

$$\Delta\nu = \frac{-v \cos \gamma \nu_0}{c}, \quad (13.5)$$

where  $\nu_0$  is the rest frequency and  $c$  is the speed of light. The core part of these calculations is implemented in the general internal function `dotprod_with_los`. The negative sign is caused by the fact the "line-of-sight" is the observation direction, not the direction of the EM waves.

# Chapter 14

## Faraday rotation

The polarisation state of an electromagnetic wave propagating through a plasma with a static magnetic field will be changed, normally denoted as Faraday rotation. The effect is present for both passive and active signals, but Faraday rotation is proportional to  $\nu^{-2}$  and can in general be neglected for emission measurements due to the relatively high frequencies applied. For Earth, the effect can in general be neglected above  $\sim 5$  GHz. Hence, Faraday rotation is a special consideration for radio/microwave radiative transfer. A brief theoretical description is found below in Section 14.2.

### 14.1 Practical usage

The first step is to ensure that the magnetic field and field of free electrons are non-zero. See Section 3.8 for how to introduce a magnetic field. Free electrons are treated as an “absorbing species”, and hence are part of `vmr_field` (Sec. 4.2.2). A further constrain is that the Stokes dimensionality (`stokes_dim`) is set to 3 or 4. This can be understood by Equation 14.4, Faraday rotation affects Stokes elements 2 and 3.

Faraday rotation is treated by `propmat_clearsky_agenda`. For the moment, there exists a single workspace method for the task and that is `propmat_clearskyAddFaraday`. That is, this method must be included in `propmat_clearsky_agenda` if you want to include Faraday rotation in your calculations.

Information on the actual rotation can be obtained as auxiliary data by `iyTransmissionStandard` and `iyRadioLink`. The total rotation along the path is selected as “Faraday rotation”. The unit is [deg]. The rotation per length unit (Eq. 14.2) is selected as “Faraday speed”. The unit is [deg/m].

### 14.2 Theory

A wave propagating through the ionosphere will force free electrons to move in curved paths. If the incident wave is circularly polarised, the motion of the electrons will be circular. The refractive index will then not be a single constant, but depending on polarisation (i.e. anisotropic). More precisely, left and right hand polarised waves will propagate with

---

#### History

121217 Written (PE), partly based on text written originally by Bengt Rydberg.

different speeds. Moreover, as a plane polarised wave can be thought of as a linear superposition of a left and a right hand polarised wave with equal amplitudes, but different phase, the plane of polarisation will then rotate as the wave is propagating through the media. This is denoted as Faraday rotation.

Birefringence is an associated mechanism, but it is not yet treated by ARTS. This later effect originates also on the fact that right- and left-hand circular polarisation have different refractive index. This can result in that the two polarisations obtain different propagation paths. For frequencies close to the “plasma frequency” the birefringence can be a strong effect, but for higher frequencies it should be secondary to Faraday rotation. Expressed roughly, a difference in optical path for the two circular polarisation of a quarter of a wavelength changes the polarisation state strongly by Faraday rotation, while additional effects coming from a difference in propagation path (birefringence) should be negligible.

According to *Rybicki and Lightman* [1979], using Gaussian (cgs) units, the angle of rotation ( $\vartheta_F$ ) of a plane polarised wave can be described as

$$\vartheta_F = \frac{e^3}{2\pi c^2 m^2 \nu^2} \int_0^d n_e(s) \mathbf{B}_{\text{geo}}(s) \cdot ds,$$

which converted to SI units becomes [*Kraus, 1966*]<sup>1</sup>

$$\vartheta_F = \frac{e^3}{8\pi^2 c \epsilon_0 m^2 \nu^2} \int_0^d n_e(s) \mathbf{B}_{\text{geo}}(s) \cdot ds \approx \frac{23648}{\nu^2} \int_0^d n_e(s) \mathbf{B}_{\text{geo}}(s) \cdot ds, \quad (14.1)$$

where  $n_e(s)$  is the density of electrons at point  $s$ ,  $\mathbf{B}_{\text{geo}}(s)$  is the geomagnetic field at point  $s$ , and  $\cdot$  denotes the dot (scalar) product. Accordingly, the Faraday rotation is proportional to the part of the magnetic field along the propagation path, the field normal to the path gives no effect.

The change in rotation angle along the propagation path,  $r$  is then given by

$$r = \frac{d\vartheta_F}{ds} = \frac{e^3}{8\pi c \epsilon_0 m^2 \nu^2} n_e(s) \mathbf{B}_{\text{geo}}(s) \cdot \hat{s}. \quad (14.2)$$

An “magneto-optical” effect (Sec. 4.2.1) of this type is mapped to a propagation matrix as

$$\mathbf{K} = \begin{bmatrix} 0 & 0 & 0 & 0 \\ 0 & 0 & 2r & 0 \\ 0 & -2r & 0 & 0 \\ 0 & 0 & 0 & 0 \end{bmatrix}. \quad (14.3)$$

If no other effects are present, the effect on the Stokes vector for some part of the propagation path can be expressed as a Mueller rotation matrix [*Goldstein, 2003; Meissner and Wentz, 2006*]:

$$\begin{bmatrix} I_F \\ Q_F \\ U_F \\ V_F \end{bmatrix} = \begin{bmatrix} 1 & 0 & 0 & 0 \\ 0 & \cos(2\vartheta_F) & -\sin(2\vartheta_F) & 0 \\ 0 & \sin(2\vartheta_F) & \cos(2\vartheta_F) & 0 \\ 0 & 0 & 0 & 1 \end{bmatrix} \begin{bmatrix} I \\ Q \\ U \\ V \end{bmatrix}. \quad (14.4)$$

<sup>1</sup>The two versions of this equation are also found in Wikipedia (under *Faraday effect*), but expressed using  $\lambda$  and an error for the numerical factor (2012-12-17). The value  $2.365 \cdot 10^4$ , derived from the fundamental constants, is confirmed by *Wright et al. [2003]*.

## Chapter 15

# Transmission calculations

The term “transmission calculations” refers here to situations when the emission from the atmosphere and surface can be neglected. These calculations can be divided into two main types. The first one is when just the transmission of the atmosphere is diagnosed (Sec. 15.1). The observation geometry is then given exactly as for emission simulations, by a position and a line-of-sight.

The second main type is radio link budgets (Sec. 15.2). For this case, the propagation path is determined solely by the position of the transmitter and the receiver. That is, the user does not need to set a line-of-sight of the sensor (receiver), it is determined by the transmitter position. A characterisation of a radio link normally involves several attenuation terms not encountered for passive measurements, such as free space loss and defocusing. Faraday rotation (Sec. 14) is an additional physical mechanism that is of special concern for active microwave devices (it can normally be neglected at the higher frequencies used for passive observations).

### 15.1 Pure transmission calculations

This section discusses the `iyTransmissionStandard` workspace method, that is relevant if you want to calculate the transmission through the atmosphere for a given position and line-of-sight. The set-up is largely the same as for simulations involving emission, such as that the observation geometry is defined by `sensor_pos` and `sensor_los` (or `rte_pos` and `rte_los` if `iyCalc` is used). The first main difference is that `iy_transmitter_agenda` replaces `iy_space_agenda` and `iy_surface_agenda`. The second main difference is that handling of cloud scattering is built-in and the need to define `iy_cloudbox_agenda` vanishes. These differences appear inside `iy_main_agenda`. Further, `blackbody_radiation_agenda` can be left undefined.

As for emission measurements (Sec. 9.1, Algorithm 2) the first main operation is to determine the propagation path through the atmosphere, but this is here done without considering the cloud-box (it is simply deactivated during this step). The possible “radiative backgrounds” are accordingly the surface or space, i.e. where the propagation path starts.

The next step is to call `iy_transmitter_agenda`. It should be noted that the same agenda is called independently if the radiative background is space or the surface. It is up to the user to

---

#### History

130206 Written (PE), partly based on text written originally by Bengt Rydberg.

decide if these two cases shall be distinguished in some manner (no workspace method for this task exists yet). For these calculations, the standard choice for `iy_transmitter_agenda` is `MatrixUnitIntensity`. If this workspace method is used, the output of `iyTransmissionStandard` shows you the fraction of unpolarised radiation that is transmitted through the atmosphere, and the polarisation state of the transmitted part.

The radiative transfer expression applied is (cf. Eq. 9.7)

$$\mathbf{s}_{i+1} = e^{-\bar{\mathbf{K}}s} \mathbf{s}_i \quad (15.1)$$

where the extinction matrix is determined in the same manner as for emission cases (Sec. 9.3). In situations where the matrix  $\mathbf{K}$  is diagonal, the scalar form shown in Eq. 9.5 is used.

The method determines automatically if any part of the propagation path is inside the cloud-box (if active). If this is the case, particle extinction is included in  $\mathbf{K}$ , following the same path step averaging as applied for pure absorbing species. For this method, scattering is purely a loss mechanism, there is no gain by scattering into the line-of-sight

A related concern is the treatment of the surface. In standard usage of the method, there is no signal reflected by the surface, and the radiative transfer calculations are started at the surface.

See the built-in documentation of `iyTransmissionStandard` for a full list of possible auxiliary quantities. These data include quantities that make it possible to determine the transmission for different parts of the propagation path. For example, the state of `iy` at each point of the propagation path can be extracted, and also the transmission matrix (Eq. 9.8) for each path step is accessible.

## 15.2 Radio link calculations

### 15.2.1 Practical usage

This type of calculations is handled by `iyRadioLink`. A sensor position must be specified, as usual. The “sensor” takes the place as the receiver of the radio link. The observation angles of the receiver are not user input (if any given they are just ignored), they are determined by the position of the transmitter. This position is given as `transmitter_pos` or `rte_pos2`, dependent on if `yCalc` or `iyCalc` is used. Specification of receiver and transmitter properties, beside their positions, is discussed in Section 15.2.3. The quantities returned by `iyRadioLink` are also described in Section 15.2.3.

It is allowed to use `iyRadioLink` together with pure geometrical propagation paths, but this option does not give realistic results as the this set-up misses the impact of “defocusing” (Sec. 15.2.7). With refraction, the propagation path can not be determined in a strict analytical manner and some search algorithm is required, as discussed in Section 15.2.2.

### 15.2.2 Determination of the radio link path

ARTS contains so far just a quite simple algorithm for this purpose, activated by applying `ppathFromRtePos2` in `ppath_agenda`. The input `rte_los` is taken as the first guess for the observation angles of the receiver. One way to set this initial value use `rte_losGeometricFromRtePosToRtePos2`, that sets `rte_los` to the angles for the geometrical path. For satellite-to-satellite links with tangent points in the lower troposphere, the geometrical zenith angle can give an intersection with the surface and it is recommended to use a lower start value for the zenith angle. For 1D cases this is simply achieved:

```
rte_losGeometricFromRtePosToRtePos2
VectorAddScalar(rte_los, rte_los, -2.5)
```

Another option is to use the angle from the last link, but this requires that the links of an occultation is treated in a specified order, which is not guaranteed when running with multi-threading.

New propagation path are calculated (from the receiver backwards towards the transmitter) until a path is found that passes the transmitter sufficiently close. The search and stop criterion is based on the smallest distance between the transmitter and the path. However, this distance is evaluated as an “angular miss”. The miss term is taken as the difference in zenith angle between the geometrical path to transmitter and path point derived. If the transmitter is placed inside the model atmosphere, the closest point is found by an interpolation between the points defining the path. If the transmitter is above the top-of-the-atmosphere (TOA), the closest point is derived by geometrically extend the path (from its end point at TOA).

For each iteration of the search, the zenith angle is updated. The first choice is to determine the new zenith angle by a least squares fit, using data from the three last “test paths”. On the same time, the zenith angles giving the smallest positive and negative angular miss are kept in memory, giving the end points for new range of new zenith angles to consider. If the least squares fit gives an angle outside this range, bi-section between the end points of the search range is used for updating the angle. A special consideration to ground intersections must be given (see the code for details). If it is determined that the ground makes a link impossible, a dummy propagation path (of length 1) having “surface” as radiative background is returned. The radiative background is otherwise set to “transmitter”.

The above is repeated until the miss term is smaller than the given accuracy criterion, defined by the argument `za_accuracy`. For a receiver in a low Earth orbit, a tangent altitude accuracy of 1 m corresponds roughly to  $2 \cdot 10^{-5}$  for `za_accuracy`.

If the selected criterion is not met, the calculations are re-started with a smaller ray tracing step length (`p_path_lraytrace`), and with last value of `rte_los` as “first guess”. The decrease of the ray tracing step length follows the argument `p_plrt_factor`. If the ray tracing length is smaller than `p_plrt_lowest`, the calculations are halted and a dummy propagation path (of length 1) flagged as “undefined” is returned. The method returns `p_path_lraytrace` set to the value used for the final calculation.

A suitable start value for `p_path_lraytrace` depends on the size of refractive index. For satellite-to-satellite links close to the Earth’s surface a suitable value can be as low as 100 m.

### 15.2.3 Definition of attenuation and loss terms

The radiance law is not applicable for the signal from a point source. The power received,  $p_r$ , by an antenna with an effective aperture size  $A_e$ , located a distance  $l$  from a transmitter, with power  $p_t$  and gain  $g_t$ , can be expressed as [e.g. *Ippolito, 2008*]

$$p_r(l) = t_a \frac{p_t g_t}{4\pi l^2} A_e, \quad (15.2)$$

where  $t_a$  is the transmission due to losses caused by the atmosphere. This total atmospheric loss is the product between losses due to defocusing,  $t_d$  (Sec. 15.2.7) and gaseous and particle extinction,  $t_e$  (Sec. 15.2.8):

$$t_a = t_d t_e. \quad (15.3)$$

The factor

$$t_f = \frac{1}{4\pi l^2} \quad (15.4)$$

represents the pure geometrical dilution of the power, following the inverse square law. This effect is encountered also for propagation in free space, and, accordingly, it is denoted as the free space loss. Please note that other definitions of this quantity exists, see Section 15.2.4.

With these definitions, Equation 15.2 can be written as

$$p_r(l) = t_d t_e t_f p'_t, \quad (15.5)$$

where  $p'_t = p_t g_t A_e$ , a term discussed further in Section 15.2.4.

The method `iyRadioLink` reports  $p_r$  as `iy`, i.e.  $p_r$  is treated as the main quantity. All loss terms ( $t_d$ ,  $t_e$  and  $t_f$ ) can be obtained as auxiliary data (`iy_aux`). The auxiliary variables include also extra path delay, bending angle and Faraday rotation. Some of these terms can be obtained as attenuation/rotation/delay (per length) along the propagation path.

Note the distinction between “loss” and “attenuation”. The first term refers here to path-integrated transmission factors, while the second term refers to local attenuation coefficients. That is, losses are dimensionless values, between 0 and 1, while the unit of attenuation is  $1/m$ . See the following sections for details.

The quantity returned in `iy` is also what ends up in `y`, outputted by `yCalc`. For increased flexibility, the method `iyReplaceFromAux` allows the user to replace the content of `iy` with some of the auxiliary variables. For example, for radio link calculations bending angle can frequently be seen as the primary observation, and this case can be handled by `iyReplaceFromAux`. The constrain for allowing this swap of variables is that the auxiliary variable to replace  $p_r$  must have the same data dimensions. In practice, this means that the auxiliary variable is a function of frequency, possibly being a Stokes vector for each frequency. Variables fulfilling this constrain are: defocusing loss ( $t_d$ ), atmospheric extinction loss ( $t_e$ ), free space loss ( $t_f$ ), bending angle, extra path delay, and (total) Faraday rotation.

#### 15.2.4 Free space loss and sensor characteristics

It is repeated that (total) free space loss is in ARTS defined as given above in Equation 15.4:

$$t_f = \frac{1}{4\pi l^2}.$$

It is stressed that this deviates from what appears to be a more common (even standard?) definition of free space loss:  $(\lambda/(4\pi l))^2$ , where  $\lambda$  is the wavelength of the signal. This expression encompasses the relationship between the receiver’s effective antenna area and its gain ( $A_e = g_r \lambda^2 / (4\pi)$ ). This later definition was avoided to keep atmospheric and sensor effects clearly separated in ARTS,

Hence, the definition of free space loss has consequences for how to specify sensor characteristics. A possible choice is to treat pure multiplicative factors such as  $p_t$ ,  $g_t$  and  $A_e$  separately, and let ARTS handle the pure radiative propagation effects. In this case,  $p'_t$  (Eq. 15.5) shall be set to unity (`MatrixUnitIntensity` handles this case). If e.g. Faraday rotation or particle scattering is of concern, `stokes.dim` must be  $> 1$  and also the polarisation of the transmitted signal is of concern, and must be included in the specification of  $p'_t$  (e.g.  $p'_t = [1, \pm 1, 0, 0]$  when V or H is transmitted). The next step towards a more complete treatment of the transmitter should be to include  $p_t$  and  $g_t$  in  $p'_t$ . In any case, `iyRadioLink` expects `iy_transmitter_agenda` to return  $p'_t$ , for each frequency in `f_grid`.



So far ARTS has no dedicated support to handle characteristics of receivers in radio link configurations. The first step here should be to consider  $A_e$ , but the simplest way to achieve this is to include  $A_e$  in  $p'_t$  (and it is here where the definition of free space loss comes into play, as with the standard definition  $p'_t$  should instead include  $g_r$ ). Some functionality developed for passive sensors could also be of use for radio links, but this has not yet been tested practically (even less validated) and these options are not commented further.

Setting  $I = p_r$  (to be consistent in the nomenclature used elsewhere) and taking the derivative of  $I(s)$  gives

$$\frac{dI(s)}{ds} = -\frac{2}{s}I(s). \quad (15.6)$$

This equals the Beer-Lambert law with an attenuation coefficient of  $2/s$ . With other words, the free space loss can be also treated as an ordinary extinction term, and when “free space attenuation”,  $k_f$ , is requested as an auxiliary variable it is calculated as

$$k_f = \frac{2}{s}. \quad (15.7)$$

This extinction coefficient can be seen as non-linear, as it varies with the distance from the transmitter. If the transmitter is placed inside the atmosphere,  $k_f$  becomes infinity for the path point corresponding to  $l = 0$ . The  $k_f$ -coefficient is not dependent on the definition differences of (total) free space loss discussed above.

### 15.2.5 Extra path delay

In the absence of an atmosphere a signal sent from a transmitter in the direction towards a receiver would follow a straight line, i.e. the shortest geometric distance between the two instruments. Moreover, the signal would propagate with the speed of light. The geometric distance,  $l_g$ , between the transmitter and receiver is

$$l_g \equiv \int_{\text{geometric}} 1 ds \quad (15.8)$$

In the presence of an atmosphere, two changes follow, the speed of the signal is retarded and the ray path gets bent. The optical path length is defined as

$$l_o \equiv \int_{\text{ray}} n(s) ds. \quad (15.9)$$

The geometrical length of the bent ray path is

$$l_r \equiv \int_{\text{ray}} 1 ds. \quad (15.10)$$

To recall what you probably heard during our physics lessons, some quotes from the Wikipedia entry on optical path length: *Fermat's principle states that the path light takes between two points is the path that has the minimum optical path length. An electromagnetic wave that travels a path of given optical path length arrives with the same phase shift as if it had travelled a path of that physical length in a vacuum.*

The total delay, compared if there would be vacuum between transmitter and receiver, expressed in units of length, is

$$d \equiv l_o - l_g \geq 0, \quad (15.11)$$

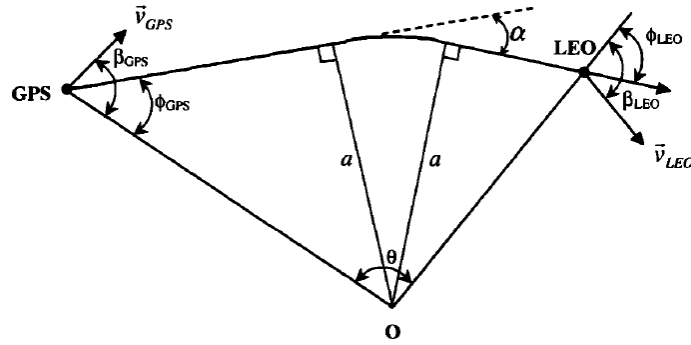


Figure 15.1: Illustration of the bending angle of a satellite-to-satellite radio occultation [copied from *Schreiner et al., 1999*, Fig. 2].

which can be expressed also as

$$d = (l_o - l_r) + (l_r - l_g) = d_n + d_g, \quad (15.12)$$

where  $d_n$  is the along-path delay due to decreased propagation velocity, and  $d_g$  is delay due to deviation from geometric propagation (refraction).

The (total) extra path delay, in units of seconds, is

$$\Delta t = \frac{d}{c}, \quad (15.13)$$

and is provided by `iyRadioLink` as an auxiliary variable.

### 15.2.6 Bending angle

The bending angle is a measure on the deviation from geometric propagation. Using the nomenclature defined in Figure 15.2.6, the bending angle,  $\alpha$ , can be calculated as [e.g. *Schreiner et al., 1999*, Eq. 6]

$$\alpha = \phi_{GPS} + \phi_{LEO} + \theta - \pi.$$

This equation is derived assuming what in ARTS is denoted as a 1D atmosphere. ARTS operates with zenith angles and the equation above becomes

$$\alpha = \psi_t - \psi_r + \theta, \quad (15.14)$$

where  $\psi_t$  and  $\psi_r$  is the zenith angle of propagation path, at the transmitter and the receiver, respectively. This equation is applied for all atmospheric dimensionalities, hence, any bending in the horizontal plane, that can occur for 3D, is neglected.

A remark here is that the ARTS' zenith angles for the path are the ones to observe the propagating radiation, and e.g.  $\psi_r = \pi - \phi_{LEO}$ . Equation 7.8 in *ARTS Theory* shows that that without refraction  $\theta = \psi_t - \psi_r$  (note the difference in notation), and Equation 15.14 is consistent with a zero bending angle for propagation in vacuum. Consequently, ARTS should theoretically return a bending angle of zero if geometrical path calculations are selected, but due to limited calculation precision a small deviation from zero can be found.

### 15.2.7 Defocusing

A special effect for radio links is defocusing. This effect is caused by the fact that refraction varies over the wavefront. In short, defocusing occurs if neighbouring ray-paths diverge more quickly than for free space propagation. This is the typical situation for limb sounding due to the vertical variation of the refractive index, causing an additional divergence of the transmitted power. The opposite, focusing, is also possible. In fact, already for an ideal spherically symmetric atmosphere a focusing effect takes place in the horizontal dimension, caused by the curvature of the planet. In this case, the middle point of the beam experiences the highest refractive index and has then the lowest propagation speed. This, in addition to symmetry around the middle point, counteracts partly the free space divergence of the power.

Defocusing can be estimated by two different algorithms, simple denoted as method 1 and 2. The user selects the method to apply by the argument `defocus_method`.

#### Defocusing, method 1

This method is intended to be general, using a very simple calculation approach. The optical path length between the transmitter and the receiver is determined, here denoted as  $l_o$ . This is followed by that two propagation paths are calculated, with slight shifts in the zenith angle. The size of the angular shift is an user input (`defocus_shift`).

The spatial position where each of the two shifted paths have an optical path length of  $l_o$  is determined. The distance between these two points are compared to what is expected for free space propagation. If, for example, the distance is double as high compared to the free space case, this is taken as a defocusing “transmission” of 0.5. The factor can be higher than 1, which corresponds to conditions of focusing. Only the zenith angle dimension is considered, any defocusing/focusing in the horizontal plane is neglected (which in general should be a good approximation).

The method can be applied for all possible links, e.g. links inside the atmosphere, for ground-to-satellite links and satellite-to-satellite links. In the last case, if the path with the highest zenith angle intersects with the ground, the defocusing is calculated using the nominal path and the low zenith angle path.

#### Defocusing, method 2

This method is restricted to satellite-to-satellite links. The defocusing effect in this case, of a transmitted signal with intensity  $I_0$ , can be described as [*Haugstad, 1978; Kursinski et al., 2000*]

$$I = I_0 M_\alpha M_\beta, \quad (15.15)$$

where  $M_\alpha$  and  $M_\beta$  is the vertical and horizontal defocusing factors, respectively. In general, the defocusing effect is fairly complex in a modelling perspective, although for special cases the defocusing factors can be calculated analytically. Such analytic expressions can be used for “test cases” of more general solutions. For a signal transmitted in a limb geometry through a spherical symmetric atmosphere (i.e. 1D), with an exponential scale height  $H$ , [*Haugstad, 1978*]

$$M_\alpha = \left[ 1 + \frac{\alpha L_r}{H} \right]^{-1},$$

$$M_\beta = \left[ 1 - \frac{\alpha L_r}{R} \right]^{-1},$$

where  $\alpha$  is the bending angle (Eq. 15.14),  $L_r$  is the distance from the tangent point to the receiver, and  $R$  is the planet radius. An alternative form of the equations above, also valid for an atmosphere with a non-exponential scale height is [Kursinski *et al.*, 2000]

$$M_\alpha = \left[ 1 + \frac{d\alpha}{da} \frac{L_t L_r}{L_r + L_t} \right]^{-1}, \quad (15.16)$$

$$M_\beta = \left[ 1 - \frac{\alpha}{R} \frac{L_t L_r}{L_r + L_t} \right]^{-1}, \quad (15.17)$$

where  $L_t$  and  $L_r$  is the distance between the tangent point and the transmitter and receiver, respectively, and  $a = nr \sin(\psi)$  is denoted as the impact parameter (and is equal to the “propagation path constant” defined in Eq. 7.30 of *ARTS Theory*).

The bending angle ( $a$ ) is given by the derived path between the transmitter and receiver. The term  $d\alpha/da$  is estimated using calculations with shifted zenith angles, with a shift set by the user (`defocus_shift`). Hence, this term is calculated in a manner similar to the approach used in method 1.

### 15.2.8 Atmospheric extinction

Atmospheric absorption and scattering are handled exactly as for `iyTransmissionStandard`. Accordingly, only scattering out-of-the propagation path is considered.

# Chapter 16

## Clear-sky Jacobians

Inversions of both OEM and Tikhonov type require that the Jacobian can be provided by the forward model [see e.g. *Eriksson, 2000*]. A retrieval characterisation following *Rodgers [1990, 2000]* raises the same demand. A column of the Jacobian,  $\mathbf{K}_x$ , is defined as

$$\frac{\partial \mathbf{y}}{\partial x_p}, \quad (16.1)$$

where  $\mathbf{y}$  is the vector of measurement data and  $x_p$  is one forward model (scalar) variable. See further Section 1.3 of *ARTS Theory*. The nomenclature of that section is also used here.

The quantity in Eq. 16.1 is in the atmospheric sounding community frequently denoted as a “weighting function”, and accordingly  $\mathbf{K}_x$  is called the weighting function matrix. In the documentation of ARTS both terms (Jacobian and weighting functions) are used. These names refer normally to  $\mathbf{K}_x$ , the partial derivatives with respect to the variables to be retrieved, forming the state vector  $\mathbf{x}$ . However, in the context of retrieval characterisation, the same matrix for the remaining model parameters is of equally high interest, denoted as  $\mathbf{K}_b$ . In the same manner, the terms inversion and retrieval are used interchangeably.

The main task of the user is to select which quantities that shall be retrieved, and to define the associated retrieval grids. These aspects must be considered for successful inversions, but are out of scope for this document. Beside for the most simple retrievals, it is further important to understand how the Jacobian is calculated. A practical point is the calculation speed, primarily determined if perturbations or analytical expressions are used (Sec. 16.1). The derivation of the different Jacobians involves some approximations due to theoretical and practical considerations. Such approximations can be accepted, if of low or moderate size, but will result in a slower convergence (the inversion will require more iterations). Due to these later aspects, and to meet the needs of more experienced users, this section is relatively detailed and contains a (high?) number of equations.

This section is restricted to Jacobians for clear-sky conditions, i.e. to be applied outside the cloudbox. So far none of the scattering methods provide Jacobians. Sections 16.1 - 16.2 contain information of general character, while the available quantities are discussed in the remaining sections (Section 16.4 and forward).

---

### History

110826 First complete version by Patrick Eriksson.

## 16.1 Introduction

There are two main approaches for calculating Jacobians, by analytical expressions and by perturbations. We start with the conceptually simplest one, but also the more inefficient approach.

### 16.1.1 Perturbations

The most straightforward method to determine the Jacobian is by perturbing the model parameter of concern. For example, the Jacobian corresponding to state variable  $p$  can always be calculated as

$$\mathbf{K}_x^p = \frac{\mathcal{F}(\mathbf{x} + \Delta x \mathbf{e}^p, \mathbf{b}) - \mathcal{F}(\mathbf{x}, \mathbf{b})}{\Delta x} \quad (16.2)$$

where  $(\mathbf{x}, \mathbf{b})$  is the linearization state,  $\mathbf{e}^p$  is a vector of zeros except for the  $p$ :th component that is unity, and  $\Delta x$  is a small disturbance (but sufficiently large to avoid numerical instabilities).

However, it is normally not needed to make a recalculation using the total forward model as the variables are either part of the atmospheric or the sensor state, but not both. In addition, in many cases it is possible to find short-cuts. For example, the perturbed state can be approximated by an interpolation of existing data (such as for a perturbed zenith angle). Such short-cuts are discussed separately for each retrieval quantity.

### 16.1.2 Analytical expressions

For most atmospheric variables, such as species abundance, it is possible to derive an analytical expression for the Jacobians. This is advantageous because they result in faster and more accurate calculations. Such expressions are derived below. Some of the terms involved are calculated as a perturbation. This is partly a consequence of the flexibility of ARTS. The high-level radiative transfer methods (e.g. `iyEmissionStandard`) do not know how the low-level methods are defining all quantities, and a fixed analytical expression can not be used (see e.g. Sec. 16.6). So, in practise, the calculations are “semi-analytical”. The analytical calculations are introduced in Sec. 16.3.

### 16.1.3 Workspace variables and methods

As a workspace variable, the complete Jacobian is denoted as `jacobian`. Auxiliary information is provided by `jacobian_quantities` and `jacobian_indices`. The actual calculations are made as part of `yCalc`.

The retrieval quantities are defined separately, before calling `yCalc`. This process is started by calling `jacobianInit`. The retrieval quantities are then introduced through workspace methods named as `jacobianAddSomething`. For example, for atmospheric temperature the method is `jacobianAddTemperature`. It does not matter in which order these “add methods” are called.

The definition of retrieval quantities is finalised by calling `jacobianClose`. To disable the calculation of the Jacobian, skip all above, and just use `jacobianOff`. The methods named `jacobianCalcSomething` shall never be used directly. Neither needs the user to consider `jacobian_agenda`.

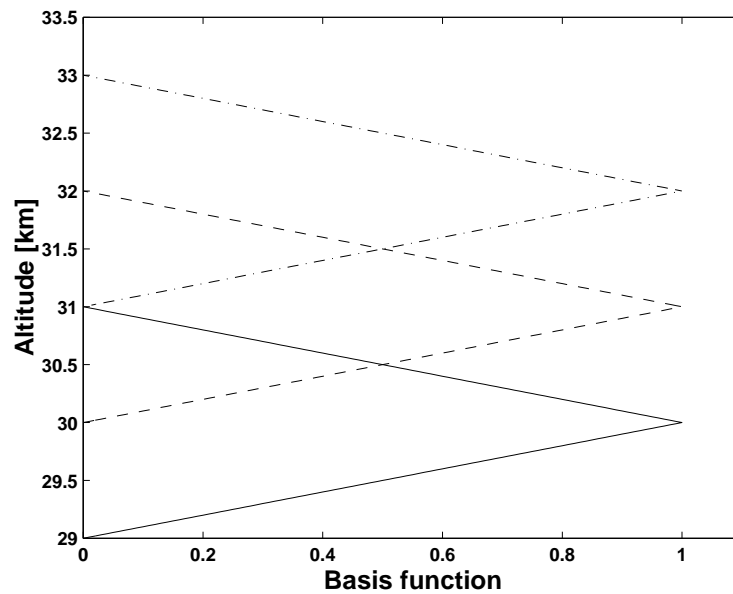


Figure 16.1: Examples on 1d basis functions for a vertical grid with a 1 km spacing: — 30 km, - - - 31 km and - · - 32 km.

The input to the “add methods” differs. In some cases you can select between the analytical and perturbation options. For all perturbation calculations you must specify the size of the perturbation. For atmospheric gases you can use different units. For atmospheric fields, and some other quantities, you must define the retrieval grid(s) to use.

## 16.2 Basis functions

A forward model must use a discrete representation: it describes each quantity with one or several variables. This is unproblematic for quantities that are of discrete nature (including scalar variables). However, for atmospheric fields and other continuous model quantities, the discrete representation inside the forward model requires consideration. To avoid inconsistencies between model input and output it is important that the mapping from the discrete variables to the “continuous view” of the quantity is well defined, and applied consistently through the forward model. This mapping is given by the basis functions. Similar arguments and nomenclature are found in *Read et al. [2006]*.

The basis functions are discussed explicitly in few places in this user guide, but it shall be noted that all interpolations imply an underlying set of basis functions. On the other hand, an understanding of both the derivation and the obtained Jacobians require direct consideration of the basis functions. ARTS operates with two types of basis functions.

### 16.2.1 Basis functions for piece-wise linear quantities

To treat an one-dimensional quantity to be piece-wise linear, or to say that a linear interpolation shall be applied, are identical definitions. The basis functions matching this definition have triangular shape, sometimes denoted as “tenth functions”. Such functions are exemplified in Fig. 16.1, see also *Buehler et al. [2005]*.

In most cases, the quantity is considered to be undefined outside the end points of the grid. Hence, the basis function for a grid end point is then just “half a tenth”. The exception to this rule is retrieval grids of piece-wise linear variables. To avoid that retrieval grids must cover the complete atmosphere, end point values are assumed to be valid to the end of the atmosphere (or data range of concern). That is, the basis functions for end points of retrieval grids follow the tenth shape inside the grid range, and have a constant value of 1 outside. In terms of interpolation, this matches to allow extrapolation, the applying a “nearest” interpolation for positions outside the covered range (the end values are valid all the way to  $\pm$ infinity). The basis functions are defined likewise for higher dimensions, but the tenth functions are then 2D or 3D “tenths”.

### 16.2.2 Polynomial basis functions

Some retrieval quantities are expressed using a polynomial basis. Sensor zenith angle pointing off-set is one such quantity. The off-set is then treated to have a polynomial variation as a function of time. If the offset is assumed to be constant in time, a zero order polynomial shall be selected. If there is also a linear drift with time, use a first order polynomial, etc.

For these basis functions, the explanatory variable (time in the example above) is normalised to cover the range  $[-1,1]$ , here denoted as  $z$ , and the continuous representation ( $f$ ) of the variable of concern can be written as

$$f(z) = x_0 + x_1(z - b_1) + x_2(z^2 - b_2) + x_3(z^3 - b_3) + x_4(z^4 - b_4) + \dots \quad (16.3)$$

where  $x_0, x_1, \dots$  are the coefficients to be retrieved (elements of  $\mathbf{x}$ ). The interpretation of a retrieval is simplified if the average of  $f$  equals  $x_{p0}$ , and the scalars  $b_1, b_2, \dots$  are selected, schematically, as

$$0 = \int_{-1}^1 (z^n - b_n) dz, \quad n > 0. \quad (16.4)$$

According to this expression,  $b_n$  is zero for odd  $n$ . However,  $z$  is in practise a discrete variable ( $z_i$ , not necessarily symmetric around 0), and  $b_n$  is taken as the average of  $z_i^n$ : all  $b_n$  can be non-zero. The normalisation of  $z$  is not only made for interpretation reasons, it can be required for pure numerical reasons, such as when  $z$  represent frequency (in Hz).

In practise, the basis functions are vectors, denoted below as  $\mathbf{z}_i$ . Element  $j$  of  $\mathbf{z}_i$  is

$$\mathbf{z}_i(j) = z(j)^i - b_i. \quad (16.5)$$

## 16.3 Atmospheric variables, common expressions

The analytically-oriented calculation procedure to obtain the Jacobian for atmospheric quantities is here outlined. The expressions are based on the chain rule, and can be applied for absorption constituents, atmospheric temperatures and winds. It is important to notice that only local effects are considered, and the expressions have limitations, as discussed below in Sec. 16.3.6.

### 16.3.1 Matrix derivatives

Some of the expressions of this section treat derivatives involving vectors and matrices. Such derivatives must be handled with some care, the standard calculation rules do not



always apply. The basic relationships used here are<sup>1</sup>

$$\frac{\partial \mathbf{a}}{\partial \mathbf{a}} = \mathbf{1}, \quad (16.6)$$

$$\frac{\partial(\mathbf{A}\mathbf{b})}{\partial \mathbf{a}} = \mathbf{A} \frac{\partial \mathbf{b}}{\partial \mathbf{a}}, \quad \text{when } \mathbf{A} \text{ independent of } \mathbf{a}, \quad (16.7)$$

$$\frac{\partial(\mathbf{b} + \mathbf{c})}{\partial \mathbf{a}} = \frac{\partial \mathbf{b}}{\partial \mathbf{a}} + \frac{\partial \mathbf{c}}{\partial \mathbf{a}}, \quad (16.8)$$

where  $\mathbf{a}$ ,  $\mathbf{b}$  and  $\mathbf{c}$  are vectors, and  $\mathbf{A}$  is a matrix.

Matrix exponential derivatives can not be expressed analytically in a general manner, but some cases can be handled. If two matrices  $\mathbf{A}$  and  $\mathbf{B}$  are commutative, i.e.  $\mathbf{AB} = \mathbf{BA}$ , then the following is valid [Dattorro, 2011]<sup>2</sup>

$$\frac{\partial}{\partial t} e^{t\mathbf{A}+\mathbf{B}} = \mathbf{A} e^{t\mathbf{A}+\mathbf{B}}, \quad (16.9)$$

where  $t$  is a scalar variable. The cases where  $\mathbf{A}$  and  $\mathbf{B}$  are commutative includes the situation where one of them is a scalar matrix (can be written as  $a\mathbf{1}$ , i.e. diagonal with all non-zero elements equal).

### 16.3.2 Separation of terms

The overall task is to calculate (Eq. 16.1 with subscript  $p$  left out)

$$\frac{\partial \mathbf{y}}{\partial x}$$

where  $x$  is the element of  $\mathbf{x}$  for which we want to obtain the weighting function. This is a column of the complete weighting function matrix.

A first step is to identify how sensor characteristics can be incorporated? To make the nomenclature simpler, we assume here that the simulations cover only a single measurement block and we have (cf. Eq. 5.2)

$$\mathbf{y} = \mathbf{H}\mathbf{i}_b. \quad (16.10)$$

We can then apply the chain-rule for a first time to obtain

$$\frac{\partial \mathbf{y}}{\partial x} = \frac{\partial \mathbf{y}}{\partial \mathbf{i}_b} \frac{\partial \mathbf{i}_b}{\partial x} = \mathbf{H} \frac{\partial \mathbf{i}_b}{\partial x} = \mathbf{H}\mathbf{k}_i. \quad (16.11)$$

Hence, sensor characteristics can be handled by calculating the weighting function column matching all monochromatic pencil beam calculation of the measurement block ( $\mathbf{k}_i$ ) and perform a multiplication with  $\mathbf{H}$ , a parallel procedure compared to how  $\mathbf{i}_b$  is compiled to obtain  $\mathbf{y}$ . The calculation procedure expands to allow that the complete weighting function matrix (for quantities covered by the analytical calculation procedure) is calculated as

$$\frac{\partial \mathbf{y}}{\partial \mathbf{x}} = \mathbf{H}\mathbf{K}_i, \quad (16.12)$$

where  $\mathbf{K}_i = \partial \mathbf{i}_b / \partial \mathbf{x}$ . One column of this matrix is  $\mathbf{k}_i$ .

<sup>1</sup>See e.g. [en.wikipedia.org/wiki/Matrix\\_calculus](http://en.wikipedia.org/wiki/Matrix_calculus).

<sup>2</sup>Available at <https://ccrma.stanford.edu/~dattorro/mybook.html>.

The vector  $\mathbf{i}_b$  consists of a number of Stokes vectors appended,  $\mathbf{i}_b = [\mathbf{s}_1^T, \mathbf{s}_2^T, \dots, \mathbf{s}_n^T]^T$ , and the calculation of  $\mathbf{k}_i$  can schematically be written as

$$\mathbf{k}_i = \sum_{j=1}^n \frac{\partial \mathbf{i}_b}{\partial \mathbf{s}_j} \frac{\partial \mathbf{s}_j}{\partial x} \quad (16.13)$$

The terms  $\partial \mathbf{i}_b / \partial \mathbf{s}_j$  are formally matrices. However, these matrices are not calculated explicitly as they only contain information on where  $\mathbf{s}_i$  is stored inside  $\mathbf{i}$ . That is, these matrices are of bookkeeping character, consisting only of zeros and ones. In practice, results matching  $\partial \mathbf{s}_j / \partial x$  are simply inserted in correct place of  $\mathbf{k}_i$ , mimicking how  $\mathbf{s}_i$  is put into  $\mathbf{i}$ .

Accordingly, the core task is to calculate  $\partial \mathbf{s}_j / \partial x$ , where for simplicity the subscript  $j$  is dropped below. This calculation is expanded as

$$\frac{\partial \mathbf{s}}{\partial x} = \sum_{i=1}^n \frac{\partial \mathbf{s}}{\partial x_i} \frac{\partial x_i}{\partial x}, \quad (16.14)$$

where  $x_i$  is the value of the quantity of concern, at each point of the propagation path. That is,  $i$  indexes the path points. The actual radiative transfer enters by the terms  $\partial \mathbf{s} / \partial x_i$ , and they are discussed separately below.

The term  $\partial x_i / \partial x$  appears due to the fact that  $x_i$  and  $x$  are placed at different positions, and the representation of the atmospheric fields must be considered here. In practise, the term is calculated as the value of the basis function for  $x$  at the location of  $x_i$  (further discussed in *Buehler et al. [2005]*). This is a slight approximation with respect to the goal of fully incorporating the piece-wise linear representation in the weighting functions [*Buehler et al., 2005*]. A low value of  $\Delta l_i$  decreases the degree of approximation.

It can be noted that  $\partial x_i / \partial x$  is normally non-zero for more than one element of  $\mathbf{x}$ . The exception is if the positions of  $x_i$  and  $x$  are identical. Reversely, the weighting function for element  $x$  can have contributions from several propagation path points ( $x_i$ ), as well as from several radiance spectra. Accordingly, the practical calculations are done by first determine all  $\partial \mathbf{s} / \partial x_i$ , of the given propagation path. These data are then used to determine  $\partial \mathbf{s} / \partial \mathbf{x}$ , for the retrieval quantity of concern. That is, each  $\partial \mathbf{s} / \partial x_i$  is combined with  $\partial x_i / \partial x$  for all elements of  $\mathbf{x}$ . Most of these combinations yield a zero result. The terms  $\partial x_i / \partial x$  are determined with help of ARTS' internal interpolation grid position routines.

### 16.3.3 $\partial \mathbf{s} / \partial x_i$ , general case

The term  $\partial \mathbf{s} / \partial x_i$  is here outlined for the general case of vector radiative transfer. In this case, the Stokes elements can not be treated separately, and matrix-vector notation is required. The final Stokes vector obtained through Eq. 9.7 can be expressed as

$$\mathbf{s} = \mathbf{s}' + \mathbf{T}' [\mathbf{T}_i \mathbf{s}_i + (\mathbf{1} - \mathbf{T}_i) \bar{\mathbf{b}}_i], \quad (16.15)$$

where  $\mathbf{s}'$  is the Stokes vector for all emission generated between the sensor and point  $i + 1$ ,  $\mathbf{T}'$  is the transmission Mueller matrix for the same part of the propagation path and  $\mathbf{T}_i$  is defined in Eq. 9.8. The quantities  $\mathbf{s}'$ ,  $\mathbf{T}'$  and  $\mathbf{s}_i$  are not function of  $x_i$ . This gives

$$\frac{\partial \mathbf{s}}{\partial x_i} = \mathbf{T}' \left[ \frac{\partial \mathbf{T}_i}{\partial x_i} (\mathbf{s}_i - \bar{\mathbf{b}}_i) + (\mathbf{1} - \mathbf{T}_i) \frac{\partial \bar{\mathbf{b}}_i}{\partial x_i} \right]. \quad (16.16)$$

The terms  $\partial \mathbf{T}_i / \partial x_i$  and  $\partial \bar{\mathbf{b}}_i / \partial x_i$  are both calculated in a pure numerical manner, for different reasons discussed below.

### 16.3.4 Including the surface

For scattered down-welling radiation the effective transmission matrix is

$$\mathbf{T}' = \mathbf{T}_2 \mathbf{R}_i \mathbf{T}_1, \quad (16.17)$$

where  $\mathbf{T}_2$  is the transmission between the surface and the sensor,  $\mathbf{R}_i$  is defined in Eq. 11.7 and  $\mathbf{T}_1$  is the transmission between the point  $i + 1$  and the surface.

### 16.3.5 $\partial \mathbf{s} / \partial x_i$ , locally unpolarised absorption

Eq. 16.16 can be simplified for some conditions. A first case is scalar radiative transfer, i.e. only the first element of the Stokes vector is considered and all terms of Eq. 16.16 are scalar quantities. For all other cases, in principle vector radiative transfer must be performed, as  $\mathbf{T}'$  can always have off-diagonal elements. Even if atmospheric absorption is totally unpolarised,  $\mathbf{T}'$  can be non-diagonal due to the surface (Eq. 16.17). However, if the absorption locally lacks polarisation, the calculations can be handled by analytical expressions in a higher degree.

To focus on the analytical expressions dealing with local radiative transfer effects, let us write Eq. 16.15 as

$$\mathbf{s} = \mathbf{s}' + \mathbf{T}' \mathbf{s}_s. \quad (16.18)$$

In the nomenclature of Eq. 9.7,  $\mathbf{s}_s = \mathbf{s}_{i+1}$  (but would be confusing to here use  $\mathbf{s}_{i+1}$ ). Hence

$$\frac{\partial \mathbf{s}}{\partial x_i} = \mathbf{T}' \frac{\partial \mathbf{s}_s}{\partial x_i}.$$

The first element of  $\mathbf{s}_s$ ,  $I$ , can be written as (cf. Eq. 9.2)

$$I = e^{-\tau_i} I_i + (1 - e^{-\tau_i}) \bar{B}_i. \quad (16.19)$$

By again using the chain rule, the derivative of  $I$  with respect to  $x_i$  can be written as

$$\frac{\partial I}{\partial x_i} = \frac{\partial I}{\partial \tau_i} \frac{\partial \tau_i}{\partial x_i} + \frac{\partial I}{\partial \bar{B}_i} \frac{\partial \bar{B}_i}{\partial x_i} = e^{-\tau_i} \frac{\partial \tau_i}{\partial x_i} (\bar{B}_i - I_i) + (1 - e^{-\tau_i}) \frac{\partial \bar{B}_i}{\partial x_i}. \quad (16.20)$$

The two remaining derivatives  $\partial \tau_i / \partial x_i$  and  $\partial \bar{B}_i / \partial x_i$  depend on the quantity considered, and are discussed further below.

For higher Stokes components of  $\mathbf{s}_s$ , or in general if emission is totally ignored, Eq. 16.19 is simplified to (here exemplified for the second Stokes element,  $Q$ )

$$Q = e^{-\tau_i} Q_i, \quad (16.21)$$

and the chain rule expression is correspondingly shorter:

$$\frac{\partial Q}{\partial x_i} = -e^{-\tau_i} \frac{\partial \tau_i}{\partial x_i} Q_i. \quad (16.22)$$

### 16.3.6 Limitations

A constraint for the analytical expressions above is that the effect of the variable must only be local. Main examples on non-local effects should occur through hydrostatic equilibrium and refraction. Significant impact of a gas through these mechanisms should only be found for water vapour in the lower troposphere, but is a general concern for temperature as discussed in Sec. 16.6.

## 16.4 Absorption species

### 16.4.1 Common practicalities

To obtain the Jacobian for absorption species, use `jacobianAddAbsSpecies`. The method handles one species at the time. The calculations can either be done in “analytical” or “perturbation” manner. For gases, weighting functions (WFs) can be provided for several units of the gas abundance:

**vmr** Volume mixing ratio (a value between 0 and 1). The WF divided by  $10^6$  corresponds to that 1 ppm of the gas is added to the atmospheric volume of concern.

**nd** Number density. The WF corresponds here to that one molecule is added.

**rel** Relative/fractional change. In a perfectly linear case, the WF corresponds here to that the gas amount is doubled.

**logrel** This option returns the same WFs as “rel”, but is included to flag that the natural logarithm of the “rel” unit is retrieved.

For the “rel” and “logrel” options it is important to note that ARTS calculate the WFs with respect to the given state, ARTS does not know anything about the actual reference state for which the “rel” unit is valid (where normally the a priori state is selected). For iterative inversions, a rescaling of the WFs provided by ARTS is likely needed, to make the WFs valid with respect to the (original) reference state. For the assumption made inside ARTS, the WFs for “rel” and “logrel” are identical.

A second main consideration is to select the retrieval grids. For analytical calculations there are no other selections to be made.

### 16.4.2 Perturbation calculations

For pure numerical calculations, also the size of the perturbation must be specified ( $\Delta x$  in Eq. 16.2). The perturbation shall given following the unit selected. The same value is applied for all WFs (which can cause practical problems ...).

### 16.4.3 Analytical expressions

If not made clear above, the only term that differs between the Jacobian quantities is  $\partial s / \partial x_i$ .

#### Unpolarised absorption

The term  $\partial \bar{B}_i / \partial x_i$  of Eq. 16.20 is zero and the chain rule expression reduces to

$$\frac{\partial I}{\partial x_i} = e^{-\tau_i} \frac{\partial \tau_i}{\partial x_i} (\bar{B}_i - I_i) \quad (16.23)$$

The absorption coefficient at point  $i$ ,  $\alpha_i$ , is here written as

$$\alpha_i = x_i \sigma_i + \alpha_i^o, \quad (16.24)$$

where  $\sigma_i$  is the absorption cross-section for the species (at point  $i$  and in a unit matching the unit of  $x$ ), and  $\alpha_i^o$  covers the summed absorption of all other atmospheric constituents. Considering Eq. 9.4, the derivative of  $\tau_i$  with respect to  $x_i$  is then

$$\frac{\partial \tau_i}{\partial x_i} = \frac{\partial \tau_i}{\partial \alpha_i} \frac{\partial \alpha_i}{\partial x_i} = \frac{\Delta l_i}{2} \sigma_i. \quad (16.25)$$

### General case

So far, the term  $\partial \mathbf{T}_i / \partial x_i$  is only estimated by performing a small perturbation, of the absorption associated with the species to be retrieved.

However, there exists a potential to use an analytical expression, as discussed below, but this is left for future consideration. The relationship between  $x_i$  and the propagation matrix of the path step can be written as

$$\bar{\mathbf{K}}_i = \frac{x_i \mathbf{C}_i + x_{i+1} \mathbf{C}_{i+1}}{2} + \bar{\mathbf{K}}_i^o, \quad (16.26)$$

where  $\mathbf{C}$  can be seen as a matrix absorption cross-section (corresponding to  $\sigma$  in Eq. 16.24) and  $\bar{\mathbf{K}}_i^o$  is the propagation matrix summed for all other atmospheric constituents. On the condition that Eq. 16.9 is valid, we have that

$$\frac{\partial \mathbf{T}_i}{\partial x_i} = \frac{\partial}{\partial x_i} e^{-\Delta l_i \left( \frac{x_i \mathbf{C}_i + x_{i+1} \mathbf{C}_{i+1}}{2} + \bar{\mathbf{K}}_i^o \right)} = \frac{-\Delta l_i}{2} \mathbf{C}_i \mathbf{T}_i. \quad (16.27)$$

The question is when Eq. 16.27 can be applied? We have three main cases:

- The equation is valid as long as the species to be retrieved has unpolarised absorption. This as  $\mathbf{C}_i$  and  $\mathbf{C}_{i+1}$  can then both be written as  $\sigma_i \mathbf{1}$ , and  $(x_i \mathbf{C}_i + x_{i+1} \mathbf{C}_{i+1})/2$  is commutative with any  $\bar{\mathbf{K}}_i^o$ .
- Eq. 16.27 is not valid when all three matrices involved ( $\bar{\mathbf{K}}_i^o$  and the two  $\mathbf{C}$ -matrices) have off-diagonal elements on the same time. However, this is unlikely case. The main causes to polarised absorption are free electrons, Zeeman splitting and particles, and these mechanisms are mainly found in the ionosphere, mesosphere and troposphere, respectively.
- The remaining case is when  $\bar{\mathbf{K}}_i^o$  is diagonal but the species to be retrieved has polarised absorption. The likely situation is that both  $\mathbf{C}_i$  and  $\mathbf{C}_{i+1}$  are non-diagonal on the same time, and the condition of Eq. 16.9 is not fulfilled. However, as argued below, Eq. 16.27 should still be approximately valid, and this is used as “working hypothesis” in ARTS.

An alternative way to express the propagation matrix is

$$\bar{\mathbf{K}}_i = \frac{x_i + x_{i+1}}{2} \bar{\mathbf{C}}_i + \bar{\mathbf{K}}_i^o,$$

with

$$\bar{\mathbf{C}}_i = \frac{\mathbf{C}_i + \mathbf{C}_{i+1}}{2}.$$

With this formulation even the third case above would be handled, as we now only have two matrices to consider (and  $\bar{\mathbf{C}}_i$  is commutative with a diagonal  $\bar{\mathbf{K}}_i^o$ ). We would then have

$$\frac{\partial \mathbf{T}_i}{\partial x_i} = \frac{-\Delta l_i}{2} \bar{\mathbf{C}}_i \mathbf{T}_i.$$

As  $\mathbf{C}_i$  and  $\mathbf{C}_{i+1}$  are (very) similar matrices (and then also close to  $\bar{\mathbf{C}}_i$ ), the practical difference between this equation and Eq. 16.27 should be small. Or reversely, Eq. 16.27 should be approximately correct as  $\mathbf{C}_i$  and  $\mathbf{C}_{i+1}$  are close to identical matrices.

## 16.5 Winds

Calculation of wind weighting functions are triggered by `jacobianAddWind`. Each wind component (see Sec. 13.1) is treated as an individual retrieval variable. That is, if you want to retrieve all three wind components, `jacobianAddWind` must be called three times. Only the analytically inclined calculation approach is at hand for winds.

Theoretically, the Doppler shift induced by winds affects the emission source term ( $\bar{B}_i$ , in the scalar case), but this impact is extremely small and the related terms are ignored. This gives a case basically identical to the one above for absorption species. The only difference is that also the term  $\partial\alpha_i/\partial x_i$  is obtained in a pure numerical manner, by recalculating the absorption coefficient with the wind perturbed slightly.

## 16.6 Atmospheric temperatures

### 16.6.1 Common practicalities

To obtain WFs for absorption species, use `jacobianAddTemperature`. The calculations can either be done in “analytical” or “perturbation” manner. Retrieval grids must be specified.

A special consideration for temperature is hydrostatic equilibrium. If effects originating in hydrostatic equilibrium shall be included in the WFs, or not, is selected by an argument denoted as `hse`. A full account of hydrostatic equilibrium is possible for perturbation calculations, while the analytical approach only treats the local effect (see further below).

### 16.6.2 Perturbation calculations

The size of the perturbation must be selected (in K). Complete radiative transfer calculations are done after perturbing the temperature field. Hence, all possible effects are included, such as changed propagation paths through the impact of temperature on the refractive index. Please, note that hydrostatic equilibrium comes in during the perturbation. If `hse` is set to “on”, also `z_field` is recalculated as part of the temperature perturbation (Section 3.5). If set to “off”, there is no change of `z_field`. That is, you must make an active choice regarding hydrostatic equilibrium, while others effects are included automatically.

### 16.6.3 Analytical expressions

#### Unpolarised absorption

Compared to atmospheric species, the expressions become here more complex as temperature also affects the propagation path length ( $\Delta l_i$ ) and the emission source term ( $\bar{B}_i$ ). Accordingly, all terms of Eq. 16.20 are relevant, and the expansion of  $\partial\tau_i/\partial x_i$  generates additional terms

$$\frac{\partial I}{\partial x_i} = e^{-\tau_i} \left[ \frac{\partial\tau_i}{\partial\alpha_i} \frac{\partial\alpha_i}{\partial x_i} + \frac{\partial\tau_i}{\partial\Delta l_i} \frac{\partial\Delta l_i}{\partial x_i} \right] (\bar{B}_i - I_i) + (1 - e^{-\tau_i}) \frac{\partial\bar{B}_i}{\partial x_i}. \quad (16.28)$$

Terms part of expressions found above are not discussed separately here. The term,  $\partial\Delta l_i/\partial x_i$ , originates in the constrain of hydrostatic equilibrium, and is set to zero when `hse` is set to “off”. Otherwise it is set as derived below. The term  $\partial\alpha_i/\partial x_i$  is calculated in a pure numerical manner, by perturbing the temperature. Eq. 9.4 gives

$$\frac{\partial\tau_i}{\partial\Delta l_i} = \frac{\alpha_i + \alpha_{i+1}}{2}. \quad (16.29)$$

The path length ( $\Delta l_i$ ), for a given pressure, is linearly proportional to the temperature, and if  $\bar{T}$  is the average temperature along the path step:

$$\frac{\partial \Delta l_i}{\partial \bar{T}} = \frac{\Delta l_i}{\bar{T}}. \quad (16.30)$$

Following the other variables, we set  $\bar{T} = (T_i + T_{i+1})/2$ , and

$$\frac{\partial \Delta l_i}{\partial x_i} = \frac{\Delta l_i}{2T_i}. \quad (16.31)$$

In summary (assuming hse set to “on”):

$$\frac{\partial I}{\partial x_i} = e^{-\tau_i} \frac{\Delta l_i}{2} \left[ \frac{\partial \alpha_i}{\partial x_i} + \frac{\alpha_i + \alpha_{i+1}}{2T_i} \right] (\bar{B}_i - I_i) + (1 - e^{-\tau_i}) \frac{\partial \bar{B}_i}{\partial x_i}. \quad (16.32)$$

The derivative of the Planck function ( $\partial B/\partial x_i$ ) can be expressed analytically [Eriksson *et al.*, 2002], but as  $B$  is provided by an agenda related terms must anyhow be determined in a pure numerical manner. For example, if the Rayleigh-Jeans approximation is for some reason applied ( $B = T$ ) the term is just 1.

The expression for higher Stokes elements, or if emission is totally ignored, is obtained by setting  $\bar{B}_i$  (and  $\partial \bar{B}_i/\partial x_i$ ) to zero.

### General case

The term  $\partial \mathbf{T}_i/\partial x_i$  is calculated in a pure numerical manner. This is done in two steps. In the first step, the transmission matrix is recalculated for a slightly perturbed temperature. If hydrostatic equilibrium is considered, the transmission is also recalculated with a disturbed  $\Delta l_i$ . To avoid making two identical disturbances of the transmission matrix, these calculations are performed as

$$\frac{\partial \mathbf{T}_i}{\partial x_i} = \frac{\partial \mathbf{T}_i}{\partial \bar{T}} \frac{\bar{T}}{2T_i},$$

a relationship that follows from Eqs. 16.30 and 16.31.

### Hydrostatic equilibrium and limitations

A changed temperature has non-local effects, originating from refraction and hydrostatic equilibrium. The expressions above ignore totally refraction effects.

As mentioned, if hse is set to “off”, the term  $\partial \Delta l_i/\partial x_i$  is set to zero. That is, the path length through the layer is not affected by a temperature change. With hse set to “on”, the complete expressions above are used.

If this treatment of hydrostatic equilibrium is sufficient or not depends on the observation geometry. It should be insufficient for limb sounding, where changes even at altitudes below the tangent point can have an influence as the geometrical altitudes of all higher layers is changed through hydrostatic equilibrium. However, this effect vanishes for ground-based observations at zenith and satellite measurements at nadir, giving a full account of hydrostatic equilibrium even with the analytical expressions. In practise it should be possible to apply the expressions outside zenith and nadir, as long as the observations are of “up” or “down-ward” type. The same applies to measurements from inside the atmosphere, (e.g. aircraft ones), if the reference pressure for hydrostatic equilibrium (p\_hse) is matched to the pressure of the observation point.

## 16.7 Sensor pointing

The term “sensor pointing” refers to deviations between nominal and actual viewing direction of the sensor. So far, only deviations in zenith angle can be considered. The workspace method to initiate such Jacobians is `jacobianAddPointingZa`.

The pointing deviation is treated as a time varying variable, then having a polynomial variation. hence, the basis functions described in Section 16.2.2 are applied. The time is taken from `sensor.time`. If the pointing error is assumed to be constant with time, the polynomial order to select is 0, and so on. As a special case, the polynomial order -1 signifies here that the pointing off-set is so highly varying that an off-set must be assigned to each spectrum (sometime called “pointing jitter”).

The Jacobian can be calculated in two manners:

**recalc** If this option is selected, radiative transfer calculations are performed for a shift of `sensor.los` (perturbation size selected by `dza`). Only a “one-sided” perturbation is applied.

**interp** The Jacobian is derived from existing data, by an interpolation of existing data. This achieved by interpolating pencil beam data to a shifted zenith angle grid. This will involve some extrapolation of the data, and this aspect should be considered when selecting `mblock_za_grid`. The average of a positive and negative shift is determined. The shift to apply (`dza`) should be smaller than the minimum spacing of `mblock_za_grid` for accurate results. As interpolation is a relative fast operation and a “double-sided” disturbance is used, this option should in general be preferred.

## 16.8 Sensor frequencies

This class of Jacobians treats deviations between nominal and actually recorded frequencies. Such differences can originate in several ways, but the exact origin can normally be ignored and the effect can be modelled as the backend (spectrometer, filter bank ...) channels are shifted from their nominal position. The workspace methods to define such Jacobians are `jacobianAddFreqShift` and `jacobianAddFreqStretch`. These Jacobians can so far only be determined by applying an interpolation of existing monochromatic data, then shifted `df` from the nominal values.

The methods treat either the “shift” or “stretch” effects. This follows standard nomenclature. A “shift” is an off-set that is of the same size for all backend channels. That is, if only a shift is assumed, the nominal distances between the channels are assumed to be valid. The “stretch” term considers the distance between the channels. For a backend with all channels equally spaced, a stretch signifies that the spacing deviates from the nominal value (but all channels still equally spaced). More generally, a stretch means that the deviation from the nominal channel position increases linearly from the middle point of the backend. In terms of the basis functions Section 16.2.2, shift and stretch correspond to polynomial order 0 and 1.

Both frequency shift and stretch can be assumed to be time varying, where exactly the same polynomial approach as for pointing is applied. This including the case of setting the order to -1.



## 16.9 Polynomial baseline fit

A “baseline” is microwave jargon for a disturbance of the spectrum that is not covered by the common sensor characteristics. The most common case is that the local oscillator signal leaks into the measurement by reflections occurring inside the sensor, causing a pattern in the spectrum of standing-wave type. Such effects are difficult to model in a physical manner, and a more general fitting procedure must be applied. A common option is then to model the baseline as a polynomial, of a specified order. That is, assuming a measurement giving a single spectrum, the measured spectrum  $\mathbf{y}$  is modelled as

$$\mathbf{y} = \mathbf{y}' + \sum_{i=0}^n x_i \mathbf{z}_i, \quad (16.33)$$

where  $\mathbf{y}'$  is the “baseline free” spectrum, and  $x_i$  and  $\mathbf{z}_i$  are introduced in Section 16.2.2.

The Jacobian for such baseline models are obtained by `jacobianAddPolyfit`. For single spectra measurements, the only consideration is the polynomial order to use. For measurements where several spectra are appended to form the measurement vector, the default option is that baseline can vary between all spectra. In some cases, it could be assumed that the baseline is common between data for different polarisations, viewing directions or measurement blocks, and flags can be set to mimic such assumptions.

For a given set of retrieved  $x_i$ , the simplest way to determine the estimated baseline is to perform a multiplication between the relevant parts of the Jacobian and the state vector:

$$\mathbf{K}_p \mathbf{x}_p, \quad (16.34)$$

where  $p$  indicates the  $n + 1$  columns/elements corresponding to  $x_i$ .

## 16.10 Sinusoidal baseline fit

If the baseline has components of sinusoidal character there is also a second option, provided the method `jacobianAddSinefit`. The baseline is in this method modelled as [Kuntz *et al.*, 1997]

$$\mathbf{y} = \mathbf{y}' + \sum_{i=1}^n a_i \sin\left(\frac{2\pi(\nu - \nu_1)}{l_i}\right) + b_i \cos\left(\frac{2\pi(\nu - \nu_1)}{l_i}\right) \quad (16.35)$$

where  $a_i$  and  $b_i$  are the coefficients to be retrieved,  $\nu$  is frequency,  $\nu_1$  is a reference frequency and  $l_i$  is period length. The reference frequency ( $\nu_1$ ) is in practice taken as the first frequency of the spectrometer.

The period lengths ( $l_i$ ) are user input. For each given period length, the corresponding sine and cosine terms are included in the Jacobian. As for the polynomial fit, there exist options to set the baseline to be common between different polarisations, viewing directions or measurement blocks. Equation 16.34 is also applicable for sinusoidal baseline fits.

An alternative way to express the expression above is

$$\mathbf{y} = \mathbf{y}' + \sum_{i=1}^n A_i \sin\left(\frac{2\pi(\nu - \nu_1)}{l_i} + \phi_i\right) \quad (16.36)$$

where

$$A_i = \sqrt{a_i^2 + b_i^2} \quad (16.37)$$

and

$$\tan \phi_i = \frac{a_i}{b_i}. \quad (16.38)$$

Equation 16.35 is used to define the weighting functions as this gives a linear retrieval problem, in contrast to if Equation 16.36 would be used, that would require an iterative process to determine  $A_i$  and  $\phi_i$ .

# Chapter 17

## Batch calculations

Quite often one wants to repeat a large number of calculations with only a few variables changed. Examples of such cases are to perform 1D calculations for a number of atmospheric states taken from some atmospheric model, generate a set of spectra to create a training database for regression based inversions or perform a numeric inversion error analysis. For such calculations it is inefficient to perform the calculations by calling ARTS repeatedly. For example, as data must be imported for each call even if the data are identical between the cases. Cases such as the ones described above are here denoted commonly as batch calculations.

### 17.1 Batch calculations of measurement vector $y$

Batch calculations of measurement vectors are done by the WSM `ybatchCalc`, which takes three inputs, the indices `ybatch_start` and `ybatch_n`, and the agenda `ybatch_calc_agenda`.

The method `ybatchCalc` will do `ybatch_n` calculations, starting at index `ybatch_start`. It will run the agenda `ybatch_calc_agenda` for each case individually. The agenda gets an input `ybatch_index`, which it should use to extract the right input data from one or more arrays or matrices of input. Execution of `ybatch_calc_agenda` must result in a new spectrum vector,  $y$ , most likely by a call of `yCalc`.

The WSV `ybatch_start` is set to a default of 0 in `general.arts`, so you do not have to set this variable unless you want to start somewhere in the middle of your batch input data.

The next section gives some examples of what could be put inside the `ybatch_calc_agenda`.

---

#### History

- 090330 Description of `ybatch_start` added by Stefan Buehler.
- 070726 Copy-edited by Stefan Buehler.
- 070618 Updated by Oliver Lemke.
- 040916 Created by Patrick Eriksson.

## 17.2 Control file examples

The WSV `Extract` can be used to extract an element from an Array, a row from a `Matrix`, a `Matrix` from a `Tensor3`, and so on. The selection is always done on the first dimension. So, for a `Tensor3` as input, it copies the page with the given index from the input `Tensor3` variable to the output `Matrix`.

The idea here is to store the batch cases in tensors or arrays with one dimension extra compared to corresponding workspace variables. For example, a set of `t_field` (which is of type `Tensor3`) is stored as `Tensor4`.

If the dimension is the same for all batch cases, tensors are appropriate. If the dimensions vary (for example you have a different number of vertical levels for each case), then arrays are appropriate.

In the following 1D example, five atmospheric scenarios have been put into the three first loaded files, and a random vector of zenith angles is found in the last file. The batch calculations are then performed as:

```
ReadXML( tensor4_1, "batch_t_field.xml" )
ReadXML( tensor4_2, "batch_z_field.xml" )
ReadXML( tensor5_1, "batch_vmr_field.xml" )
ReadXML( tensor3_1, "batch_za.xml" )
IndexSet( ybatch_n, 5 )

AgendaSet ( ybatch_calc_agenda ){
  Print( ybatch_index, 0 )
  Extract( t_field,    tensor4_1, ybatch_index )
  Extract( z_field,    tensor4_2, ybatch_index )
  Extract( vmr_field,  tensor5_1, ybatch_index )
  Extract( sensor_los, tensor3_1, ybatch_index )

  yCalc
}

ybatchCalc

WriteXML( "ascii", ybatch )
```

If you then want to repeat the calculations, for example with another propagation path step length (e.g. 25 km), it is sufficient to add the lines:

```
AgendaSet( ppath_step_agenda ){
  ppath_stepGeometric( ppath_step, atmosphere_dim, lat_grid,
                      lon_grid, z_field, refellipsoid, z_surface,
                      25e3 )
}

ybatchCalc

WriteXML( "ascii", ybatch, "ybatch_run2.xml" )
```

## **Part IV**

# **Radiative transfer: dedicated scattering methods**



# Chapter 18

## Scattering - DOIT module

The Discrete Ordinate Iterative (DOIT) method is one of the scattering algorithms in ARTS. Besides the DOIT method a backward Monte Carlo scheme has been implemented (see *ARTS Theory*, Section 8). The DOIT method is unique because a discrete ordinate iterative method is used to solve the scattering problem in a spherical atmosphere. Although the DOIT module is implemented for 1D and 3D atmospheres, it is strongly recommended to use it only for 1D, because the Monte Carlo module (*ARTS Theory*, Chapter 8) is much more appropriate for 3D calculations. More appropriate in the sense that it is much more efficient. A literature review about scattering models for the microwave region, which is presented in *Emde and Sreerekha [2004]*, shows that former implementations of discrete ordinate schemes are only applicable for (1D-)plane-parallel or 3D-cartesian atmospheres. All of these algorithms can not be used for the simulation of limb radiances. A description of the DOIT method, similar to what is presented in this chapter, has been published in *Emde et al. [2004]* and in *Emde [2005]*.

### 18.1 The discrete ordinate iterative method

#### 18.1.1 Radiation field

The Stokes vector depends on the position in the cloud box and on the propagation direction specified by the zenith angle ( $\psi$ ) and the azimuth angle ( $\omega$ ). All these dimensions are discretized inside the model; five numerical grids are required to represent the radiation field  $\mathcal{I}$ :

$$\begin{aligned}\vec{P} &= \{P_1, P_2, \dots, P_{N_P}\}, \\ \vec{\alpha} &= \{\alpha_1, \alpha_2, \dots, \alpha_{N_\alpha}\}, \\ \vec{\beta} &= \{\beta_1, \beta_2, \dots, \beta_{N_\beta}\}, \\ \vec{\psi} &= \{\psi_1, \psi_2, \dots, \psi_{N_\psi}\}, \\ \vec{\omega} &= \{\omega_1, \omega_2, \dots, \omega_{N_\omega}\}.\end{aligned}\tag{18.1}$$

---

#### History

- 020601 Created and written by Claudia Emde
- 050223 Rewritten by Claudia Emde, mostly taken from Chapter 4 of Claudia's PhD thesis
- 050929 Included technical part, example control file

Here  $\vec{P}$  is the pressure grid,  $\vec{\alpha}$  is the latitude grid and  $\vec{\beta}$  is the longitude grid. The radiation field is a set of Stokes vectors ( $N_P \times N_\alpha \times N_\beta \times N_\psi \times N_\omega$  elements) for all combinations of positions and directions:

$$\mathcal{I} = \{ \mathbf{s}_1(P_1, \alpha_1, \beta_1, \psi_1, \omega_1), \mathbf{s}_2(P_2, \alpha_1, \beta_1, \psi_1, \omega_1), \dots, \mathbf{s}_{N_P \times N_\alpha \times N_\beta \times N_\psi \times N_\omega}(P_{N_P}, \alpha_{N_\alpha}, \beta_{N_\beta}, \psi_{N_\psi}, \omega_{N_\omega}) \}. \quad (18.2)$$

In the following we will use the notation

$$\begin{aligned} i &= 1 \dots N_P \\ j &= 1 \dots N_\alpha \\ k &= 1 \dots N_\beta \\ l &= 1 \dots N_\psi \\ m &= 1 \dots N_\omega \end{aligned} \quad \mathcal{I} = \{ \mathbf{s}_{ijklm} \} \quad (18.3)$$

### 18.1.2 Vector radiative transfer equation solution

Figure 18.1 shows a schematic of the iterative method, which is applied to solve the vector radiative transfer equation (compare *ARTS Theory*, Equation 6.35)

$$\frac{d\mathbf{s}(\hat{\mathbf{n}}, \nu, T)}{ds} = - \langle \mathbf{K}(\hat{\mathbf{n}}, \nu, T) \rangle \mathbf{s}(\hat{\mathbf{n}}, \nu, T) + \langle \mathbf{a}(\hat{\mathbf{n}}, \nu, T) \rangle B(\nu, T) \quad (18.4)$$

$$+ \int_{4\pi} d\hat{\mathbf{n}}' \langle \mathbf{Z}(\hat{\mathbf{n}}, \hat{\mathbf{n}}', \nu, T) \rangle \mathbf{s}(\hat{\mathbf{n}}', \nu, T), \quad (18.5)$$

where  $\mathbf{s}$  is the specific intensity vector,  $\langle \mathbf{K} \rangle$  is the ensemble-averaged extinction matrix,  $\langle \mathbf{a} \rangle$  is the ensemble-averaged absorption vector,  $B$  is the Planck function and  $\langle \mathbf{Z} \rangle$  is the ensemble-averaged phase matrix. Furthermore  $\nu$  is the frequency of the radiation,  $T$  is the temperature,  $ds$  is a path-length-element of the propagation path and  $\hat{\mathbf{n}}$  the propagation direction. The vector radiative transfer equation is explained in more detail in *ARTS Theory*, Section 6.4.

The first guess field

$$\mathcal{I}^{(0)} = \{ \mathbf{s}_{ijklm}^{(0)} \}, \quad (18.6)$$

is partly determined by the boundary condition given by the radiation coming from the clear sky part of the atmosphere traveling into the cloud box. Inside the cloud box an arbitrary field can be chosen as a first guess. In order to minimize the number of iterations it should be as close as possible to the solution field.

The next step is to solve the scattering integrals

$$\langle \mathbf{S}_{ijklm}^{(0)} \rangle = \int_{4\pi} d\hat{\mathbf{n}}' \langle \mathbf{Z}_{ijklm} \rangle \mathbf{s}_{ijklm}^{(0)}, \quad (18.7)$$

using the first guess field, which is now stored in a variable reserved for the *old radiation field*. For the integration we use equidistant angular grids in order to save computation time (cf. Section 18.3.1). The radiation field, which is generally defined on finer angular grids ( $\vec{\omega}, \vec{\psi}$ ), is interpolated on the equidistant angular grids. The integration is performed over all incident directions  $\hat{\mathbf{n}}'$  for each propagation direction  $\hat{\mathbf{n}}$ . The evaluation of the scattering integral is done for all grid points inside the cloud box. The obtained integrals are interpolated on  $\vec{\omega}$  and  $\vec{\psi}$ . The result is the first guess *scattering integral field*  $\mathcal{S}^0$ :

$$\mathcal{S}^{(0)} = \{ \langle \mathbf{s}_{ijklm}^{(0)} \rangle \}. \quad (18.8)$$



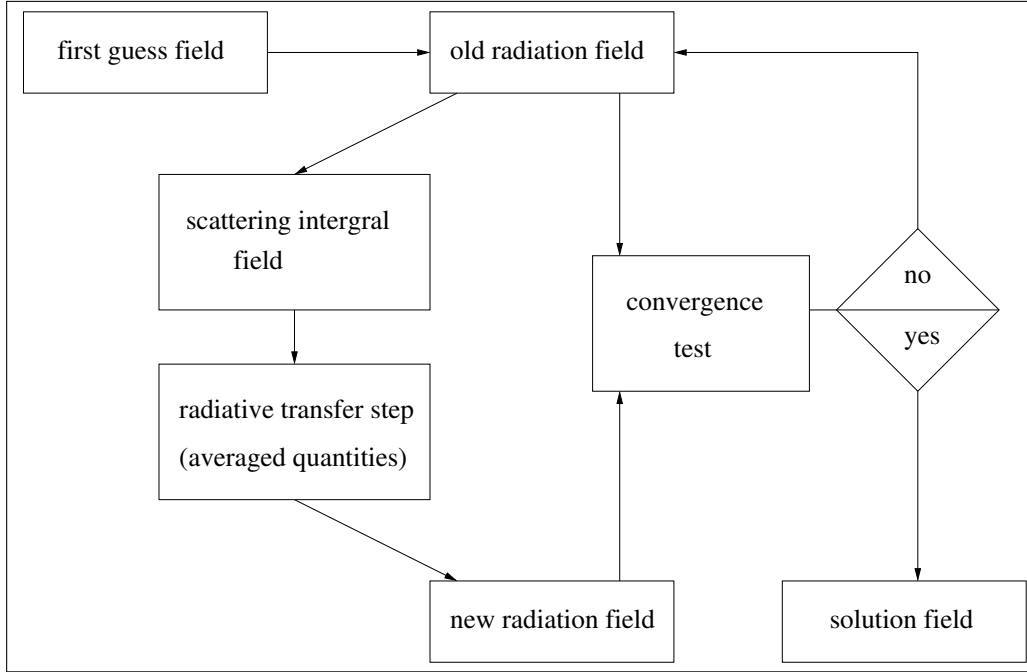


Figure 18.1: Schematic of the iterative method to solve the VRTE in the cloud box.

Figure 18.2 shows a propagation path step from a grid point  $\mathbf{P} = (P_i, \alpha_j, \beta_k)$  into direction  $\hat{\mathbf{n}} = (\psi_l, \omega_m)$ . The radiation arriving at  $\mathbf{P}$  from the direction  $\hat{\mathbf{n}}'$  is obtained by solving the linear differential equation:

$$\frac{ds^{(1)}}{ds} = -\overline{\langle \mathbf{K} \rangle} s^{(1)} + \overline{\langle \mathbf{a} \rangle} \bar{B} + \overline{\langle s^{(0)} \rangle}, \quad (18.9)$$

where  $\overline{\langle \mathbf{K} \rangle}$ ,  $\overline{\langle \mathbf{a} \rangle}$ ,  $\bar{B}$  and  $\overline{\langle s^{(0)} \rangle}$  are *averaged quantities*. This equation can be solved analytically for constant coefficients. Multi-linear interpolation gives the quantities  $\mathbf{K}'$ ,  $\mathbf{a}'$ ,  $s'$  and  $T'$  at the intersection point  $\mathbf{P}'$ . To calculate the radiative transfer from  $\mathbf{P}'$  towards  $\mathbf{P}$  all quantities are approximated by taking the averages between the values at  $\mathbf{P}'$  and  $\mathbf{P}$ . The average value of the temperature is used to get the averaged Planck function  $\bar{B}$ .

The solution of Equation 18.9 is found analytically using a matrix exponential approach:

$$\mathbf{s}^{(1)} = e^{-\overline{\langle \mathbf{K} \rangle} s} \mathbf{s}^{(0)} + \left( \mathbf{1} - e^{-\overline{\langle \mathbf{K} \rangle} s} \right) \overline{\langle \mathbf{K} \rangle}^{-1} \left( \overline{\langle \mathbf{a} \rangle} \bar{B} + \overline{\langle s^{(0)} \rangle} \right), \quad (18.10)$$

where  $\mathbf{1}$  denotes the identity matrix and  $\mathbf{s}^{(0)}$  the initial Stokes vector. The *radiative transfer step* from  $\mathbf{P}'$  to  $\mathbf{P}$  is calculated, therefore  $\mathbf{s}^{(0)}$  is the incoming radiation at  $\mathbf{P}'$  into direction  $(\psi'_l, \omega'_m)$ , which is the first guess field interpolated on  $\mathbf{P}'$ . This radiative transfer step calculation is done for all points inside the cloud box in all directions. The resulting set of Stokes vectors ( $\mathbf{s}^{(1)}$  for all points in all directions) is the first order iteration field  $\mathcal{I}^{(1)}$ :

$$\mathcal{I}^{(1)} = \left\{ \mathbf{s}_{ijklm}^{(1)} \right\}. \quad (18.11)$$

The first order iteration field is stored in a variable reserved for the *new radiation field*.

In the *convergence test* the *new radiation field* is compared to the *old radiation field*. For the difference field, the absolute values of all Stokes vector elements for all cloud box positions are calculated. If one of the differences is larger than a requested accuracy limit,

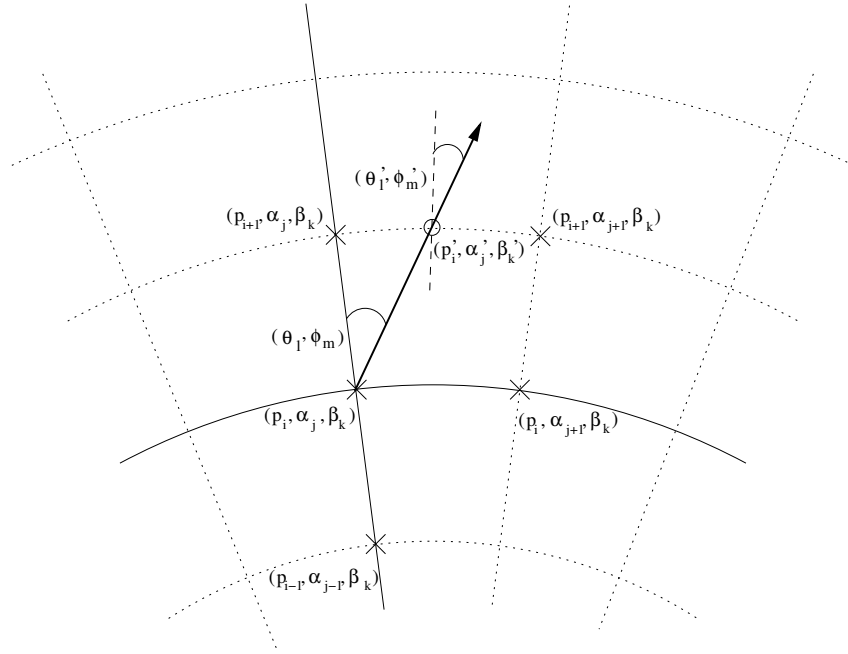


Figure 18.2: Path from a grid point  $((P_i, \alpha_j, \beta_k) - (\times))$  to the intersection point  $((P_i', \alpha_j', \beta_k') - (\circ))$  with the next grid cell boundary. Viewing direction is specified by  $(\psi_l, \omega_m)$  at  $(\times)$  or  $(\psi_l', \omega_m')$  at  $(\circ)$ .

the convergence test is not fulfilled. The user can define different convergence limits for the different Stokes components.

If the convergence test is not fulfilled, the first order iteration field is copied to the variable holding the *old radiation field*, and is then used to evaluate again the scattering integral at all cloud box points:

$$\langle \mathbf{s}_{ijklm}^{(1)} \rangle = \int_{4\pi} d\hat{\mathbf{n}}' \langle \mathbf{Z} \rangle \mathbf{s}_{ijklm}^{(1)}. \quad (18.12)$$

The second order iteration field

$$\mathcal{I}^{(2)} = \{ \mathbf{s}_{ijklm}^{(2)} \}, \quad (18.13)$$

is obtained by solving

$$\frac{d\mathbf{s}^{(2)}}{ds} = -\overline{\langle \mathbf{K} \rangle} \mathbf{s}^{(2)} + \overline{\langle \mathbf{a} \rangle} \bar{B} + \overline{\langle \mathbf{s}^{(1)} \rangle}, \quad (18.14)$$

for all cloud box points in all directions. This equation contains already the averaged values and is valid for specified positions and directions.

As long as the convergence test is not fulfilled the scattering integral fields and higher order iteration fields are calculated alternately.

We can formulate a differential equation for the  $n$ -th order iteration field. The scattering integrals are given by

$$\langle \mathbf{s}_{ijklm}^{(n-1)} \rangle = \int_{4\pi} d\hat{\mathbf{n}}' \langle \mathbf{Z} \rangle \mathbf{s}_{ijklm}^{(n-1)}, \quad (18.15)$$

and the differential equation for a specified grid point into a specified direction is

$$\frac{d\mathbf{s}^{(n)}}{ds} = -\overline{\langle \mathbf{K} \rangle} \mathbf{s}^{(n)} + \overline{\langle \mathbf{a} \rangle} \bar{B} + \overline{\langle \mathbf{s}^{(n-1)} \rangle}. \quad (18.16)$$

Thus the  $n$ -th order iteration field

$$\mathcal{I}^{(n)} = \left\{ \mathbf{s}_{ijklm}^{(n)} \right\}, \quad (18.17)$$

is given by

$$\mathbf{s}^{(n)} = e^{-\overline{\langle \mathbf{K} \rangle} s} + \cdot \mathbf{s}^{(n-1)} (\mathbf{1} - e^{-\overline{\langle \mathbf{K} \rangle} s}) \overline{\langle \mathbf{K} \rangle}^{-1} (\overline{\langle \mathbf{a} \rangle} \bar{B} + \overline{\langle \mathbf{s}^{(n-1)} \rangle}), \quad (18.18)$$

for all cloud box points and all directions defined in the numerical grids.

If the convergence test

$$\left| \mathbf{s}_{ijklm}^{(N)} (P_i, \alpha_j, \beta_k, \psi_l, \omega_m) - \mathbf{s}_{ijklm}^{(N-1)} (P_i, \alpha_j, \beta_k, \psi_l, \omega_m) \right| < \epsilon, \quad (18.19)$$

is fulfilled, a solution to the vector radiative transfer equation has been found:

$$\mathcal{I}^{(N)} = \left\{ \mathbf{s}_{ijklm}^{(N)} \right\}. \quad (18.20)$$

### 18.1.3 Scalar radiative transfer equation solution

In analogy to the *scattering integral* vector field the scalar scattering integral field is obtained:

$$\left\langle S_{ijklm}^{(0)} \right\rangle = \int_{4\pi} d\hat{\mathbf{n}}' \langle Z_{11} \rangle I_{ijklm}^{(0)}. \quad (18.21)$$

The *scalar radiative transfer* equation (compare *ARTS Theory*, 6.44) with a fixed scattering integral is

$$\frac{dI^{(1)}}{ds} = -\langle K_{11} \rangle I^{(1)} + \langle a_1 \rangle B + \langle S^{(0)} \rangle. \quad (18.22)$$

Assuming constant coefficients this equation is solved analytically after averaging extinction coefficients, absorption coefficients, scattering vectors and the temperature. The averaging procedure is done analogously to the procedure described for solving the VRTE. The solution of the averaged differential equation is

$$I^{(1)} = I^{(0)} e^{-\overline{\langle K_{11} \rangle} s} + \frac{\overline{\langle a_1 \rangle} \bar{B} + \overline{\langle S^{(0)} \rangle}}{\overline{\langle K_{11} \rangle}} \left( 1 - e^{-\overline{\langle K_{11} \rangle} s} \right), \quad (18.23)$$

where  $I^{(0)}$  is obtained by interpolating the initial field, and  $\overline{\langle K_{11} \rangle}$ ,  $\overline{\langle a_1 \rangle}$ ,  $\bar{B}$  and  $\overline{\langle S^{(0)} \rangle}$  are the averaged values for the extinction coefficient, the absorption coefficient, the Planck function and the scattering integral respectively. Applying this equation leads to the first iteration scalar intensity field, consisting of the intensities  $I^{(1)}$  at all points in the cloud box for all directions.

As the solution to the vector radiative transfer equation, the solution to the scalar radiative transfer equation is found numerically by the same iterative method. The convergence test for the scalar equation compares the values of the calculated intensities of two successive iteration fields.

### 18.1.4 Single scattering approximation

The DOIT method uses the single scattering approximation, which means that for one propagation path step the optical depth is assumed to be much less than one so that multiple-scattering can be neglected along this propagation path step. It is possible to choose a rather coarse grid inside the cloud box. The user can define a limit for the maximum propagation path step length. If a propagation path step from one grid cell to the intersection point with the next grid cell boundary is greater than this value, the path step is divided in several steps such that all steps are less than the maximum value. The user has to make sure that the optical depth due to cloud particles for one propagation path sub-step is sufficiently small to assume single scattering. The maximum optical depth due to ice particles is

$$\tau_{max} = \langle \mathbf{K}^p \rangle \cdot \Delta s, \quad (18.24)$$

where  $\Delta s$  is the length of a propagation path step. In all simulations presented in [Emde \[2005\]](#),  $\tau_{max} \ll 0.01$  is assumed. This threshold value is also used in [Czekala \[1999\]](#). The radiative transfer calculation is done along the propagation path through one grid cell. All coefficients of the VRTE are interpolated linearly on the propagation path points.

## 18.2 Sequential update

In the previous Section 18.1 the iterative solution method for the VRTE has been described. For each grid point inside the cloud box the intersection point with the next grid cell boundary is determined in each viewing direction. After that, all the quantities involved in the VRTE are interpolated onto this intersection point. As described in the sections above, the intensity field of the previous iteration is taken to obtain the Stokes vector at the intersection point. Suppose that there are  $N$  pressure levels inside the cloud box. If the radiation field is updated taking into account for each grid point only the adjacent grid cells, at least  $N-1$  iterations are required until the scattering effect from the lower-most pressure level has propagated throughout the cloud box up to the uppermost pressure level. From these considerations, it follows, that the number of iterations depends on the number of grid points inside the cloud box. This means that the original method is very ineffective where a fine resolution inside the cloud box is required to resolve the cloud inhomogeneities.

A solution to this problem is the “sequential update of the radiation field”, which is shown schematically in Figure 18.3. For simplicity it will be explained in detail for a 1D cloud box. We divide the update of the radiation field, i.e., the radiative transfer step calculations for all positions and directions inside the cloud box, into three parts: Update for “up-looking” zenith angles ( $0^\circ \leq \psi_{up} \leq 90^\circ$ ), for “down-looking” angles ( $\psi_{limit} \leq \psi_{down} \leq 180^\circ$ ) and for “limb-looking” angles ( $90^\circ < \psi_{limb} < \psi_{limit}$ ). The “limb-looking” case is needed, because for angles between  $90^\circ$  and  $\psi_{limit}$  the intersection point is at the same pressure level as the observation point. The limiting angle  $\psi_{limit}$  is calculated geometrically. Note that the propagation direction of the radiation is opposite to the viewing direction or the direction of the line of sight, which is indicated by the arrows. In the 1D case the radiation field is a set of Stokes vectors each of which depend upon the position and direction:

$$\mathcal{I} = \{ \mathbf{s}(P_i, \psi_l) \}. \quad (18.25)$$

The *boundary condition* for the calculation is the incoming radiation field on the cloud box boundary  $\mathcal{I}^{bd}$ :

$$\mathcal{I}^{bd} = \{ \mathbf{s}(P_i, \psi_l) \} \text{ where } P_i = P_N \forall \psi_l \in [0, \psi_{limit}]$$

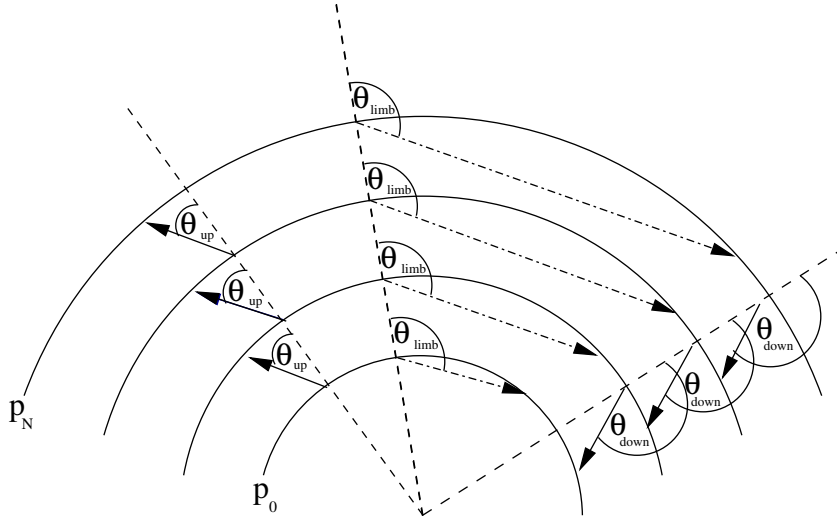


Figure 18.3: Schematic of the sequential update (1D) showing the three different parts: “up-looking” corresponds to zenith angles  $\psi_{\text{up}}$ , “limb-looking” corresponds to  $\psi_{\text{limb}}$  “down-looking” corresponds to  $\psi_{\text{down}}$ .

$$P_i = P_0 \forall \psi_l \in (\psi_{\text{limit}}, 180^\circ], \quad (18.26)$$

where  $P_0$  and  $P_N$  are the pressure coordinates of the lower and upper cloud box boundaries respectively. For down-looking directions, the intensity field at the lower-most cloud box boundary and for up- and limb-looking directions the intensity field at the uppermost cloud box boundary are the required boundary conditions respectively.

### 18.2.1 Up-looking directions

The first step of the sequential update is to calculate the intensity field for the pressure coordinate  $P_{N-1}$ , the pressure level below the uppermost boundary, for all up-looking directions. Radiative transfer steps are calculated for paths starting at the uppermost boundary and propagating to the  $(N - 1)$  pressure level. The required input for this radiative transfer step are the averaged coefficients of the uppermost cloud box layer and the Stokes vectors at the uppermost boundary for all up-looking directions. These are obtained by interpolating the boundary condition  $\mathcal{I}^{bd}$  on the appropriate zenith angles. Note that the zenith angle of the propagation path for the observing direction  $\psi_l$  does not equal  $\psi'_l$  at the intersection point due to the spherical geometry. If  $\psi_l$  is close to  $90^\circ$  this difference is most significant.

To calculate the intensity field for the pressure coordinate  $P_{N-2}$ , we repeat the calculation above. We have to calculate a radiative transfer step from the  $(N - 1)$  to the  $(N - 2)$  pressure level. As input we need the interpolated intensity field at the  $(N - 1)$  pressure level, which has been calculated in the last step.

For each pressure level  $(m - 1)$  we take the interpolated field of the layer above ( $\mathcal{I}(P_m)^{(1)}$ ). Using this method, the scattering influence from particles in the upper-most cloud box layer can propagate during one iteration down to the lower-most layer. This means that the number of iterations does not scale with the number of pressure levels, which would be the case without sequential update.

The radiation field at a specific point in the cloud box is obtained by solving Equation

18.10. For up-looking directions at position  $P_{m-1}$  we may write:

$$\begin{aligned} \mathbf{s}(P_{m-1}, \psi_{\text{up}})^{(1)} &= e^{-\overline{\mathbf{K}(\psi_{\text{up}})}s} \mathbf{s}(P_m, \psi_{\text{up}})^{(1)} \\ &+ \left( \mathbf{1} - e^{-\overline{\mathbf{K}(\psi_{\text{up}})}s} \right) \overline{\mathbf{K}(\psi_{\text{up}})}^{-1} \left( \overline{\mathbf{a}(\psi_{\text{up}})} \bar{B} + \overline{\mathbf{s}(\psi_{\text{up}})^{(0)}} \right). \end{aligned} \quad (18.27)$$

For simplification we write

$$\mathbf{s}(P_{m-1}, \psi_{\text{up}})^{(1)} = \mathbf{A}(\psi_{\text{up}}) \mathbf{s}(P_m, \psi_{\text{up}})^{(1)} + \mathbf{B}(\psi_{\text{up}}). \quad (18.28)$$

Solving this equation sequentially, starting at the top of the cloud and finishing at the bottom, we get the updated radiation field for all up-looking angles.

$$\mathcal{I}(P_i, \psi_{\text{up}})^{(1)} = \left\{ \mathbf{s}^{(1)}(P_i, \psi_l) \right\} \quad \forall \psi_l \in [0, 90^\circ]. \quad (18.29)$$

### 18.2.2 Down-looking directions

The same procedure is done for down-looking directions. The only difference is that the starting point is the lower-most pressure level  $P_1$  and the incoming clear sky field at the lower cloud box boundary, which is interpolated on the required zenith angles, is taken as boundary condition. The following equation is solved sequentially, starting at the bottom of the cloud box and finishing at the top:

$$\mathbf{s}(P_m, \psi_{\text{down}})^{(1)} = \mathbf{A}(\psi_{\text{down}}) \mathbf{s}(P_{m-1}, \psi_{\text{down}})^{(1)} + \mathbf{B}(\psi_{\text{down}}). \quad (18.30)$$

This yields the updated radiation field for all down-looking angles.

$$\mathcal{I}(P_i, \psi_{\text{down}})^{(1)} = \left\{ \mathbf{s}^{(1)}(P_i, \psi_l) \right\} \quad \forall \psi_l \in [\psi_{\text{limit}}, 180^\circ]. \quad (18.31)$$

### 18.2.3 Limb directions

A special case for limb directions, which correspond to angles slightly above  $90^\circ$  had to be implemented. If the tangent point is part of the propagation path step, the intersection point is exactly at the same pressure level as the starting point. In this case the linearly interpolated clear sky field is taken as input for the radiative transfer calculation, because we do not have an already updated field for this pressure level:

$$\mathbf{s}(P_m, \psi_{\text{limb}})^{(1)} = \mathbf{A}(\psi_{\text{limb}}) \mathbf{s}(P_m, \psi_{\text{limb}})^{(0)} + \mathbf{B}(\psi_{\text{limb}}) \quad (18.32)$$

By solving this equation the missing part of the updated radiation field is obtained

$$\mathcal{I}(P_i, \psi_{\text{limb}})^{(1)} = \left\{ \mathbf{s}(P_i, \psi_l) \right\} \quad \forall \psi_l \in ]90^\circ, \psi_{\text{limit}}[ \quad (18.33)$$

For all iterations the sequential update is applied. Using this method the number of iterations depends only on the optical thickness of the cloud or on the number of multiple-scattering events, not on the number of pressure levels.

## 18.3 Numerical Issues

### 18.3.1 Grid optimization and interpolation

The accuracy of the DOIT method depends very much on the discretization of the zenith angle. The reason is that the intensity field strongly increases at about  $\psi = 90^\circ$ . For angles below  $90^\circ$  (“up-looking” directions) the intensity is very small compared to angles above  $90^\circ$  (“down-looking” directions), because the thermal emission from the lower atmosphere and from the ground is much larger than thermal emission from trace gases in the upper atmosphere. Figure 18.4 shows an example intensity field as a function of zenith angle for different pressure levels inside a cloud box, which is placed from 7.3 to 12.7 km altitude, corresponding to pressure limits of 411 hPa and 188 hPa respectively. The cloud box includes 27 pressure levels. The frequency of the sample calculation was 318 GHz. A midlatitude-summer scenario including water vapor, ozone, nitrogen and oxygen was used. The atmospheric data was taken from the FASCOD [Anderson *et al.*, 1986] and the spectroscopic data was obtained from the HITRAN database [Rothman *et al.*, 1998]. For simplicity this 1D set-up was chosen for all sample calculations in this section. As the intensity (or the Stokes vector) at the intersection point of a propagation path is obtained by interpolation, large interpolation errors can occur for zenith angles of about  $90^\circ$  if the zenith angle grid discretization is too coarse. Taking a very fine equidistant zenith angle grid leads to very long computation times. Therefore a zenith angle grid optimization method is required.

For the computation of the scattering integral it is possible to take a much coarser zenith angle resolution without losing accuracy. It does not make sense to use the zenith angle grid, which is optimized to represent the radiation field with a certain accuracy. The integrand is the product of the phase matrix and the radiation field. The peaks of the phase matrices can be at any zenith angle, depending on the incoming and the scattered directions. The multiplication smooths out both the radiation field increase at  $90^\circ$  and the peaks of the phase matrices. Test calculations have shown that an increment of  $10^\circ$  is sufficient. Taking the equidistant grid saves the computation time of the scattering integral to a very large extent, because much less grid points are required.

#### Zenith angle grid optimization

As a reference field for the grid optimization the DOIT method is applied for an empty cloud box using a very fine zenith angle grid. The grid optimization routine finds a reduced zenith angle grid which can represent the intensity field with the desired accuracy. It first takes the radiation at  $0^\circ$  and  $180^\circ$  and interpolates between these two points on all grid points contained in the fine zenith angle grid for all pressure levels. Then the differences between the reference radiation field and the interpolated field are calculated. The zenith angle grid point, where the difference is maximal is added to  $0^\circ$  and  $180^\circ$ . After that the radiation field is interpolated between these three points forming part of the reduced grid and again the grid point with the maximum difference is added. Using this method more and more grid points are added to the reduced grid until the maximum difference is below a requested accuracy limit.

The top panel of Figure 18.5 shows the clear sky radiation in all viewing directions for a sensor located at 13 km altitude. This result was obtained with a switched-off cloud box. The difference between the clear sky part of the ARTS model and the scattering part is that in the clear sky part the radiative transfer calculations are done along the line of sight of the instrument whereas inside the cloud box the RT calculations are done as described in

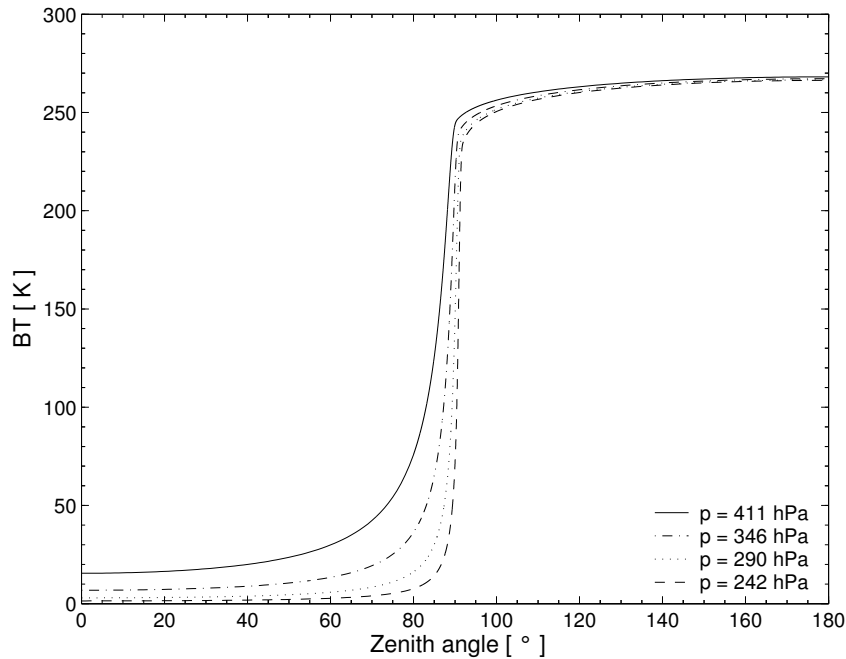


Figure 18.4: Intensity field for different pressure levels.

the previous section to obtain the full radiation field inside the cloud box. In the clear sky part the radiation field is not interpolated, therefore we can take the clear sky solution as the exact solution.

The interpolation error is the relative difference between the exact clear sky calculation (cloud box switched off) and the clear sky calculation with empty cloud box. The bottom panels of Figure 18.5 show the interpolation errors for zenith angle grids optimized with three different accuracy limits (0.1%, 0.2% and 0.5%). The left plot shows the critical region close to  $90^\circ$ . For a grid optimization accuracy of 0.5% the interpolation error becomes very large, the maximum error is about 8%. For grid accuracies of 0.2% and 0.1% the maximum interpolation errors are about 0.4% and 0.2% respectively. However for most angles it is below 0.2%, for all three cases. For down-looking directions from  $100^\circ$  to  $180^\circ$  the interpolation error is at most 0.14% for grid accuracies of 0.2% and 0.5% and for a grid accuracy of 0.1% it is below 0.02%.

### Interpolation methods

Two different interpolation methods can be chosen in ARTS for the interpolation of the radiation field in the zenith angle dimension: linear interpolation or three-point polynomial interpolation. The polynomial interpolation method produces more accurate results provided that the zenith angle grid is optimized appropriately. The linear interpolation method on the other hand is safer. If the zenith angle grid is not optimized for polynomial interpolation one should use the simpler linear interpolation method. Apart from the interpolation of the radiation field in the zenith angle dimension linear interpolation is used everywhere in the model. Figure 18.6 shows the interpolation errors for the different interpolation methods. Both calculations are performed on optimized zenith angle grids, for polynomial interpolation 65 grid points were required to achieve an accuracy of 0.1% and for linear interpolation



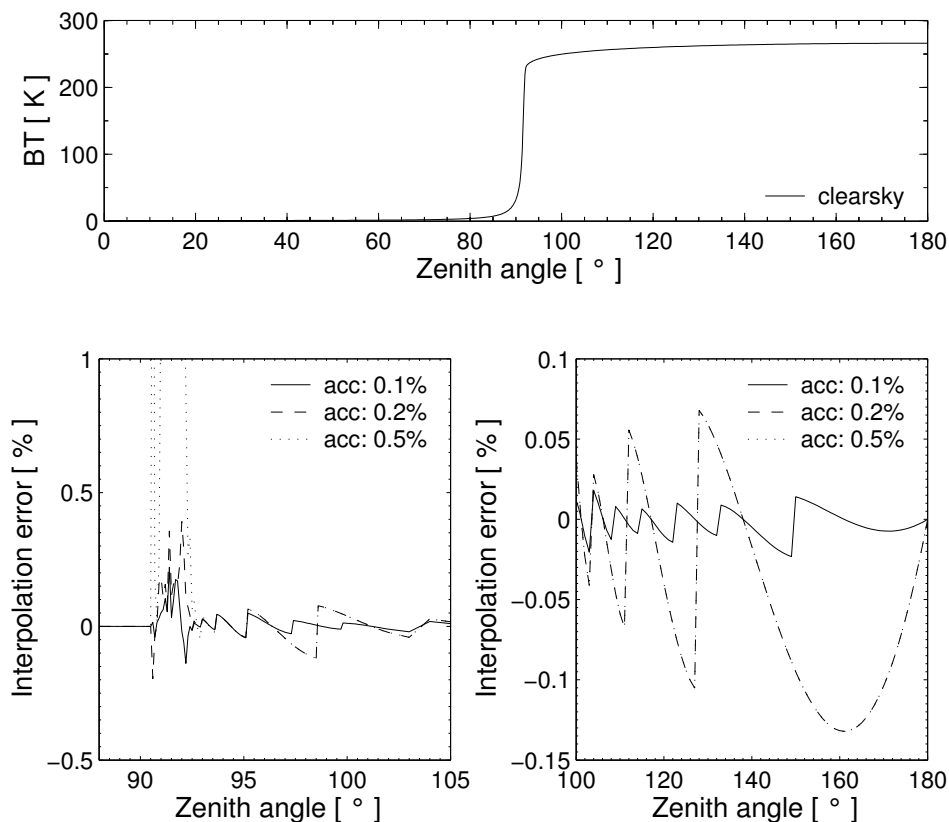


Figure 18.5: Interpolation errors for different grid accuracies. Top panel: Clear sky radiation simulated for a sensor at an altitude of 13 km for all viewing directions. Bottom left: Grid optimization accuracy for limb directions. Bottom right: Grid optimization accuracy for down-looking directions.

101 points were necessary to achieve the same accuracy. In the region of about  $90^\circ$  the interpolation errors are below 1.2% for linear interpolation and below 0.2% for polynomial interpolation. For the other down-looking directions the differences are below 0.08% for linear and below 0.02% for polynomial interpolation. It is obvious that polynomial interpolation gives more accurate results. Another advantage is that the calculation is faster because less grid points are required, although the polynomial interpolation method itself is slower than the linear interpolation method. Nevertheless, we have implemented the polynomial interpolation method so far only in the 1D model. In the 3D model, the grid optimization needs to be done over the whole cloud box, where it is not obvious that one can save grid points. Applying the polynomial interpolation method using non-optimized grids can yield much larger interpolation errors than the linear interpolation method.

### Error estimates

The interpolation error for scattering calculations can be estimated by comparison of a scattering calculation performed on a very fine zenith angle grid (resolution  $0.001^\circ$  from  $80^\circ$  to  $100^\circ$ ) with a scattering calculation performed on an optimized zenith angle grid with 0.1% accuracy. The cloud box used in previous test calculations is filled with spheroidal particles with an aspect ratio of 0.5 from 10 to 12 km altitude. The ice mass content is assumed to be

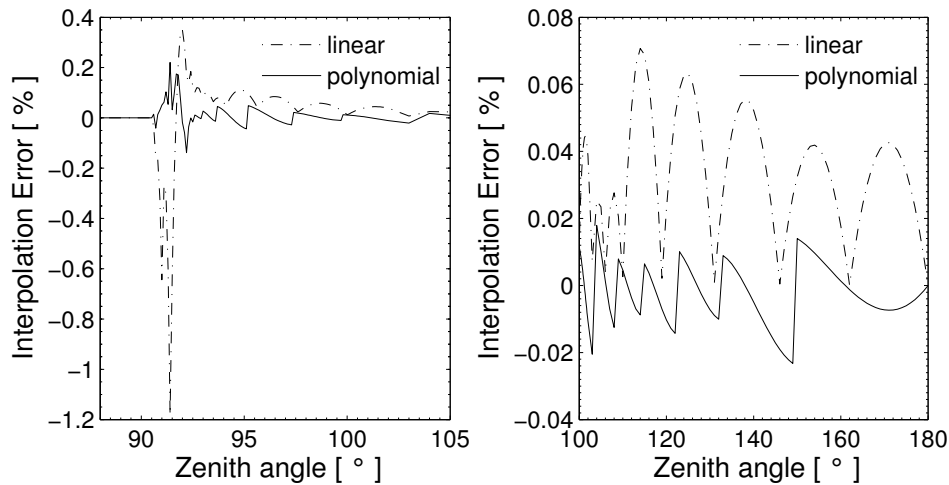


Figure 18.6: Interpolation errors for polynomial and linear interpolation.

$4.3 \cdot 10^{-3} \text{ g/m}^3$  at all pressure levels. An equal volume sphere radius of  $75 \mu\text{m}$  is assumed. The particles are either completely randomly oriented (p20) or azimuthally randomly oriented (p30) (cf. Section 8.2.3). The top panels of Figure 18.7 show the interpolation errors of the intensity. For both particle orientations the interpolation error is in the same range as the error for the clear sky calculation, below 0.2 K. The bottom panels show the interpolation errors for  $Q$ . For the randomly oriented particles the error is below 0.5%. For the horizontally aligned particles with random azimuthal orientation it goes up to 2.5% for a zenith angle of about  $91.5^\circ$ . It is obvious that the interpolation error for  $Q$  must be larger than that for  $I$  because the grid optimization is accomplished using only the clear-sky field, where the polarization is zero. Only the limb directions about  $90^\circ$  are problematic, for other down-looking directions the interpolation error is below 0.2%.

## 18.4 Implementation

The workspace methods required for DOIT calculations are implemented in the files `m.scattrte.cc`, `m.cloudbox.cc` and `m.optproperties.cc`.

### 18.4.1 1D control file example

This example demonstrates how to set up a 1D DOIT calculation. A full running controlfile example for a DOIT calculation can be found in the ARTS package in the `controlfiles/artscomponents/doit` directory. The file is called `TestDOIT.arts`. For detailed descriptions of the workspace methods and variables please refer also to the online help (`arts -d ...`).

### 18.4.2 DOIT frame

As a first step for a DOIT calculation we have to calculate the incoming field on the boundary of the cloudbox. This is done using the workspace method `CloudboxGetIncoming`:

```
CloudboxGetIncoming
```

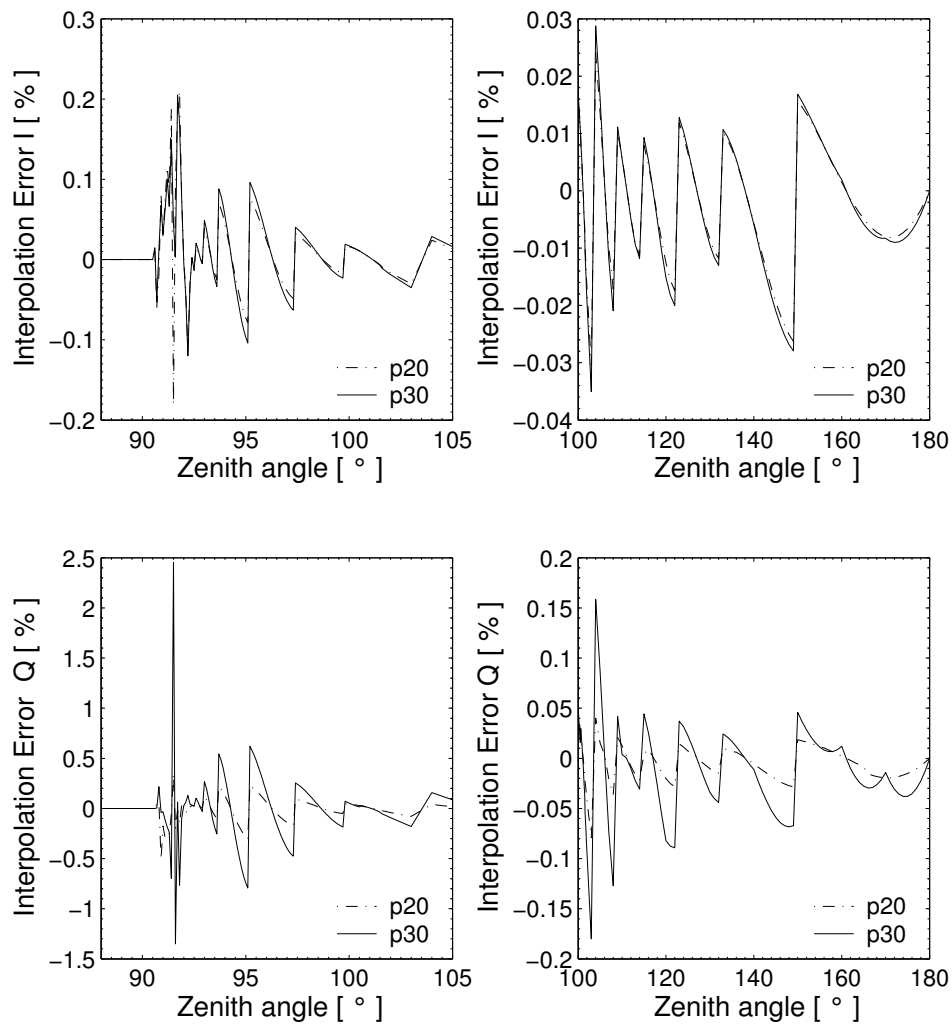


Figure 18.7: Interpolation errors for a scattering calculation. Left panels: Interpolation errors for limb directions. Right panels: Interpolation errors for down-looking directions. Top: Intensity  $I$ , Bottom: Polarization difference  $Q$

The next step is the initialization of variables required for a DOIT calculation using **DoitInit**:

```
DoitInit
```

The grid discretization plays a very significant role in discrete ordinate methods. In spherical geometry the zenith angular grid is of particular importance (cf. Section 18.3.1). The angular discretization is defined in the workspace method **DoitAngularGridsSet**:

```
DoitAngularGridsSet ( doit_za_grid_size,
                      scat_aa_grid, scat_za_grid,
                      19, 10, "doit_za_grid_opt.xml" )
```

For down-looking geometries it is sufficient to define the generic inputs:

N\_za\_grid Number of grid points in zenith angle grid, recommended value: 19

N\_aa\_grid Number of grid points in azimuth angle grid, recommended value: 37

From these numbers equally spaced grids are created and stored in the work space variables **scat\_za\_grid** and **scat\_aa\_grid**.

For limb simulations it is important to use an optimized zenith angle grid with a very fine resolution about 90° for the RT calculations. Such a grid can be generated using the workspace method **doit\_za\_grid\_optCalc**. Please refer to the online documentation of this method. The filename of the optimized zenith angle grid can be given as a generic input. If a filename is given, the equidistant grid is taken for the calculation of the scattering integrals and the optimized grid is taken for the radiative transfer part. Otherwise, if no filename is specified (`za_grid_opt_file = ""`) the equidistant grid is taken for the calculation of the scattering integrals and for the radiative transfer calculations. This option makes sense for down-looking cases to speed up the calculation.

The main agenda for a DOIT calculation is **doit\_mono\_agenda**. The agenda is executed by the workspace method **ScatteringDoit**:

```
ScatteringDoit
```

### The DOIT main agenda

The agenda **doit\_mono\_agenda** requires the incoming clearsky field on the cloudbox boundary as an input and gives as output the scattered field on the cloudbox boundary if the sensor is placed outside the cloudbox or the full scattered field in the cloudbox if the sensor is placed inside the cloudbox.

```
AgendaSet( doit_mono_agenda ){
  # Prepare scattering data for DOIT calculation (Optimized method):
  DoitScatteringDataPrepare
  # Alternative method (needs less memory):
  # scat_data_array_monoCalc
  # Set first guess field:
  doit_i_fieldSetClearsky
  # Perform iterations: 1. scattering integral. 2. RT calculations with
  # fixed scattering integral field, 3. convergence test
  doit_i_fieldIterate
  # Put solution into interface for clearsky calculation
  DoitCloudboxFieldPut
}
```

The first method `DoitScatteringDataPrepare` reads the single scattering data and interpolates it on the requested frequency. It also performs the transformation from the scattering frame into the laboratory frame. Alternatively the method `scat_data_array_monoCalc` can be used. In this case only the frequency interpolation is done and the transformations are done later. The advantage is that this method needs less memory. For 1D calculation it is recommended to use `DoitScatteringDataPrepare` because it is much more efficient.

The method `doit_i_fieldSetClearsky` interpolates the incoming radiation field on all points inside the cloudbox to obtain the initial field (`doit_i_field`) for the DOIT calculation. As a test one can alternatively start with a constant radiation field using the method `doit_i_fieldSetConst`.

The iteration is performed in the method `doit_i_fieldIterate`, which includes the calculation of the scattering integral field (`doit_scat_field`), the radiative transfer calculations in the cloudbox with fixed scattering integral and the convergence test.

After convergence is obtained the radiation field has to be stored in an interface variable that creates the link between the scattering solver solution and the evaluation of the radiative transfer equation. This is done by the workspace method `DoitCloudboxFieldPut`. The radiation field at the boundary of the cloudbox is stored in the interface variable `scat_i_p.doit_i_field1D_spectrum` is used as interface variable storing the cloudbox radiation field. In contrast to `doit_i_field` the interface variables include an additional dimension for the frequency.

#### Agendas used in `doit_i_fieldIterate`

There are several methods which can be used in `doit_i_fieldIterate`, for instance for the calculation of the scattering integral. The methods are selected in the control-file by defining several agendas.

**Calculation of the scattering integral:** To calculate the scattering integral (Equation 18.7) the phase matrix (`pha_mat`) is required. How the phase matrix is calculated is defined in the agenda `pha_mat_spt_agenda`:

```
# Calculation of the phase matrix
AgendaSet( pha_mat_spt_agenda ){
  # Optimized option:
  pha_mat_sptFromDataDOITOpt
  # Alternative option:
  # pha_mat_sptFromMonoData
}
```

If in `doit_mono_agenda` the optimized method `DoitScatteringDataPrepare` is used we have to use here the corresponding method `pha_mat_sptFromDataDOITOpt`. Otherwise we have to use `pha_mat_sptFromMonoData`.

To do the integration itself, we have to define `doit_scat_field_agenda`:

```
AgendaSet( doit_scat_field_agenda ){
  doit_scat_fieldCalcLimb
  # Alternative:
  # doit_scat_fieldCalc
}
```

Here we have two options. One is `doit_scat.fieldCalcLimb`, which should be used for limb simulations, for which we need a fine zenith angle grid resolution to represent the radiation field. This method has to be used if a zenith angle grid file is given in `DoitAngularGridsSet`. The scattering integral can be calculated on a coarser grid resolution, hence in `doit_scat.fieldCalcLimb`, the radiation field is interpolated on the equidistant angular grids specified in `DoitAngularGridsSet` by the generic inputs `Nza` and `Naa`. Alternatively, one can use `doit_scat.fieldCalc`, where this interpolation is not performed. This function is efficient for simulations in up- or down-looking geometry, where we do not need the fine zenith angle grid resolution about  $90^\circ$ .

**Radiative transfer with fixed scattering integral term:** With a fixed scattering integral field the radiative transfer equation can be solved (Equation 18.9). The workspace method to be used for this calculation is defined in `doit_rte_agenda`. The most efficient and recommended workspace method is `doit_i.fieldUpdateSeq1D` where the sequential update which is described in Section 18.2 is applied. The workspace method `doit_i.fieldUpdate1D` does the same calculation without sequential update and is therefore much less efficient because the number of iterations depends in this case on the number of pressure levels in the cloudbox. Other options are to use a plane-parallel approximation implemented in the workspace method `doit_i.fieldUpdateSeq1DPP`. This method is not much more efficient than `doit_i.fieldUpdateSeq1D`, therefore it is usually better to use `doit_i.fieldUpdateSeq1D` since it is more accurate.

```
AgendaSet( doit_rte_agenda ){
    doit_i.fieldUpdateSeq1D
    # Alternatives:
    # doit_i.fieldUpdateSeq1DPP
    # i.fieldUpdate1D
}
```

The optical properties of the particles, i.e., extinction matrix and absorption vector are required for solving the radiative transfer equation. How they are calculated is specified in `spt_calc_agenda`. The workspace method `opt_prop_sptFromMonoData` requires that the raw data is already interpolated on the frequency of the monochromatic calculation. This requirement is fulfilled when `DoitScatteringDataPrepare` or `scat_data_array_monoCalc` is executed before `doit_i.fieldIterate` (see Section 18.4.2). The workspace method `ext_matAddPart` and `abs_vecAddPart` are used to extract the absorption vector `abs_vec` and extinction matrix `ext_mat` from the workspace variable `ext_mat_spt`. The gas absorption is added internally.

```
AgendaSet( spt_calc_agenda ){
    opt_prop_sptFromMonoData
}
AgendaSet( opt_prop_part_agenda ){
    ext_matInit
    abs_vecInit
    ext_matAddPart
    abs_vecAddPart
}
```

**Convergence test:** After the radiative transfer calculations with a fixed scattering integral field are complete the newly obtained radiation field is compared to the old radiation field

by a convergence test. The functions and parameters for the convergence test are defined in the agenda `doit_conv_test_agenda`. There are several options. The workspace methods `doit_conv_flagAbsBT` and `doit_conv_flagAbs` compare the absolute differences of the radiation field element-wise as described in Equation 18.19. The convergence limits are specified by the generic input `epsilon` which specifies the convergence limit. A limit must be given for each Stokes component. In `doit_conv_flagAbsBT` the limits must be specified in Rayleigh Jeans brightness temperatures whereas in `doit_conv_flagAbs` they must be defined in the basic radiance unit ( $[W/(m^2Hz sr)]$ ). Another option is to perform a least square convergence test using the workspace method `doit_conv_flagLsq`. Test calculations have shown that this test is not safe, therefore the least square convergence test should only be used for test purposes.

```
AgendaSet( doit_conv_test_agenda ) {
  doit_conv_flagAbsBT( doit_conv_flag, doit_iteration_counter,
                      doit_i_field, doit_i_field_old,
                      f_grid, f_index,
                      [0.1, 0.01, 0.01, 0.01] )
  # Alternative: Give limits in radiances
  #   doit_conv_flagAbs( doit_conv_flag, doit_iteration_counter,
  #                     doit_i_field, doit_i_field_old,
  #                     [0.1e-15, 0.1e-18, 0.1e-18, 0.1e-18] )
  #
  # If you want to look at several iteration fields, for example
  # to investigate the convergence behavior, you can use
  # the following workspace method:
  # DoitWriteIterationFields( doit_iteration_counter, doit_i_field,
  #                           [2, 4] )
}
```

### 18.4.3 Propagation of the DOIT result towards the sensor

In order to propagate the result of the scattering calculation towards the sensor, the fields needs to be interpolated on the direction of the sensor's line of sight. This is done in the workspace method `iyInterpCloudboxField`, which has to be put into the agenda `iy_cloudbox_agenda`:

```
AgendaSet( iy_cloudbox_agenda ) {
  iyInterpCloudboxField
}
```

### 18.4.4 3D DOIT calculations

The DOIT method is implemented for 1D and 3D spherical atmospheres, but it is strongly recommended to use it only for 1D calculations, because there are several numerical difficulties related to the grid discretizations. It is difficult to find appropriate discretizations to get sufficiently accurate results in reasonable computation time. Therefore only experienced ARTS users should use DOIT for 3D calculations only for smaller cloud scenarios. Please refer to the online documentation for the workspace method for 3D scattering calculations (`doit_i_fieldUpdateSeq3D`). All other workspace methods adapt automatically to the atmospheric dimensionality.





## Chapter 19

# Cloud radar simulations

ARTS provides some support for modelling measurements of backscattering inside the atmosphere. This deviates for the active measurements discussed in the previous chapter, as in this case the transmitter and receiver are placed at the same position. Here backscattering is recorded, while in the “transmission case” the attenuation through the atmosphere is probed. This has the consequence that the measurement data not only span the frequency and a polarisation dimensions, but also has a time (or distance) dimension. That is, the backscattering is basically reported as a function of distance from the sensor, for one or several frequencies frequencies and combinations of transmitted and received polarisations. Accordingly, these data differ in nature from the other types of measurements, and the standard main function (`yCalc`) is not applicable.

A very important restriction applies, only single scattering is treated. That is, no other scattering than the targeted backscattering is considered. This is frequently an acceptable simplification for precipitation and cloud radars observations, and such observations should be the main applications of the discussed workspace methods. The basic measurement approach is the same for lidars, but the assumption of single scattering is much less commonly met for such instruments.

### 19.1 Theory

The transmitted pulses are treated to be monochromatic pencil beams. Effects due to antenna patterns and the geometrical distance between the instrument and the scattering particles are assumed to be treated as a separate “calibration”, and only the “forward model” treats only the actual backscattering and atmospheric extinction.

For the conditions given above, the backscattered radiation,  $s_b$ , can be written as

$$s_b = \mathbf{T}_h \mathbf{Z}(\Omega = 0) \mathbf{T}_a s_t. \quad (19.1)$$

The terms in this equation are:

$s_t$  Stokes vector describing the transmitted pulse.

$\mathbf{T}_a$  A matrix describing the transmission from the receiver to the scattering point (the away direction).

---

#### History

121108 Written by Patrick Eriksson.

$\mathbf{Z}(\Omega = 0)$  The scattering (or phase) matrix value for the backward direction.

$\mathbf{T}_h$  As  $\mathbf{T}_a$ , but for the reversed direction (the home direction). Note that for vector radiative transfer, in general  $\mathbf{T}_a \neq \mathbf{T}_h$ .

The (attenuated) “backscatter coefficient” recorded by the receiver is

$$\beta' = \mathbf{p} \cdot \mathbf{s}_b \quad (19.2)$$

where  $\mathbf{p}$  is the (normalised) vector describing the polarisation response of the receiver and  $\cdot$  signifies the dot product.

The corresponding unattenuated backscattering coefficient is

$$\beta = \mathbf{p} \cdot [\mathbf{Z}(\Omega = 0)\mathbf{s}_t] \quad (19.3)$$

## 19.2 Units

The unit of  $\beta$  (and  $\beta'$ ) is  $1/(\text{m sr}^{-1})$ . For radar applications this is not the most common choice, but is here preferred as it directly matches  $\mathbf{Z}$ . It is also the standard definition in the lidar community. The more common definition of radar reflectivity is simply  $4\pi\beta$ .

However, even more common is to report radar data in unit of equivalent reflectivity,  $Z_e$ . This quantity is defined as [e.g. *Donovan and van Lammeren, 2001*]

$$Z_e = \frac{4\lambda_r}{\pi^4 |K|^2} \beta \quad (19.4)$$

where  $\lambda_r$  is wavelength of the radar and the “reference dielectric factor” is calculated using the complex refractive index of ice or liquid water,  $n$ :

$$K = \frac{n^2 - 1}{n^2 + 2}. \quad (19.5)$$

## 19.3 Practical usage

As for other measurements, the main radiative transfer calculations are performed inside `iy_main_agenda`. The workspace method to be used inside this agenda is `iyCloudRadar`. This method returns  $\mathbf{s}_b$  for each point of the propagation path, and for each frequency in `f_grid`. The calculated data are packed into `iy`. Here the difference to other measurement types emerge. For example, the second row holds  $\mathbf{s}_b$  corresponding to the second point of the propagation path (not the second frequency). If `f_grid` contains several frequencies, the data for the second frequency are placed below (in the row dimension) the data for the first frequency etc.

The polarisation of the transmitted pulses ( $\mathbf{s}_b$ ) are taken from `iy_transmitter_agenda`. The agenda shall here return a Stokes vector for each frequency in `f_grid`, of unit intensity.

The unit of returned data is selected by `iy_unit`. There are two options “1” and “Ze”. For the first option no unit conversion is performed, while for the second option Equation 19.4 is applied on all Stokes elements of  $\mathbf{s}_b$ . In the later case, liquid water at a user specified temperature is used as reference. That is,  $K$  is calculated for the refractive index of water at the specified temperature.

Hence, the basic calculations are performed in standard manner, using `iy_main_agenda`. However, the deviating data pattern in `iy` results in that an alternative to `yCalc` is needed

and it is `yCloudRadar`. The method applies two instrument effects. Firstly, the polarisation response of the receiver is incorporated (Eq. 19.2). Secondly, the data are averaged as a function of “range”, following the `range_bins`. These range bins can be specified either as geometrical altitude or the two-way propagation time. The range binning is described further in the built-in documentation. Further, the data are rearranged into a vector and returned as `y`.

A number of auxiliary data can be obtained by `iyCloudRadar`, this including  $\beta$ . For a list of possible variables:

```
arts -d iyCloudRadar
```

A difference of `yCloudRadar`, compared to `yCalc`, is that all auxiliary quantities provided by `iyCloudRadar` are treated.



## **Part V**

# **Bibliography and Appendices**



# Bibliography

- Anderson, G. P., S. A. Clough, F. X. Kneizys, J. H. Chetwynd, and E. P. Shettle, AFGL atmospheric constituent profiles (0–120 km), *Tech. Rep. TR-86-0110*, AFGL, 1986.
- Buehler, S. A., P. Eriksson, T. Kuhn, A. von Engeln, and C. Verdes, ARTS, the Atmospheric Radiative Transfer Simulator, *Journal of Quantitative Spectroscopy and Radiative Transfer*, *91*, 65–93, 2005.
- Buehler, S. A., A. von Engeln, E. Brocard, V. O. John, T. Kuhn, and P. Eriksson, Recent developments in the line-by-line modeling of outgoing longwave radiation, *Journal of Quantitative Spectroscopy and Radiative Transfer*, *98*, 446–457, 2006.
- Buehler, S. A., V. O. John, A. Kottayil, M. Milz, and P. Eriksson, Efficient radiative transfer simulations for a broadband infrared radiometer - Combining a weighted mean of representative frequencies approach with frequency selection by simulated annealing, *Journal of Quantitative Spectroscopy and Radiative Transfer*, *111*, 602–615, 2010.
- Buehler, S. A., P. Eriksson, and O. Lemke, Absorption lookup tables in the radiative transfer model arts, *Journal of Quantitative Spectroscopy and Radiative Transfer*, *112*, 1559–1567, 2011.
- Czekala, H., Microwave radiative transfer calculations with multiple scattering by non-spherical hydrometeors, Ph.D. thesis, Rheinische Friedrich-Wilhelms-Universität Bonn, Auf dem Hgel 20, 53121 Bonn, 1999.
- Dattorro, J., *Convex Optimization & Euclidean Distance Geometry*, Meboo Publishing USA, 2011.
- Davis, C., C. Emde, and R. Harwood, A 3D polarized reversed monte carlo radiative transfer model for mm and sub-mm passive remote sensing in cloudy atmospheres, *IEEE Transactions on Geoscience and Remote Sensing*, *43*, 1096–1101, 2005.
- Donovan, D. P., and A. C. A. P. van Lammeren, Cloud effective particle size and water content profile retrievals using combined lidar and radar observations 1. Theory and examples, *Journal of Geophysical Research*, *106*, 27425–27448, 2001.
- Emde, C., A polarized discrete ordinate scattering model for radiative transfer simulations in spherical atmospheres with thermal source, Ph.D. thesis, University of Bremen, 2005.
- Emde, C., and T. R. Sreerexha, Development of a RT model for frequencies between 200 and 1000 GHz, WP1.2 Model Review, *Tech. rep.*, ESTEC Contract No AO/1-4320/03/NL/FF, 2004.

- Emde, C., S. A. Buehler, C. Davis, P. Eriksson, T. R. Sreerekha, and C. Teichmann, A polarized discrete ordinate scattering model for simulations of limb and nadir longwave measurements in 1D/3D spherical atmospheres, *Journal of Geophysical Research*, 109, 2004.
- Eriksson, P., Analysis and comparison of two linear regularization methods for passive atmospheric observations, *Journal of Geophysical Research*, 105(D14), 18157–18167, 2000.
- Eriksson, P., F. Merino, D. Murtagh, P. Baron, P. Ricaud, and J. de La Noë, Studies for the Odin sub-millimetre radiometer: 1. Radiative transfer and instrument simulation, *Canadian Journal of Physics*, 80, 321–340, 2002.
- Eriksson, P., M. Ekström, S. Bühler, and C. Melzheimer, Efficient forward modelling by matrix representation of sensor responses, *International Journal of Remote Sensing*, 27, 1793–1808, 2006.
- Eriksson, P., S. A. Buehler, C. P. Davis, C. Emde, and O. Lemke, ARTS, the atmospheric radiative transfer simulator, version 2, *Journal of Quantitative Spectroscopy and Radiative Transfer*, 112, 1551–1558, 2011.
- Evans, K. F., S. J. Walter, A. J. Heymsfield, and M. N. Deeter, Modeling of submillimeter passive remote sensing of cirrus clouds, *J. Appl. Met.*, 37, 184–205, 1998.
- Goldstein, D., *Polarized light*, chap. The Stokes parameters and Mueller matrices for optical activity and Faraday rotation, Marcel Dekker, Inc., USA, 2003.
- Haugstad, B. S., Turbulence in planetary occultations iii. effects on atmospheric profiles derived from intensity measurements, *Icarus*, 3, 422–435, 1978.
- Ippolito, L. J., *Satellite communications systems engineering*, chap. The RF link, John Wiley and Sons Ltd, UK, 2008.
- John, V. O., S. A. Buehler, A. von Engeln, P. Eriksson, T. Kuhn, E. Brocard, and G. Koenig-Langlo, Understanding the variability of clear-sky outgoing long-wave radiation based on ship-based temperature and water vapor measurements, *Quarterly Journal of the Royal Meteorological Society*, 132, 2675–2691, 2006.
- Kraus, J. D., *Radio astronomy*, McGraw-Hill Book Company, 1966.
- Kuntz, M., G. Hochschild, and R. Krupa, Retrieval of ozone mixing ratio profiles from ground-based millimeter wave measurements disturbed by standing waves, *Journal of Geophysical Research*, 102, 21965–21975, 1997.
- Kursinski, E. R., G. A. Hajj, S. S. Leroy, and B. Herman, The gps radio occultation technique, *Terrestrial Atmospheric Oceanic Studies*, 11, 53–114, 2000.
- Larsson, R., S. A. Buehler, P. Eriksson, and J. Mendrok, A treatment of the Zeeman effect using Stokes formalism and its implementation in the Atmospheric Radiative Transfer Simulator ARTS, *Journal of Quantitative Spectroscopy and Radiative Transfer*, submitted 2013.



- Makarov, D. S., M. Y. Tretyakov, and P. W. Rosenkranz, 60-GHz oxygen band: Precise experimental profiles and extended absorption modeling in a wide temperature range, *Journal of Quantitative Spectroscopy and Radiative Transfer*, *112*, 1420–1428, 2011.
- McFarquhar, G. M., and A. J. Heymsfield, Parametrization of tropical cirrus ice crystal size distributions and implications for radiative transfer: Results from CEPEX, *Journal of the Atmospheric Sciences*, *54*, 2187–2200, 1997.
- Meissner, T., and F. J. Wentz, Polarization rotation and the third stokes parameter: the effects of spacecraft attitude and faraday rotation, *IEEE Transactions on Geoscience and Remote Sensing*, *44*, 506–515, 2006.
- Mishchenko, M. I., Calculation of the amplitude matrix for a nonspherical particle in a fixed orientation, *Appl. Opt.*, pp. 1026–1031, 2000.
- Mishchenko, M. I., and L. D. Travis, Capabilities and limitations of a current fortran implementation of the t-matrix method for randomly oriented rotationally symmetric scatterers, *J. Quant. Spectrosc. Radiat. Transfer*, *60*, 309–324, 1998.
- Mishchenko, M. I., L. D. Travis, and A. A. Lacis, *Scattering, Absorption and Emission of Light by Small Particles*, Cambridge University Press, 2002, ISBN 0-521-78252.
- Newell, A. C., and R. C. Baird, Absolute determination of refractive indices of gases at 47.7 Gigahertz, *J. Appl. Phys.*, *36*, 1965.
- Read, W. G., Z. Shippony, M. J. Schwartz, N. J. Livesey, and W. V. Snyder, The clear-cky unpolarized forward model for the EOS Aura Microwave Limb Sounder (MLS), *IEEE Transactions on Geoscience and Remote Sensing*, *44*, 1367–1379, 2006.
- Richard, C., et al., New section of the HITRAN database: Collision-induced absorption (CIA), *Journal of Quantitative Spectroscopy and Radiative Transfer*, *113*, 1276–1285, 2012.
- Rodgers, C., *Inverse methods for atmospheric sounding: Theory and practise*, 1st ed., World Scientific Publishing, 2000.
- Rodgers, C. D., Characterization and error analysis of profiles retrieved from remote sounding measurements, *Journal of Geophysical Research*, *95*, 5587–5595, 1990.
- Rosenkranz, P. W., Absorption of microwaves by atmospheric gases, in *Atmospheric remote sensing by microwave radiometry*, edited by M. A. Janssen, pp. 37–90, John Wiley & Sons, Inc., 1993, [ftp://mesa.mit.edu/phil/lbl\\_rt](ftp://mesa.mit.edu/phil/lbl_rt).
- Rothman, L. S., et al., The HITRAN molecular spectroscopic database and HAWKS (HITRAN atmospheric workstation): 1996 edition, *Journal of Quantitative Spectroscopy and Radiative Transfer*, *60*, 665–710, 1998.
- Rybicki, G. B., and A. P. Lightman, *Radiative processes in astrophysics*, chap. Plasma effects, John Wiley and Sons, Inc., USA, 1979.
- Schreiner, W. S., S. Sokolovskiy, V. C. Rocken, , and D. C. Hunt, Analysis and validation of gps/met radio occultation data in the ionosphere, *Radio Science*, *34*, 949–966, 1999.

Wright, P., S. Quegan, N. Wheadon, and C. Hall, Faraday rotation effects on l-band spaceborne sar data, *IEEE Transactions on Geoscience and Remote Sensing*, 41, 2735–2744, 2003.

**Part VI**

**Index**



# Index

- 1D, 16
- 2D, 16
- 3D, 17
- agenda, 9
- antenna pattern dimensionality, 31
- ARTS, 3
- ARTS files
  - agendas.arts, 10, 37, 39
  - continua.arts, 43
  - controlfiles, 10, 41
  - controlfiles/artscomponents, 50
  - controlfiles/artscomponents/cia, 45
  - controlfiles/artscomponents/faraday, 49
  - gas\_abs\_lookup.cc, 53
  - gas\_abs\_lookup.h, 53, 54
  - general.arts, 10, 53
  - hitran\_cia2012\_adapted.xml.gz, 45
  - m\_cloudbox.cc, 66, 136
  - m\_optproperties.cc, 66, 136
  - m\_scatrte.cc, 136
  - optproperties.cc, 66
  - optproperties.h, 60
  - README, 5, 10
- ARTS-1, 3
- ARTS\_INCLUDE\_PATH, 10
- atmosphere, 3
- atmospheric dimensionality, 16
- atmospheric field, 18
- azimuth angle, 30
- basis function, 19, 109
- birefringance, 98
- built-in documentation, 5
- cloud box, 20
- command line parameters, 6
- controlfile, 6
- Coordinate systems, 59
- curvature radius, 88
- data reduction, 31
- data types
  - GasAbsLookup, 53, 54
  - GField3, 59, 66
  - Ppath, 84
  - SingleScatteringData, 59, 60, 66
- default value, 8
- Discrete Ordinate ITERative (DOIT) method, 125
- dispersion, 57, 73, 78
- Doppler effect, 95
- DOXYGEN, 5
- ellipsoid, 87
- engine, 6
- example controlfiles, 10
- Faraday rotation, 97
- generic, 7
- geo-location, 19
- geocentric latitude, 88
- geodetic latitude, 88
- geometrical altitude, 15
- groups, 7, 8
- include, 10
- internal ARTS functions
  - dotprod\_with\_los, 96
  - ppath\_calc, 82, 83
  - surface\_specular\_los, 90
- laboratory frame, 59
- latitude, 17
- line-of-sight, 30
- longitude, 18
- magnetic field, 21
- measurement block, 31
- measurement sequence, 31
- meridian plane, 30
- methods, 6
- model atmosphere, 18

- n2-law of radiance, 77
- parser, 6
- particle size distribution, 64
- particle types, 62
- polar coordinate system, 16
- predefined variables, 7
- pressure, 15
- pressure altitude, 15
- propagation path, 73
- radiation field, 125
- radiative background, 73
- radius, 15
- ray tracing, 73
- refractive index, 57
- report file, 11
- reporting level, 11
- retrievals, 3
- scalar radiative transfer, 24, 129
- scattering, 4
- scattering frame, 59
- scripting language, 6
- sensor characteristics, 31
- sensor position, 29
- sensor transfer matrix, 31
- sensor, the, 29
- Sequential update, 130
- single scattering approximation, 130
- Single scattering properties, 59
- specific, 7
- spherical coordinate system, 17
- surface, 4
- surface altitude, 90
- tangent point, 83
- vector radiative transfer, 24
- vector radiative transfer equation, 126
- verbosity, 11
- workspace agendas
  - abs\_xsec\_agenda, 36
  - blackbody\_radiation\_agenda, 25, 77
  - doit\_conv\_test\_agenda, 141
  - doit\_mono\_agenda, 138, 139
  - doit\_rte\_agenda, 140
  - doit\_scatter\_field\_agenda, 139
  - iy\_cloudbox\_agenda, 75, 99, 141
  - iy\_main\_agenda, 29, 72, 78, 79, 99
  - iy\_space\_agenda, 73, 77, 99
  - iy\_sub\_agenda, 78
  - iy\_surface\_agenda, 75, 77, 90, 99
  - iy\_transmitter\_agenda, 99, 102, 144
  - jacobian\_agenda, 108
  - pha\_mat\_spt\_agenda, 139
  - ppath\_agenda, 78, 81, 100
  - ppath\_step\_agenda, 81
  - propmat\_clearsky\_agenda, 9, 25, 36, 37, 42, 54, 97
  - refr\_index\_air\_agenda, 57, 73, 78, 81
  - spt\_calc\_agenda, 140
  - ybatch\_calc\_agenda, 121
- workspace methods, 6, 7
  - abs\_coefCalcFromXsec, 42
  - abs\_lines\_per\_speciesAddMirrorLines, 42
  - abs\_lines\_per\_speciesCompact, 42
  - abs\_lines\_per\_speciesCreateFromLines, 42
  - abs\_lines\_per\_speciesReadFromCatalogues, 42
  - abs\_lineshape\_per\_tgDefine, 42
  - abs\_lineshapeDefine, 42
  - abs\_linesReadFromArts, 42
  - abs\_linesReadFromHitran, 42
  - abs\_linesReadFromHitranPre2004, 42
  - abs\_linesReadFromJpl, 42
  - abs\_linesReadFromMytran2, 42
  - abs\_linesReadFromSplitArtscat, 42
  - abs\_lookupAdapt, 42, 53
  - abs\_lookupCalc, 39, 42, 53
  - abs\_lookupSetup, 53
  - abs\_lookupSetupBatch, 53
  - abs\_lookupSetupWide, 53
  - abs\_speciesSet, 39, 41, 43
  - abs\_vecAddPart, 140
  - abs\_xsec\_per\_speciesAddCIA, 42, 45
  - abs\_xsec\_per\_speciesAddConfs, 42, 43
  - abs\_xsec\_per\_speciesAddLines, 42
  - abs\_xsec\_per\_speciesInit, 42
  - AtmosphereSet1D, 16
  - AtmosphereSet2D, 16
  - AtmosphereSet3D, 16
  - blackbody\_radiationPlanck, 77
  - CloudboxGetIncoming, 136
  - cloudboxOff, 20

- cloudboxSetManually, 66
- cloudboxSetManuallyAltitude, 66
- doit\_conv\_flagAbs, 141
- doit\_conv\_flagAbsBT, 141
- doit\_conv\_flagLsq, 141
- doit\_i\_fieldIterate, 139, 140
- doit\_i\_fieldSetClearsky, 139
- doit\_i\_fieldSetConst, 139
- doit\_i\_fieldUpdate1D, 140
- doit\_i\_fieldUpdateSeq1D, 140
- doit\_i\_fieldUpdateSeq1DPP, 140
- doit\_i\_fieldUpdateSeq3D, 141
- doit\_scat\_fieldCalc, 140
- doit\_scat\_fieldCalcLimb, 140
- doit\_zs\_grid\_optCalc, 138
- DoitAngularGridsSet, 138, 140
- DoitCloudboxFieldPut, 139
- DoitInit, 138
- DoitScatteringDataPrepare, 139, 140
- ext\_matAddPart, 140
- Extract, 122
- isotopologue\_ratiosInitFromBuiltin, 51
- iyApplyUnit, 77, 78
- iyCalc, 29, 78
- iyCloudRadar, 144
- iyEmissionStandard, 29, 76, 79
- iyInterpCloudboxField, 141
- iyLoopFrequencies, 78, 80
- iyRadioLink, 100, 102
- iyReplaceFromAux, 102
- iySurfaceRtpropAgenda, 90
- iyTransmissionStandard, 99
- jacobianAddAbsSpecies, 114
- jacobianAddFreqShift, 118
- jacobianAddFreqStretch, 118
- jacobianAddPointingZa, 118
- jacobianAddPolyfit, 119
- jacobianAddSinefit, 119
- jacobianAddTemperature, 116
- jacobianAddWind, 116
- jacobianClose, 108
- jacobianInit, 108
- jacobianOff, 108
- line\_mixing\_dataInit, 48
- line\_mixing\_dataMatch, 48
- MatrixCBR, 77
- MatrixUnitIntensity, 100, 102
- opt\_prop\_sptFromMonoData, 140
- ParticleType2abs\_speciesAdd, 50
- ParticleTypeAdd, 66, 67
- ParticleTypeAddAll, 67
- pha\_mat\_sptFromDataDOITOpt, 139
- pha\_mat\_sptFromMonoData, 139
- pnd\_fieldCalc, 67
- ppath\_stepGeometric, 81
- ppath\_stepRefractionBasic, 81
- ppathCalc, 73
- ppathFromRtePos2, 100
- ppathStepByStep, 81
- Print, 6
- propmat\_clearsky\_fieldCalc, 42, 43, 55
- propmat\_clearskyAddFaraday, 42, 49, 97
- propmat\_clearskyAddFromLookup, 42, 54
- propmat\_clearskyAddOnTheFly, 38, 39, 42, 43
- propmat\_clearskyAddParticles, 42, 50
- propmat\_clearskyAddZeeman, 42, 45
- propmat\_clearskyInit, 42
- ReadXML, 42
- refellipsoidEarth, 87
- refellipsoidForAzimuth, 88
- refellipsoidMars, 87
- refellipsoidOrbitPlane, 88
- refr\_index\_airFreeElectrons, 58, 78
- refr\_index\_airIR, 58
- refr\_index\_airMWgeneral, 58
- refr\_index\_airThayer, 58
- rte\_losGeometricFromRtePosToRtePos2, 100
- scat\_data\_array\_monoCalc, 139, 140
- ScatteringDoit, 138
- sensor\_responseInit, 93
- sensorOff, 93
- StringCreate, 6
- StringSet, 6
- surfaceBlackbody, 90
- surfaceFlatRefractiveIndex, 90
- surfaceFlatScalarReflectivity, 90
- surfaceLambertianSimple, 91
- TangentPointExtract, 84
- wind\_u\_fieldIncludePlanetRotation, 95
- WriteXML, 7
- yApplyUnit, 77
- ybatchCalc, 121

- yCalc, 27, 29, 71, 78–80
- yCloudRadar, 145
- z\_fieldFromHSE, 19
- workspace variable, 6
- workspace variables, 7
  - abs\_cia\_data, 36, 43
  - abs\_coef, 42
  - abs\_cont\_models, 43
  - abs\_cont\_names, 43
  - abs\_cont\_parameters, 43
  - abs\_lines, 42
  - abs\_lines\_per\_species, 42
  - abs\_lineshape, 42, 47
  - abs\_lookup, 42, 53
  - abs\_lookup\_is\_adapted, 53
  - abs\_species, 24, 39, 41, 43, 49
  - abs\_vec, 140
  - abs\_xsec\_per\_species, 36
  - antenna\_dim, 31
  - atmosphere\_dim, 16
  - blackbody\_radiation, 25
  - cloudbox\_limits, 20
  - cloudbox\_on, 20
  - doit\_i\_field, 139
  - doit\_i\_field1D\_spectrum, 139
  - doit\_scatter\_field, 139
  - ext\_mat, 140
  - ext\_mat\_spt, 140
  - f\_grid, 7, 73
  - isotopologue\_quantum, 45
  - isotopologue\_ratios, 51
  - iy, 27, 36, 72, 78, 144
  - iy\_aux, 79
  - iy\_aux\_vars, 79, 80
  - iy\_unit, 72, 77, 144
  - iyb, 72
  - jacobian, 108
  - jacobian\_indices, 108
  - jacobian\_quantities, 108
  - lat\_grid, 17
  - lat\_true, 19
  - lon\_grid, 18
  - lon\_true, 19
  - mag\_u\_field, 21, 47
  - mag\_v\_field, 21, 47
  - mag\_w\_field, 21, 47
  - mblock\_aa\_grid, 31
  - mblock\_z\_a\_grid, 31
  - output\_file\_format, 7
  - p\_grid, 15, 17
  - p\_hse, 19
  - pha\_mat, 139
  - pnd\_field, 20, 25, 67
  - pnd\_field\_raw, 67
  - ppath, 79, 82
  - ppath\_lmax, 80, 81, 83
  - ppath\_lraytrace, 81, 83, 101
  - ppath\_step, 82
  - propmat\_clearsky, 25, 36, 37, 42, 49
  - propmat\_clearsky\_field, 42
  - range\_bins, 145
  - refellipsoid, 19, 87
  - refr\_index\_air, 57
  - refr\_index\_air\_group, 57
  - rte\_alonglos\_v, 96
  - rte\_los, 31, 78, 99
  - rte\_pos, 29, 78, 99
  - rte\_pos2, 100
  - rtp\_mag, 21
  - scat\_aa\_grid, 138
  - scat\_data\_array, 25, 26, 50
  - scat\_i\_p, 139
  - scat\_z\_a\_grid, 138
  - sensor\_los, 31, 99
  - sensor\_norm, 94
  - sensor\_pos, 29, 99
  - sensor\_response, 31, 72, 93
  - sensor\_time, 118
  - stokes\_dim, 23, 72, 97
  - surface\_emission, 90
  - surface\_los, 90
  - surface\_rmatrix, 90
  - t\_field, 18
  - transmitter\_pos, 100
  - vmr\_field, 18, 24, 39, 41, 97
  - wind\_u\_field, 21, 95
  - wind\_v\_field, 21, 95
  - wind\_w\_field, 21, 95
  - y, 27, 72, 77
  - y\_f, 79
  - y\_los, 79
  - y\_pol, 79
  - y\_pos, 79
  - ybatch\_index, 121
  - ybatch\_n, 121
  - ybatch\_start, 121



z\_field, 18, 19

z\_surface, 19, 90

zenith angle, 30